

Characterization of Summertime Aerosols at Ny-Ålesund in the Arctic

by

Jianqiong Zhan

A Dissertation submitted to the

Graduate School - Newark

Rutgers, The State University of New Jersey

in partial fulfillment of the requirements

for the degree of

Doctor of Philosophy

Graduate Program in

Environmental Science

Written under the direction of

Dr. Yuan Gao

and approved by

Newark, New Jersey

May 2014

ABSTRACT OF THE DISSERTATION

Characterization of Summertime Aerosols at Ny-Ålesund in the Arctic

By Jianqiong Zhan

Dissertation Director:

Dr. Yuan Gao

Characteristics of atmospheric aerosols have implications for aerosol radiative forcing, aerosol-cloud interactions, heterogeneous chemistry, and climate. To characterize summertime aerosols in the Arctic, aerosol samples were collected at Ny-Ålesund in July of 2011 and 2012. The specific objectives were: (1) to determine aerosol compositions, (2) to investigate the sources and deposition of selected aerosol components, (3) to identify the effects of ship emissions on aerosol concentrations, and (4) to investigate the formation of secondary inorganic aerosols (SIAs), aerosol acidity and chloride (Cl^-) depletion.

The results showed that the mean equivalent black carbon (EBC) concentration was 17 ng m^{-3} at the Ny-Ålesund settlement, higher than the mean value of 5.4 ng m^{-3} observed outside the Ny-Ålesund settlement in July 2011. The average local emission rate of EBC was 8.1 g h^{-1} , with an uncertainty of approximately a factor of two. The EBC plumes from local emissions were confined to 10 km downwind, with the total EBC deposition estimated to be $6.4\text{--}44 \text{ ng m}^{-2} \text{ h}^{-1}$. When two cruise ships with more than 1500 passengers visited Ny-Ålesund in July 2012, the concentrations of the nc-V,

nc-Ni and nss-SO₄²⁻ were 0.976 ng m⁻³, 0.572 ng m⁻³ and 203 ng m⁻³, which were 38-fold, 8-fold and 2-fold higher than their median values of the sampling period. In July 2012, the mean SIAs concentration, defined as the sum of nss-SO₄²⁻, NO₃⁻ and NH₄⁺, was 158 ng m⁻³, accounted for 33% of the total mass of ionic species. The mean neutralization ratio (NR) was 0.53, indicating that SO₄²⁻ and NO₃⁻ was not fully neutralized by NH₄⁺. The Cl⁻ depletion occurred in samples that had high concentrations of [nss-SO₄²⁻ + NO₃⁻ - NH₄⁺] and sea salt, indicating that the Cl⁻ depletion could be affected by interactions of acidic species (SO₄²⁻, NO₃⁻) with sea salt.

Results from this study fill the data gap of the chemical properties of summertime aerosols and the effects of local emissions on air quality at Ny-Ålesund in the Arctic. These results may serve for future research that seeks to assess aerosol radiative forcing and for developing emission reduction strategies in the Arctic.

ACKNOWLEDGEMENTS

The efforts of a significant number of individuals and organizations have enabled me to complete this doctoral dissertation. I would like to express my sincere gratitude to all those who provide me the possibility to complete this dissertation.

First and foremost, I would like to express sincerest gratitude to my advisor, Dr. Yuan Gao. It was Dr. Yuan Gao who instigated me on the atmospheric chemistry direction at Rutgers University. Her unfaltering support, tremendous guidance, and continuous trust have helped me to successfully pursue a Ph.D. degree.

I would like to thank my committee members, Dr. James Andersen, Dr. Chao Luo and Dr. Evert Elzinga, for their valuable time, comments, and encouragement. Thanks to Dr. James Andersen, who generously gave his time and challenged the scope of my work by posing questions that helped to expand my work. I am grateful to Dr. Evert Elzinga who patiently laid the foundation of environmental chemistry theory at Rutgers. His insightful comments helped in the refinement of my manuscripts. It has also been an honor to have Dr. Luo Chao as a member of my dissertation committee. His intellectual feedback has helped tremendously in my studies from an aerosol modeling perspective.

I would like to show my greatest appreciation to Dr. Lee Slater for his tremendous support. I feel motivated and encourage every time I attend his meetings. I would especially like to thank Ms. Liz Morrin for her constant support and help. I am sincerely grateful to Dr. Kristina Keating and Dr. Jenny Lockard at Rutgers-Newark,

Dr. Robert Sherrell, Dr. Yair Rosenthal, Dr. Silke Severmann, and Dr. Gary Taghon at Rutgers-New Brunswick, Dr. Joseph Bozzelli at NJIT, for their patience to explain me the knowledge of environmental physics and chemistry using the theoretical reasoning and observation to reveal and interpret basic physical and chemical processes. I thank Marne Benson, Jordan Burke, and Paula Neves at Rutgers-Newark, for their patience to teach me oral, visual and written communication skills through commenting on the manuscript, proposal, poster and oral presentations.

I thank professors, students, and staff in the department of Earth & Environmental sciences at Rutgers. I am extraordinarily lucky to have been part of such a friendly, collaborative, open-minded, and supportive department. I would like to thank past and present members, especially those who have helped to make my doctoral journal at Rutgers enjoyable and productive, which includes Guojie Xu, Rafael Jusino-Astrino, Tianyi Xu, Ying Zhu, Zhongjie Yu, Joshua Lefkowitz, Ashley Samuel, Dawn Roberts-Semple, Michael Kalczynski, Simla Shin, Yves Personna, Chi Zhang, Pami Mukherjee, Jonathan Algeo, Peter Argyrakakis, Samuel Falzon, Neil Terry, Judy Rabinson, and Gordon Osterman for their support and encourage. All of you have been there to support me and incited me to strive towards my goal.

I would like to acknowledge the financial and technical support of the National Natural Science Foundation of China and Chinese Arctic and Antarctic Administration, particularly in the award of Foundation Young Scientist that provided the necessary financial support for this research. I will always be forever grateful for a special group from the Third Institute of Oceanography, State Oceanic Administration for their technical support and assistance in sampling and chemical analysis. I am extremely

grateful to my former advisor Professor Liqi Chen for always encouraging and expecting me to think more independently about experiments and results, and providing a friendly and safe environment for me to develop into an independent thinker. I would also like to express appreciation to Senior Engineer Wei Li, for his mentorship, support, patience, and guidance. Wei Li has always been very supportive of my research ideas and is always willing to discuss in great detail with me.

Finally, I want to thank my parents, my sister, and my brother for their endless love, encouragement and support. I am so blessed to have such a loving family who accepts me for who I am, and who instills in me the directive to always work hard and to learn new things for the pure joy of it. Last, but not least, I must thank my friends (too many to list here but you know who you are) for supporting and encouraging me through the rough road to finish this thesis.

TABLE OF CONTENTS

Chapter 1: Introduction	1
1.1 Background and Overview	1
1.2 Overall Objectives and Organization of the thesis	2
Chapter 2: Impact of summertime anthropogenic emissions on atmospheric black carbon at Ny-Ålesund in the Arctic	5
Abstract	5
2.1 Introduction	6
2.2 Methods	9
2.2.1 Measurement sites	9
2.2.2 Black carbon measurement and meteorological data collection	10
2.2.3 Atmospheric transport and dispersion model	13
2.2.4 Time-frequency analysis	13
2.3 Results and discussion	14
2.3.1 EBC concentrations	14
2.3.2 Local meteorological influences	15
2.3.3 EBC concentration from local emissions and long-range transport	19
2.3.4 Local emissions	21
2.3.5 Long-range transport	27
2.4 Conclusions	33
Chapter 3: Effects of ship emissions on summertime aerosols at Ny-Ålesund in the Arctic	35
Abstract	35
3.1 Introduction	36
3.2 Methods	39

3.2.1 Sampling site.....	39
3.2.2 Meteorological conditions	39
3.2.3 Back trajectory analysis	43
3.2.4 Sample collection.....	45
3.2.5 Sample analysis.....	46
3.2.6 Data analysis	49
3.3 Results and discussion	55
3.3.1 Composition of total Aerosol mass	55
3.3.2 Episodes from ship emissions.....	58
3.3.3 Periods with few-ship visits	62
3.4 Conclusions.....	67
Chapter 4: Characterization of major ionic species and carbonaceous components in summertime aerosols at Ny-Ålesund in the Arctic.....	69
Abstract.....	69
4.1 Introduction.....	70
4.2 Methods.....	72
4.2.1 Sample and data collection	72
4.2.2 Chemical analysis	73
4.2.3 Data analysis	75
4.3 Results and discussion	78
4.3.1 Major ions in aerosols.....	78
4.3.2 Formation of secondary inorganic aerosol.....	84
4.3.3 Aerosol acidity	85
4.3.4 Chloride depletion.....	89
4.3.5 Organic carbon and elemental carbon.....	90

4.4 Conclusions.....	92
Chapter 5: Conclusions and future work	94
5.1. Overall conclusions.....	94
5.2. Recommendations for future research	96
Reference	97
Curriculum vitae	110

LIST OF TABLES

Table 2.1 Comparison of equivalent black carbon (EBC) concentrations in Svalbard, Alert (Nunavut) and Barrow (Alaska).	12
Table 2.2 Correlations between equivalent black carbon (EBC) concentration and Meteorological parameters at Yellow River Station (YRS), Ny-Ålesund.	19
Table 2.3 Atmospheric deposition fluxes of equivalent black carbon (EBC) in Ny-Ålesund, Svalbard, and Fairbanks, Alaska	28
Table 3.1 Sampling data and time, meteorological data ^b , origin of air masses arriving at Ny-Ålesund and nc-Mn/nc-V in July 2012	44
Table 3.2 Chemical concentrations and ratios in aerosols during cruise ships present and during few-cruise ships present in Ny-Ålesund in July, 2012	50
Table 3.3 Element concentrations in soils at Ny-Ålesund (mg kg ⁻¹).	51
Table 3.4 Major chemical species in aerosols derived from calculations.	54
Table 4.1 Sampling dates, meteorological data, chemical concentrations (ng m ⁻³), neutralization ratios, [H ⁺] _{total} , [H ⁺] _{strong} , [H ⁺] _{free} (nmol m ⁻³), and pH	77
Table 4.2 Non-sea salt sulfate (nss-SO ₄ ²⁻) and methanesulfonate (MSA ⁻) concentrations and the nss-SO ₄ ²⁻ /MSA ⁻ ratio in the Arctic in summer	82
Table 4.3 Aerosol acidities found at Ny-Ålesund and at other sites	87
Table 4.4 Correlation matrix for the parameters measured	88

LIST OF FIGURES

Figure 2.1 Map of Ny-Ålesund community and sampling sites (Chinese ‘Yellow River’ station (YRS, 11.93°E, 78.92°N, 13 m a.s.l), S2(12.07°E, 78.90°N, 126 m a.s.l), S3(12.06°E, 78.99°N, 134 m a.s.l), S4(11.60°E, 78.96°N, 33 m a.s.l).	10
Figure 2.2 Time series of equivalent black carbon (EBC) concentrations, air mass transport pathways (dash line; AO represents the Arctic Ocean sector, EU stands for Western Europe, and CR stands for central Russia) and metrological parameters (total precipitation, relative humidity, wind speed, wind direction, air temperature, and pressure).....	16
Figure 2.3 Variations in equivalent black carbon (EBC) concentration (ng m^{-3}) affected by wind directions at Yellow River Station (YRS). Individual wind direction measurements are accumulated and the relative frequency is shown as a percentage.	17
Figure 2.4 (a) Contour plot of the average equivalent black carbon (EBC) concentrations during the entire experiment period at Yellow River Station (YRS) attributed to local emissions. (b) The wind rose plot was made for the entire experiment period at YRS. Individual wind direction measurements were accumulated and the relative frequency is shown as a percentage. Wind speed (m s^{-1}) is expressed by different color bars.....	24
Figure 2.5 (a) Contour plot of dry deposition averaged over the entire experiment period and (b) wet deposition from local emissions.	29
Figure 2.6 (a) Ten-day back trajectories were colored by air pressure and major transport pathways calculated by cluster analysis, labeled by identification of each cluster and frequency of occurrence. Both were generated by the	

HYSPLIT_4 model. AO represents the Arctic Ocean sector, EU stands for western Europe and CR stands for central Russia. (b) Map of potential precipitation contribution function probability.	32
Figure 3.1 Aerosol sampling site (Yellow River Station) and soil sampling sites (S1-S5) at Ny-Ålesund.....	40
Figure 3.2 The profiles of temperature and humidity at Ny-Ålesund in July 1, 2012, based on the Radiosounding data provide by The German Alfred Wegener Institute for Polar and Marine Research (AWI) and the French Polar Institute Paul Emile Victor (IPEV).	41
Figure 3.3 Geopotential heights (shaded colors and contour lines) and wind fields (vectors) at 950hPa based on the data from the European center for medium range weather forecasts (ECMWF) reanalysis project. (a) The averages of fields at 950 hPa in July 4-22 from 1981 to 2010, (b) the averages of fields at 950 hPa in July 4-22, 2012, and (c) the anomalies of fields in 2012 to the climate averages in 1981-2010. The unit is gpm for geopotential heights and m s^{-1} for winds. The contour line intervals are 5 gpm for both (a) and (b) and 10 gpm for (c). The red circle marks the location of this study at Ny-Ålesund.	42
Figure 3.4 The wind rose plot for the entire experiment period (July 4-22, 2012) at Ny-Ålesund. Individual wind direction measurements were accumulated and the relative frequency is shown as a percentage. Wind speed (m s^{-1}) is expressed by different color bars.	43
Figure 3.5 Correlation of elemental composition between soils at Ny-Ålesund and crustal materials in Taylor (1964).	52

Figure 3.6 Comparison between chemical reconstructed mass and gravimetric mass.....	57
Figure 3.7 Comparison of element concentrations observed in July 2012 with the concentrations observed in the summer from others at Ny-Ålesund [Maenhaut and Cornille, 1989; Pacyna and Ottar, 1985].....	61
Figure 3.8 Comparison of the concentrations of nc-V versus those of nc-Mn obtained at Ny-Ålesund in the summer during this study with those from Barrow [Quinn et al., 2009], Eurasia, Northeast USA , Barrow and Mould Bay in the North American Arctic and Bear Island and Spitsbergen in the Norwegian Arctic [Rahn, 1981]......	63
Figure 4.1 Sampling location at Ny-Ålesund, Svalbard	74
Figure 4.2 Ten days air mass backward trajectories associated with the high concentrations of MSA. The trajectories were calculated at the 500m, 1000m, and 5000m heights every 6 hours by the Hybrid Single-Particle Lagrangian Integrated Trajectory Model 4 (HYSPLIT_4) [Draxier and Hess, 1998]. The National Centers for Environmental Prediction (NCEP)-National Center for Atmospheric Research (NCAR) reanalysis meteorological data was fed into the model.....	81
Figure 4.3 Relationships between the methanesulfonate/non-sea salt sulfate ($\text{MSA}^-/\text{nss-SO}_4^{2-}$) ratios and the MSA^- concentrations. The dish line was the result from linear regression model using all of the data. The solid line was the result from linear regression model excluding one sample affected by ship emission which was highlighted with back circle.....	82

Figure 4.4 (a) The relationships between the organic carbon and sea salt concentrations. (b) The relationship between the organic carbon concentrations and the number of ship passengers.	91
---	----

Chapter 1: Introduction

1.1 Background and Overview

Arctic temperatures have increased at almost twice the global rate, causing Arctic sea ice to melt at an unprecedented rate [IPCC, 2013]. Declining Arctic sea ice during the summer has spurred an increase in anthropogenic activities in the Arctic [AMAP, 2011]. These developments could lead to elevated concentrations of aerosols in the Arctic [DeAngelo, 2011], which may further contribute to the changing Arctic climate via snow-albedo feedback [Bond *et al.*, 2013] and the formation of cloud condensation nuclei [Bauer and Menon, 2012]. In the summer, the transport of air and pollutants are limited because the Arctic front is weak and in a more northerly position, so Arctic air mass is separated from mid-latitudes [Garrett *et al.*, 2011; Stohl *et al.*, 2006]. In addition, clouds and precipitation during the summertime can remove pollutant from the air before they are carried far [Bourgeois and Bey, 2011]. Therefore, the transport of contaminants to the Arctic is less frequent in the summer than in the winter. There are relatively low particle number concentrations in the air in the summer. In the relative clean arctic regimes, typically in summer, the addition of aerosols into the air can dramatically increase cloud cover, and this may change the energy balance in the atmosphere and at the earth's surface [IPCC, 2013].

Observations and modeling have shown that the summertime Arctic aerosol has been influenced by anthropogenic activities within the Arctic. Ship emissions contribute about 30–40% of the total PM_{2.5} concentrations during tourist seasons in the Gulf of Alaska [Mölders *et al.*, 2010]. The shipping emissions in the Arctic may increase black carbon by 50% in 2030 and increase ozone by 10% in the Arctic lower

troposphere [*Dalsøren et al.*, 2013]. In the Svalbard archipelago during 2007, ship emissions were responsible for 90% of the total nitrogen oxides (NO_x) and 93% of the black carbon [*Vestreng et al.*, 2009]. At Ny-Ålesund, equivalent black carbon (EBC) and 60 nm particles increased 45% and 72%, respectively when cruise ships with more than 50 passengers were present at Ny-Ålesund [*Eckhardt et al.*, 2013]. Under the influence of anthropogenic emissions, the particles can be modified by the interaction of naturally generated and pollution-derived compounds [*Anderson et al.*, 1992], resulting in alternation in aerosol acidity and the formations of secondary inorganic aerosols [*Weinbruch et al.*, 2012]. This further influences aerosol radiative forcing and aerosol-cloud interaction [*Bauer and Menon*, 2012].

Aerosol chemical compositions, sources, depositions and their chemical properties (such as acidity and chloride depletion) are still not well characterized due to the lack of measurements at this location. The purpose of this study was to fill in these gaps and improve understanding of the characteristics of summertime aerosol in the Arctic.

1.2 Overall Objectives and Organization of the Thesis

This thesis aims to improve understanding of the chemical composition of aerosols and their potential sources and sinks at Ny-Ålesund in summer. To achieve this goal, field sampling, lab chemical analyses, and model calculations were employed to improve understanding of the characteristics of aerosols in Ny-Ålesund during the summer. Chapter two focuses on investigating the sources, transport, distribution and deposition of black carbon at Ny-Ålesund in the summer Arctic. Chapter three describes the evaluation of the effects of ship emissions on aerosol concentrations.

Chapter four focuses on major ionic species and carbonaceous components in the aerosol to assess the formation of secondary inorganic aerosols (SIAs), aerosol acidity, and chloride depletion. Chapter five summarizes the major findings of this research project and offer recommendations for future research.

Chapter 2 - To investigate the sources, transport, distribution and deposition of black carbon at Ny-Ålesund in the summer Arctic.

- a. EBC concentrations measurements were carried out in Ny-Ålesund in July 2011;
- b. Pearson's correlation coefficient and principal component regression (PCR) were used to estimate the influence of meteorological parameters on the EBC concentrations;
- c. Ensemble empirical mode decomposition method was used to quantify the contribution from local emissions and long-rang transport;
- d. Atmospheric transport and dispersion model were used to estimate the influence from local emissions on EBC distribution and deposition;
- e. Potential precipitation contribution function (PPCF), back-trajectories and cluster trajectory analysis were used to interpret the contribution from long-range transport.

Chapter 3 – To evaluate the effects of ship emissions on aerosol concentrations

- a. Selected trace elements, ionic species and organic/elemental carbon in aerosols were measured at Ny-Ålesund in July 2012;

- b. Chemical tracer, non-crust vanadium (nc-V), nc-nickel (Ni) and non-sea salt (nss) sulfate (SO_4^{2-}) were used to identify the signals from ship emissions and to evaluate the effects of ship emissions on aerosol concentrations;
- c. The features of aerosol concentrations with few ships visited were interpreted by employing the ratios of nc-V/nc-Mn (magnesium), backward trajectories and enrichment factors of trace elements in aerosols.

Chapter 4 - To investigate major ionic species and carbonaceous components in the aerosol, to assess the formation of secondary inorganic aerosols (SIAs), aerosol acidity, and Cl^- depletion

- a. Water soluble components and organic/elemental carbon (OC/EC) in aerosols were measured at Ny-Ålesund in July 2012;
- b. Potential sources of ionic species and OC was investigated.
- c. Formation of SIA were discussed;
- d. Aerosol acidity and factors affect aerosol acidity were studied.
- e. Cl^- depletion was evaluated.

Chapter 5 – Summarize the major findings of this research and offer recommendations for future research.

Chapter 2: Impact of summertime anthropogenic emissions on atmospheric black carbon at Ny-Ålesund in the Arctic¹

Abstract

Measurements of equivalent black carbon (EBC), calculated from aethalometer measurements of light attenuation, were carried out in July 2011 at Ny-Ålesund in the Arctic. Highly elevated EBC concentrations were observed within the settlement of Ny-Ålesund, with a median value of 17 ng m^{-3} , which was about two times the background level. Results from the ensemble empirical mode decomposition method suggested that about 60–80% of atmospheric EBC concentrations at Ny-Ålesund were from local emissions, while only 20–40% arrived via atmospheric transport. The estimated average local emission rate was 8.1 g h^{-1} , with an uncertainty of approximately a factor of two. The pollution plume was confined to 10 km downwind of the settlement, with the total EBC deposition estimated to be $6.4\text{--}44 \text{ ng m}^{-2} \text{ h}^{-1}$. This may affect snow black carbon (BC) concentrations in nearby glaciated areas. The efficiencies of the long-range transport were estimated based on cluster analysis and potential precipitation contribution function, and the results implied that transport from western Europe is more efficient than from central Russia, on account of relatively rapid transport from western Europe and infrequent precipitation along this route. However, there was no correlation between air mass back-trajectories and EBC concentrations, suggesting that the contribution of long-range transport to EBC measured in Ny-Ålesund might be not significant in this season.

¹ **Zhan, J.**, Gao, Y., 2014. Impact of summertime anthropogenic emissions on atmospheric black carbon at Ny-Ålesund in the Arctic. *Polar Research* 33, 21821, doi: 10.3402/polar.v33.21821.

Key words: Equivalent black carbon, human influences, transport efficiency.

2.1 Introduction

Black carbon (BC) in the atmosphere affects the radiative balance of the Arctic due to its strong light absorption [*Shindell and Faluvegi*, 2009]. Although organic carbon has an overall cooling effect on the atmosphere [*IPCC*, 2007], for the highly reflective snow/ice surface of the Arctic, the mixtures of organic carbon and BC still exert positive top-of-atmosphere radiative forcing [*Flanner et al.*, 2009]. The impact of BC can continue even after it is removed from the atmosphere and deposited on ice or snow, through the reduction of surface albedo [*Doherty et al.*, 2010; *Hadley and Kirchstetter*, 2012]. Over the 20th century, about 20% of the warming and snow/ice-cover melting in the Arctic is due to the BC-albedo effect [*Koch et al.*, 2011]. These findings identify BC as a critical climate forcing agent in the Arctic.

Several ground- and aircraft-based investigations of atmospheric BC have been carried out in the Arctic. Annual mean concentrations of BC ranged from 26 to 49 ng.m^{-3} , with values at Alert and Zeppelin Station higher than those at Barrow and Summit [*Hirdman et al.*, 2010b]. A pronounced seasonal cycle has been found, with a maximum in winter/early spring (i.e., the haze season) and a minimum in summer [*Eleftheriadis et al.*, 2009; *Sharma et al.*, 2006]. Strong seasonal variations are consistent with atmospheric transport patterns in the Arctic [*Hirdman et al.*, 2010a; *Stohl et al.*, 2006]. Vertical concentration profiles of BC were observed during the Arctic Research of the Composition of the Troposphere from Aircraft and Satellites mission in 2008. In the spring, two peaks were revealed in the profile of BC mass

mixing ratio: one was at 5.5 km, with a mass mixing ratio of 150 ng kg^{-1} in the aged air mass; the other one, at 4.5 km, had a mass mixing ratio of 250 ng kg^{-1} and was associated with biomass burning [Spackman *et al.*, 2010]. The vertical stratification of BC increased with altitude at lower altitudes (650 hPa), whereas at higher altitudes it decreased toward the middle troposphere [Jacob *et al.*, 2010; Spackman *et al.*, 2010]. The summertime BC concentrations varied between 5 and 100 ng kg^{-1} from 0 to 12 km in altitude, with higher BC concentrations in the lower troposphere in July. As there were widespread fires during the aircraft campaigns, the enhancement of BC could have resulted from increased biomass burning [Spackman *et al.*, 2010], which might not be representative of typical BC distributions in summer. Northern Eurasia has repeatedly been shown to be the major source for the BC concentrations observed at the Arctic surface stations in winter and spring [Hirdman *et al.*, 2010a; Stohl *et al.*, 2006]. In summer, transport from the surrounding continental locations is limited by the weaker and more northern extent of the polar dome [Klonecki *et al.*, 2003; Law and Stohl, 2007] as well as more frequent precipitation [Barrie, 1996; Bourgeois and Bey, 2011]. As result of low efficiency of long-range transport, local aerosol sources become much more important in summer.

Recent studies have highlighted the role of local emissions within the Arctic.

Measurements made at Barrow, Alert and Zeppelin Station over more than a decade have indicated that BC concentrations measured in the Arctic are highly sensitive to emissions within the Arctic [Hirdman *et al.*, 2010b]. In the last 10 years, human activities such as general transport (aviation and shipping), oil and gas flaring and resource exploitation have increased; these could lead to strongly elevated

concentrations of BC in the Arctic [AMAP, 2011; Corbett *et al.*, 2010; Dalsøren *et al.*, 2007; DeAngelo, 2011; Granier *et al.*, 2006; Lack *et al.*, 2008; Lee *et al.*, 2010; Vestreng *et al.*, 2009]. Around 4.5 Gg yr⁻¹ of BC is contributed from Arctic shipping, and this may increase global climate forcing by at least 17% compared to warming due to CO₂ emissions from these vessels (ca. 42 000 Gg yr⁻¹) [Corbett *et al.*, 2010]. Lee *et al.* [2010] also highlighted aviation emissions associated with major routes in the vicinity of 60°N. Johnson *et al.* [2011] suggested the mean soot emission rate is 2.0 g s⁻¹ at a calculated uncertainty of 33%, from measurement of the emission rate from oil and gas flaring in Uzbekistan. However, these emissions are still not well characterized and specific emission factors are still uncertain due to the lack of measurements at many locations. In Svalbard, local human activities, such as motor vehicle use, electric power production and domestic combustion, persistently occur, contributing to the loading of BC in the air, but more quantitative evaluations of these contributions are needed.

To characterize the anthropogenic emissions affecting the BC concentration in Svalbard, field measurements were carried out within and near the settlement of Ny-Ålesund in July 2011, the peak season of local human activities. In this paper, we present the measurement results and estimate the contribution of local emissions, the emission rates and the BC deposition rates using model simulations. These results will be useful for interpreting other data sets in the region, for planning future measurement campaigns in this region and for developing emission reduction strategies in the Arctic.

2.2 Methods

2.2.1 Measurement sites

The measurements were made in Ny-Ålesund, on the island of Spitsbergen in the Svalbard Archipelago. The sampling sites were one site at the Chinese Yellow River Station (78.92°N, 11.93°E, 13 m a.s.l) within the Ny-Ålesund settlement and three sites around Ny-Ålesund: S2 (78.90°N, 12.07°E, 126 m a.s.l), S3 (78.99°N, 12.06°E, 134 m a.s.l), and S4 (78.96°N 11.60°E, 33 m a.s.l; Figure 2.1) Data measured at Zeppelin Station (78.90°N, 11.88°E, 474 m a.s.l) by *Eleftheriadis et al.* [2009] were used in this study for comparison. Zeppelin Station is situated on the mountain of Zeppelinfjellet, 1 km south of, and over 400 m above, the settlement, where contaminants from Ny-Ålesund are minimal [*Hirdman et al.*, 2010b]. The YRS is situated in Ny-Ålesund, directly below Zeppelin Station; it was therefore directly affected by local emissions from tourism and research-related activities in the settlement. S2 was located 4 km south-east of Ny-Ålesund, on the glacier Midtre Lovénbreen. S3 lay on the island of Blomstrandhalvøya, on the other side of the fjord from Ny-Ålesund and at a distance of about 5 km from the settlement. S4 was situated on the coastal plain of Kvadehuksletta at the north-west point of the peninsula Brøggerhalvøya, about 10 km away from Ny-Ålesund.

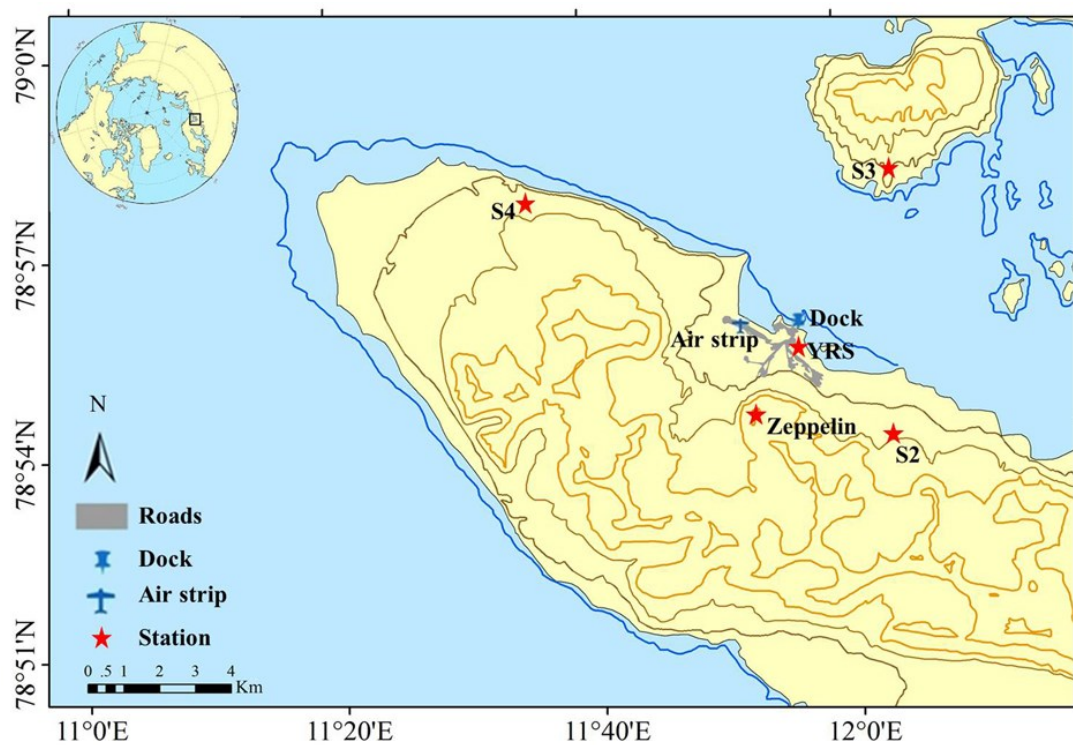


Figure 2.1 Map of Ny-Ålesund community and sampling sites (Chinese ‘Yellow River’ station (YRS, 11.93°E, 78.92°N, 13 m a.s.l), S2(12.07°E, 78.90°N, 126 m a.s.l), S3(12.06°E, 78.99°N, 134 m a.s.l), S4(11.60°E, 78.96°N, 33 m a.s.l).

2.2.2 Black carbon measurement and meteorological data collection

Aethalometers have been widely used for measuring BC concentrations in the Arctic [Eleftheriadis *et al.*, 2009; Hirdman *et al.*, 2010a; Sharma *et al.*, 2006]. The device measures the attenuation of light transmitted through particles that accumulate on a quartz fiber filter, and interprets the rate of increase of optical attenuation in terms of the concentration of optically-absorbing material in the sample air stream. Since these optically-based measurements rely on some assumptions to convert particle light absorption to BC concentrations, the data derived from this method are also called equivalent BC (EBC) [Sharma *et al.*, 2004]. In this study, an AE42 Model

Aethalometer (7-wavelength; only λ ca. 880 nm reported here; Magee Scientific, Berkeley, CA, USA) was used at the Yellow River Station site, while model AE51 instruments (Magee Scientific) were used at sites S2, S3 and S4. Temporal resolutions were 10 minutes for the AE42 unit and 5 minutes for the AE51 units during the measuring period of 5-19 July 2011. The specific mass absorption coefficient $\alpha_{ap} = 15.9 \text{ m}^2 \text{ g}^{-1}$ was used to calculate BC mass concentrations from the AE42 device. This value was derived from simultaneous measurements of light absorption and thermo-optical elemental carbon mass concentration by *Nyeki et al.* [2005], which was also applied in EBC calculations at Zeppelin Station by *Eleftheriadis et al.* [2009]. Data from the AE51 units were corrected by comparing AE42 and AE51 measurements at the same place. The scattering correction wasn't employed in this study since aerosols in these remote areas were well-aged, requiring little or no correction [*Hansen et al.*, 2007]. The overall uncertainty on the aggregated data is on the order of 10% [*Hansen et al.*, 2007]. To circumvent the potential error induced through the use of two different instruments, co-location experiments were carried out both before and after experiments. Measurement data are summarized in Table 2.1. Meteorological parameters, for example, air temperature, wind speed, wind direction and relative humidity, were collected simultaneously with a temporal resolution of one hour. Precipitation data was from Ny-Ålesund station, which is around 0.2 km away from Yellow River Station. The arithmetic mean, maximum and minimum for each parameter are presented in Table 2.1.

Table 2.1 Comparison of equivalent black carbon (EBC) concentrations in Svalbard, Alert (Nunavut) and Barrow (Alaska).

Station	Location	EBC concentration (ng m^{-3}) ^a	Time period	References
Yellow River station	11.93°E, 78.92°N, 13 m a.s.l	17 (4.1–38)	July, 2011	This work
S2	12.07°E, 78.90°N, 126 m a.s.l	5.3 (1.0–7.8)	July, 2011	This work
S3	12.06°E, 78.99°N, 134 m a.s.l	6.6 (0.0–15)	July, 2011	This work
S4	11.60°E, 78.96°N, 33 m a.s.l	4.7 (0.0–12)	July, 2011	This work
Zeppelin	11.92°E, 78.93°N, 474 m a.s.l	7 (3–11)	Summers 1998–2007	[Eleftheriadis et al., 2009]
		11	Summers 1990–1992	[Heintzenberg and Leck, 1994]
Gruvebadet	11.92°E, 78.93°N, 10 m a.s.l	5	Summers 1979–1990	[Heintzenberg and Leck, 1994]
Alert	62.3°W, 82.5°N, 210 m a.s.l	12–26	Summers 1989–2003	[Sharma et al., 2006; Sharma et al., 2004]
Barrow	156.6°W, 71.3°N, 11 m a.s.l	9–24	Summers 1989–2003	[Sharma et al., 2006]

^a Mean (minimum-maximum).

2.2.3 Atmospheric transport and dispersion model

The Hybrid Single-Particle Lagrangian Integrated Trajectory 4 (HYSPLIT_4) model, created by the US National Ocean and Atmospheric Administration [*Draxler and Hess, 1998*], was used to generate both forward and backward trajectories and complex dispersion/deposition simulations, using US National Centers for Environmental Prediction/National Center for Atmospheric Research (NCAR/NCEP) reanalysis data. The data were provided at a horizontal resolution of 2.5×2.5 degrees, 17 vertical levels up to 10hPa, and a temporal resolution of six hours. Emission rates were estimated by fitting the predictions from dispersion model to the observed concentration difference between within and outside the community, and then the subsequent advection, dispersion and deposition of EBC were simulated, using NCAR/NCEP reanalysis meteorological data fed into the HYSPLIT model. Wet deposition was calculated using precipitation data from the European Centre for Medium-Range Weather Forecasts (ECMWF). The washout ratio was calculated from the Scott washout ratio [*Scott, 1978*].

2.2.4 Time-frequency analysis

To better understand the properties and physical mechanism hidden in the EBC data, ensemble empirical mode decomposition (EEMD) was used to isolate and extract various temporal scales in data. These various temporal scales were further linked to different sources. There are other popular tools, such as Fourier analysis, wavelet analysis and Wigner-Ville distribution, which can also decompose the data into the components of different timescales, but they are limited to either linear or stationary processes, and require a priori function basis. This often makes their applications to

data from nonlinear and non-stationary processes problematic. EEMD is an adaptive method that is designed specifically for analyzing nonlinear and non-stationary data without imposing irrelevant mathematical rules [Wu and Huang, 2009]. This approach consists of sifting an ensemble of white noise-added signal, and obtains the mean of corresponding intrinsic mode functions (IMFs) that bear the full physical meaning and a time-frequency distribution, and also gets the corresponding average residual which is identical to the trend. Further details on the EEMD method can be found in Wu and Huang [2009]. The results are tested by statistical significance at the 95% confidence level based on a testing method suggested by Wu and Huang [2004] against the white noise null hypothesis.

2.3 Results and discussion

2.3.1 EBC concentrations

The concentrations of EBC (Figure 2.2) at YRS ranged from 4.1 to 38 ng m⁻³, with a median value of 17 ng m⁻³, which was higher than values observed outside the Ny-Ålesund settlement at S2, S3 and S4, where median EBC concentrations were 5.3, 6.6 and 4.4 ng m⁻³, respectively. The median value found at YRS was in the range of the summer monthly average at Alert (12–26 ng m⁻³) and Barrow (9–24 ng m⁻³) from 1989 to 2003 [Sharma *et al.*, 2006], but higher than EBC concentrations at Zeppelin Station (3–11 ng m⁻³) [Eleftheriadis *et al.*, 2009]. The levels of EBC at S2, S3 and S4 were comparable to measurements taken at Zeppelin Station (474 m a.s.l.) with a median EBC concentration of 7 ng m⁻³ [Eleftheriadis *et al.*, 2009]. These levels were also similar to aircraft measurements over the Arctic in July 2008, where the BC mass concentration was ca. 10 ng kg⁻¹ above 3 km and ca. 5 ng kg⁻¹ below 3 km [Liu *et al.*,

2011] as well as the Gruvebadet sea level site near YRS (78.92°N, 11.89°E) measured by *Heintzenberg and Leck* [1994], who reported 5 ng m⁻³ for summer/autumn from 1979 to 1990.

The results showed that the EBC concentration at YRS was higher than the levels of EBC at Zeppelin Station and ground-based stations around the settlement. Similar results were reported by *Hermansen et al.* [2011]: SO₂ and soot levels were higher in the Ny-Ålesund settlement than at Zeppelin Station. The aerosol scattering coefficient was also ca. 13–66% lower at Zeppelin, suggesting relative cleanliness at Zeppelin Station due to its elevation at 474 m a.s.l., above a temperature inversion layer, which limited vertical mixing [*Di Liberto et al.*, 2012]. Residential emissions were presumably a factor contributing to the elevated EBC concentration at YRS. This observation is further illustrated in Figure 2.3. As shown, EBC concentrations corresponded to wind directions; higher EBC concentrations were associated with being downwind— especially south—of Ny-Ålesund. Variations and average EBC concentration during the daytime were larger than those at night, indicating more complicated and stronger sources in the daytime than at night. This confirms that local human activities were one of the major sources affecting the concentration of EBC at Ny-Ålesund.

2.3.2 Local meteorological influences

The relationships between meteorological parameters and EBC concentrations were tested for statistical significance. Pearson's correlation coefficient and principal component regression (PCR) were used to estimate the influence of meteorological

parameters on the EBC concentrations. PCR assumes that the variables have normal distributions. However, some of our measured data are not normally distributed; therefore logarithmic transformations were done for the EBC concentrations, wind speed and relative humidity to avoid violation of the normality assumption.

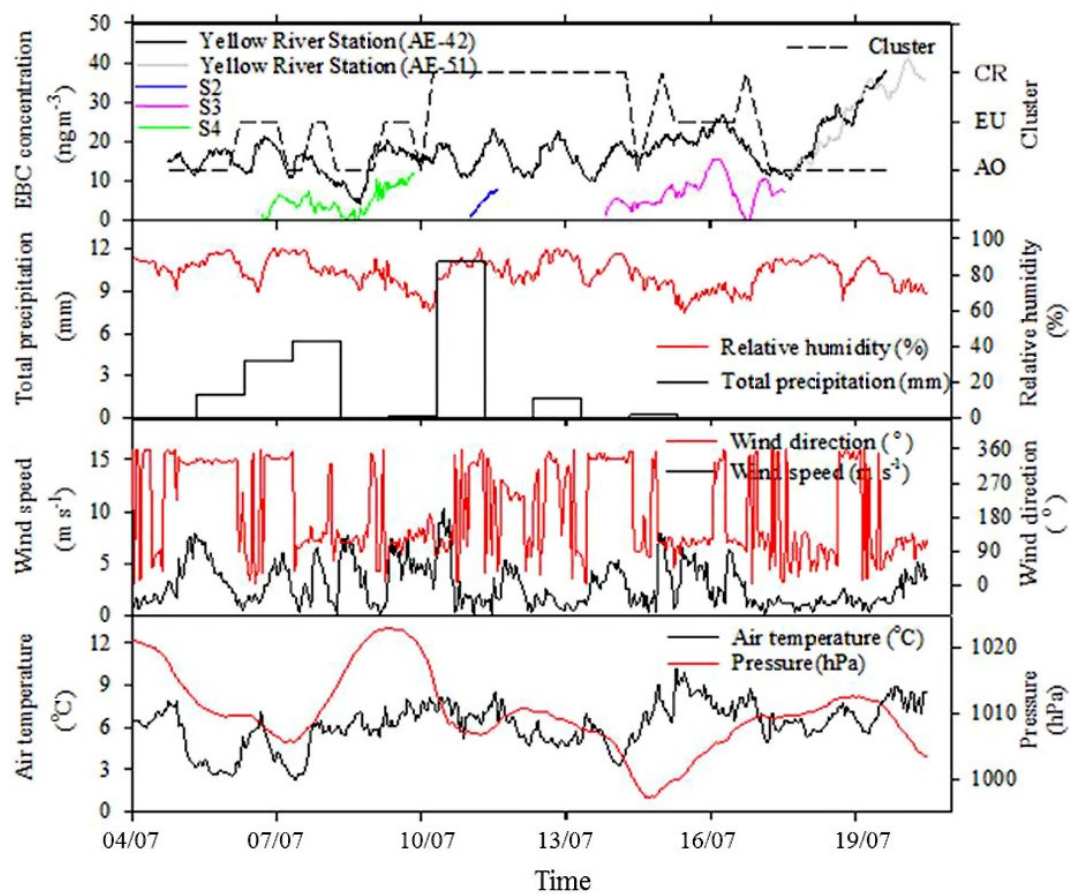


Figure 2.2 Time series of equivalent black carbon (EBC) concentrations, air mass transport pathways (dash line; AO represents the Arctic Ocean sector, EU stands for Western Europe, and CR stands for central Russia) and metrological parameters (total precipitation, relative humidity, wind speed, wind direction, air temperature, and pressure).

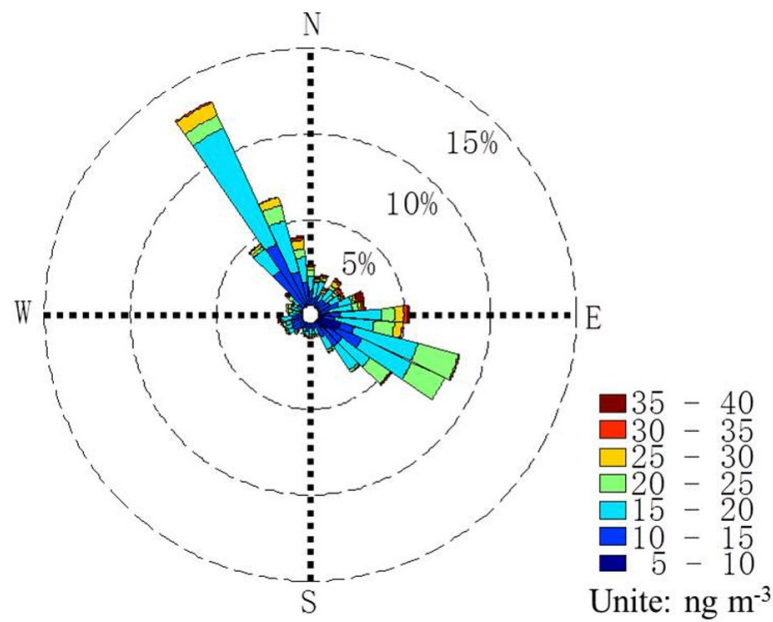


Figure 2.3 Variations in equivalent black carbon (EBC) concentration (ng m^{-3}) affected by wind directions at Yellow River Station (YRS). Individual wind direction measurements are accumulated and the relative frequency is shown as a percentage.

The levels of EBC were significantly ($p < 0.000$) related to temperature, wind speed, atmospheric pressure and total precipitation (Table 2.2). Among the meteorological parameters, temperature had the greatest effect on the EBC concentration, with a Pearson's correlation coefficient of 0.22 ($p < 0.000$), indicating higher levels of EBC during higher temperature periods. A negative correlation was found between temperature and boundary layer height, with a Pearson correlation of -0.38 ($p < 0.000$). This suggests that high EBC concentrations in warm air might relate to shallow boundary layer, which was created by temperature inversion [Tjernström, 2005]. Observations and NCAR/NCEP reanalysis data reveal that elevated temperature inversion dominates 91% of summer months [Tjernström and Graversen, 2009], and this was more pronounced in a warmer summer (e.g., 2007) compared to

other years (2003-06 and 2008) [Devasthale *et al.*, 2010]. Temperature inversion creates a stable and shallow mixing layer, which limits the vertical transfer of EBC between the surface and the free troposphere, trapping EBC close to the ground. This suggests that temperature may indirectly influence EBC concentration when a shallow boundary layer is capped by temperature inversion in the summer.

As expected, a negative correlation was found between EBC concentration and total precipitation due to removal via wet deposition. A negative relationship was found between the EBC concentration and wind speed, with a Pearson correlation of -0.10 ($p < 0.000$), indicating the dilution effect of winds on the EBC concentrations.

Relative humidity showed less significant correlation with the EBC concentrations, with a Pearson correlation of 0.033 ($p = 0.34$), suggesting that humidity did not directly affect EBC concentrations since most of the BC particles were hydrophobic.

The association between selected meteorological parameters (temperature, wind speed, relative humidity, atmospheric pressure and total precipitation) and EBC concentration was analyzed by PCR. The selected meteorological parameters can only explain 19% of the variation in EBC concentrations ($p < 0.000$), suggesting that other factors are influencing EBC levels in the area, such as the distance to sources and the strength of sources and sinks.

Table 2.2 Correlations between equivalent black carbon (EBC) concentration and Meteorological parameters at Yellow River Station (YRS), Ny-Ålesund.

	Mean and Range	Correlation Coefficient	
		r	p-value
Temperature	6.5	.22**	.000
(°C)	(2.4–10.5)		
Pressure	1011.0	-.21**	.000
(hPa)	(997.2–1023.1)		
Wind speed	3.2	-.10**	.000
(m s ⁻¹)	(0.0–12.5)		
Total precipitation	0.8	-.10**	.000
(mm/day)	(0.0–11.1)		
Relative humidity	80	.03	.125
(%)	(57–93)		

**. Correlation is significant at the 0.01 level (2-tailed).

2.3.3 EBC concentration from local emissions and long-range transport

Ny-Ålesund can be both a source and receptor for pollutants because some are locally generated and some are transported there over long distances. To evaluate these two factors, local emissions were assumed to be generated by both intermittent, short-term activities and continuous activities, while long-range transport, which is controlled by atmospheric circulation, occurs at various temporal scales [Stohl *et al.*, 2006]. In order to separate various signals hiding in the data, EEMD was used to decompose the EBC

data into various frequency signals. The results included IMFs, which represent some specific scale of oscillation, and a residual that is identical to the trend, expressed as:

$$EBC_{total} = IMF_1 + IMF_2 + \dots + IMF_n + Trend \quad (2.1)$$

BC at Ny-Ålesund can come from local emissions (EBC_{lo}) and long-range transport (EBC_{tr}).

$$EBC_{total} = EBC_{lo} + EBC_{tr} \quad (2.2)$$

Here, we assume that local emissions were generated by both random and continuous activities, which can be represented by high frequency ($IMF_1, IMF_1 \dots IMF_m$), and extremely low signals (E_{low-lo}), which were included in Trend. Hence, EBC_{lo} was defined as follows:

$$EBC_{lo} = IMF_1 + IMF_2 + \dots + IMF_m + E_{low-lo} \quad (2.3)$$

Long-range transport is controlled by atmospheric circulation at various temporal scales [Stohl *et al.*, 2006]; therefore, it can be expressed with specific frequency IMFs and as part of the signal in Trend. So EBC_{tr} were expressed as:

$$EBC_{tr} = IMF_{m+1} + IMF_{m+2} + IMF_{m+3} + \dots + IMF_n + E_{low-tr} \quad (2.4)$$

where $IMF_{m+1}, IMF_{m+2}, IMF_{m+3}, \dots, IMF_n$ are relatively low-frequency signals in IMFs and E_{low-tr} was the result from longer time scales of atmospheric circulation.

Based on these assumptions and principles of EEMD, the residual is understood to represent longer term oscillation, which is associated with continuous local emissions and longer timescales of transport. That is:

$$Trend = E_{low-lo} + E_{low-tr} \quad (2.5)$$

In this study, EBC data were decomposed into 10 IMFs, corresponding to periods ranging from two hours to more than five days. Generally, the frequencies of local human activities are higher than those of long-range transport and they are characterized by diurnal variation or shorter periods of variations. *Eleftheriadis et al.* [2009] pointed out that diurnal variation in EBC concentration was less than ± 1 standard deviation range at Zeppelin Station during the summer months (JJA), suggesting that the diurnal variation was negligible; therefore, one day was chosen as a cut-off point and frequencies of one day or less were identified as being associated with local emissions, while variances lasting more than one day were ascribed to long-range transport. When Eqns. 2.1-2.5 were applied to the data measured at YRS, S2, S3 and S4, the results indicated that 60–80% of EBC at the YRS was from local emissions. The processes controlling BC in the atmospheric boundary layer include emissions, atmospheric transport and deposition or eventual ventilation [*Wang et al.*, 2011]. These are considered below.

2.3.4 Local emissions

EBC emission rates. The atmospheric dispersion factor (D , h m^{-3}) from the source to the receptor was calculated using the HYSPLIT model, and then the emission rates (Q , ng h^{-1}) were obtained by dividing the EBC concentrations (M , ng m^{-3}) from local emissions by the relevant dispersion factors, according to the equation: $Q = M/D$.

EBC concentrations (M , ng m^{-3}) from local emissions were calculated using Eqn. 3. Here, a six-hour time average of the dispersion factor was set as the model output, and the average emission rate was calculated. A median value of 8.1 g h^{-1} was estimated, with a range from 1.0 to 25 g h^{-1} . The uncertainty in these factors was approximately a

factor of two due to the uncertainty associated with measurements and accuracy of the dispersion model and meteorological data. According to the average PM 2.5 emission rates measured during on-road testing in South East Queensland, Australia, the emission factor was 15 g h^{-1} for diesel buses or 1.7 g h^{-1} for light-duty vehicles driving at an average speed of 50 km h^{-1} [Keogh *et al.*, 2010]. The emission rate at Ny-Ålesund was equivalent to about half the emission produced by a bus, or to emissions from about five light-duty vehicles constantly driving. Although emissions from local human activities were miniscule compared to the emissions released from the mainland, these emissions in the vulnerable Arctic may change the physical and chemical properties of BC particles and more efficiently deposit to snow/ice surfaces [DeAngelo, 2011].

EBC concentration distribution estimate. Using the HYSPLIT_4 model, the spatial pattern of near-ground level EBC concentration due to local emissions was modeled every six hours and then averaged over the measurement period of this study. A contour plot of the average EBC concentration around Ny-Ålesund is shown in Figure 2.4a. Hourly wind speed and direction at 2-m height during the measurement period is shown by the wind rose diagram (also in Figure 2.4b). The prevailing winds during the experiments were typically either from the east–south-east or north–north-west. The concentration contour maps demonstrated that the trajectories of the EBC plumes released from Ny-Ålesund correlated well with the wind direction, and the plume shifted as wind changed in direction. The highest EBC concentration was about 14 ng m^{-3} at Ny-Ålesund, decreasing markedly with distance from the settlement as EBC was dispersed in the atmosphere. The concentrations of EBC reduced to 4.0 ng m^{-3}

(30%) within 2 km of the source, with the majority of the downwind area having concentrations of less than 2.0 ng m^{-3} . However, the impact of these emissions was irregular, such that puffs were more likely to cover the southern sectors (south–south-east, south, and south–south-west), where the snow- or ice-covered surface was more sensitive to pollution compared to other exposed land, rather than the west–north-west sector.

EBC dry deposition estimate In this study, dry deposition of EBC was estimated by the product of dry deposition velocities (V_d) and atmospheric EBC concentrations. Generally, V_d was calculated by surface resistance, which was a function of aerodynamic resistance, friction velocity and surface type [Vignati *et al.*, 2010]. Here, a deposition velocity of 0.030 cm s^{-1} was chosen based on results presented by Nilsson and Rannik [2001] and Held *et al.* [2011] of eddy-covariance flux measurements in the Arctic, which was input to the model to determine the EBC dry deposition flux from local emissions around Ny-Ålesund. Each six-hour dry deposition flux was calculated; a contour map for the average of the whole period is shown in Figure 2.5a. The deposition distribution pattern was similar to the concentration distributions, with the highest deposition of EBC directly downwind of the source, which was then immediately reduced to $4.0 \text{ ng m}^{-2} \text{ h}^{-1}$ (30% of the central value) within 2 km of the source. Major depositions occurred in glaciated areas in the south–south-west and south–south-east sector. EBC dry deposition from local emissions in summer ranged from 0.0 to $18 \text{ ng m}^{-2} \text{ h}^{-1}$ and total dry deposition (local emissions + long range transport) ranged from 4.3 to $32 \text{ ng m}^{-2} \text{ h}^{-1}$ (100 – $770 \text{ ng m}^{-2} \text{ d}^{-1}$) within 10 km (Table 2.3). This is in the lower range of dry deposition flux over

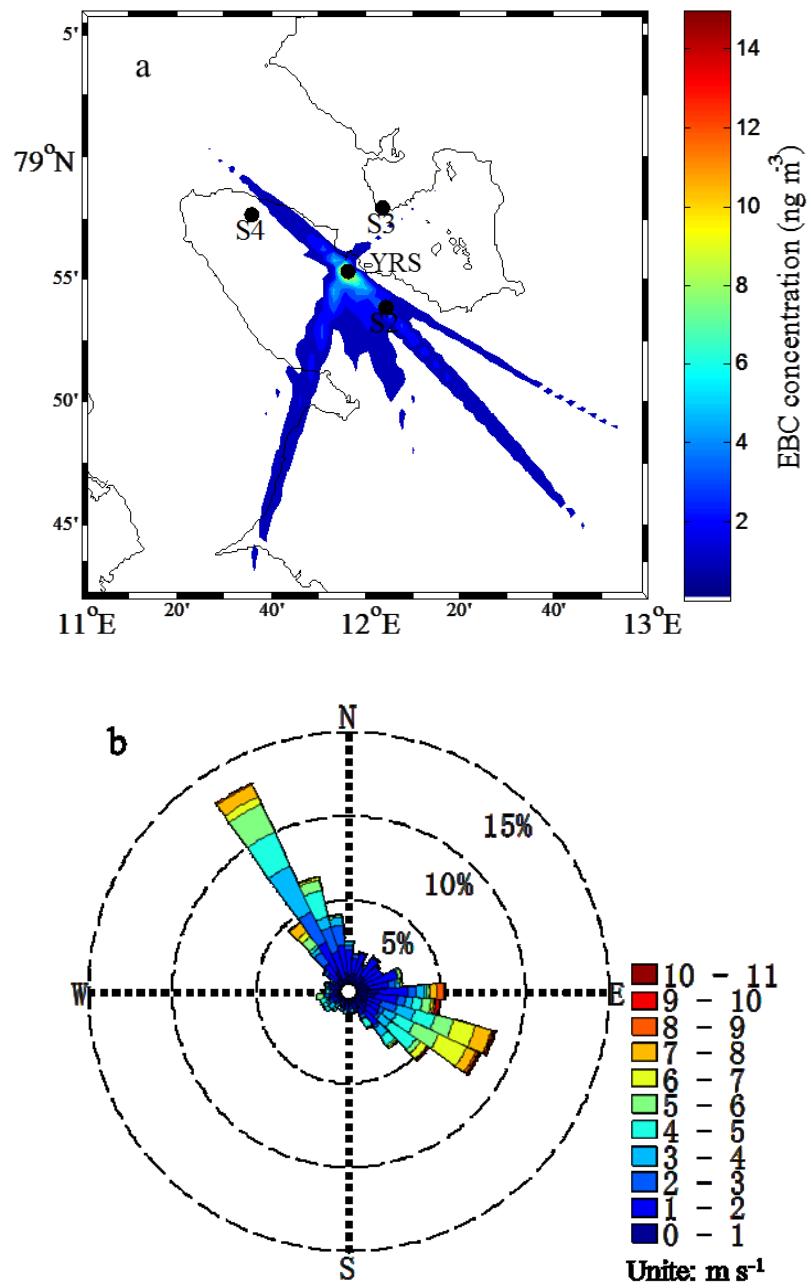


Figure 2.4 (a) Contour plot of the average equivalent black carbon (EBC) concentrations during the entire experiment period at Yellow River Station (YRS) attributed to local emissions. (b) The wind rose plot was made for the entire experiment period at YRS. Individual wind direction measurements were accumulated and the relative frequency is shown as a percentage. Wind speed (m s^{-1}) is expressed by different color bars.

snow/ice (about 100–5300 ng m⁻² day⁻¹) based on the observed BC depletion in the boundary layer in spring, including the period of biomass-burning that was documented [Spackman *et al.*, 2010].

EBC wet deposition estimate Wet deposition was also considered as a process controlling atmospheric BC concentration and affecting BC concentration in the snow surface since the observation site was subjected to periods of heavy precipitation during summer, and a substantial fraction of aerosol might be washed out and deposited on the snow/ice surface [Liu *et al.*, 2011]. Here, wet deposition flux was calculated as follows:

$$F_w = C \times P = 10^{-3} \times \text{EBC}_{\text{air}} \times \text{WR} \times P \quad (2.6)$$

where EBC_{air} is the EBC concentration in the air (ng m⁻³), WR is the washout ratio, P is precipitation rate (mm h⁻¹) and F_w is the wet deposition flux (ng m⁻² h⁻¹). The washout ratio,

$$\text{WR} = \text{BC}_{\text{snow or rain}} / \text{BC}_{\text{air}} \quad (2.7)$$

can be calculated by comparing of the amount of snow or rain with the concentration of BC in the air. Hegg *et al.* [2011] compared the washout ratio from fieldwork and the Scott washout ratio model [Scott, 1978], and found that the washout ratio predicted by the model was in reasonable agreement with the observed value. Hence, the Scott washout ratio was used in this study as follows:

$$\text{WR}(\text{BC}) = \frac{14000 \times M_s(0)}{\text{BC}_{\text{air}} \times P^{0.88}} + \frac{1000 \times F_{\text{BC}} \times (1 - 0.0441 \times P^{-0.88})}{1.56 + 0.44 \times \ln P}, \quad (2.8)$$

where $\text{WR}(\text{BC})$ was the BC washout ratio, $M_s(0)$ was the concentration of BC (ng m⁻³) in hydrometeors at the top of the riming zone, F_{BC} was scavenging efficiency, BC_{air} was the air concentration of BC, and P is the precipitation rate in mm h⁻¹. Here, we set

$M_s(0) = 0.1 BC_{\text{air}}$ (Scott's warm rain value) and $F_{\text{BC}} = 0.5$, since *Hegg et al.* [2011] reported that a predicted washout ratio using these two parameters agreed reasonably with the observed value for warm rain. The total precipitation was from the ECMWF database. The wet deposition due to local emissions was calculated every six hours; the average was calculated for the whole period as shown in the contour map (Figure 2.5b). Wet deposition from emissions ranged from 0.10 to 9.6 $\text{ng m}^{-2} \text{h}^{-1}$; total wet deposition ranged from 2.1 to 12 $\text{ng m}^{-2} \text{h}^{-1}$ within 10 km (Table 2.3). Wet deposition accounted for 22-44% of total EBC deposition, which was lower than $78 \pm 17\%$ inferred from the AeroCom multimodel assessment (Textor et al. 2006) as well as the results from *Spackman et al.* [2010], who reported that wet deposition accounted for 91% of total BC deposition to the Arctic in spring and 85% in winter.

The total EBC depositions, which were defined as the sum of dry and wet deposition, were about 6.4–44 $\text{ng m}^{-2} \text{h}^{-1}$. Local emissions of BC contribute ca. 15% to the total deposition within a radius of 10 km at Ny-Ålesund. This was similar to the figure reported for Svalbard by Norway's Climate and Pollution Agency: 20% of total deposition came from local emissions [*Vestreng et al.*, 2009].

This analysis demonstrates that the environmental impacts of deposition from an individual source can be localized, with dispersion of pollutants in the atmosphere resulting in negligible environmental burdens beyond about 10 km downwind. Even though the pollution puffs from local emissions were more likely to pass over the glaciated areas in the southern sectors, the total deposition flux of EBC from local emission over these areas was less than 10 $\text{ng m}^{-2} \text{h}^{-1}$. If we assume that all of this BC

is deposited on the top 1cm of snow and the density of snow is 0.40 g cm^{-3} , then local emissions only contribute 1.8 ng BC per gram of snow each month. However, it is comparable to the average BC concentration (about 5 ng g^{-1}) in fresh snow previously measured in the same region in late May [Hegg *et al.*, 2011]. However, this analysis only considers a single emission source. A variety of uncertainties should be included in these calculations because the physical and chemical characteristics of BC are not constant. Rather, they involve different source and emission conditions, as well as the size, mixing state and chemical composition of BC particles. Hence, a more sophisticated model should be used to evaluate BC dispersion and deposition.

2.3.5 Long-range transport

Cluster analysis. Backward trajectories can provide information about the transport patterns and potential sources of the observed aerosols [Draxler and Hess, 1998; Stohl *et al.*, 2006]. The ten-day backward trajectories were calculated every six hours using HYSPLIT_4 and meteorological data to investigate the effect of long-range transport. Here, the arrival elevation of 540 m a.s.l. was chosen for each trajectory calculation, which was the most representative arriving height [Huang *et al.*, 2010; Worthy *et al.*, 1994]. Cluster analysis was used to classify the trajectories into different groups. The results of trajectories and cluster analysis (Figure 2.6a) showed that Ny-Ålesund was impacted by three different atmospheric transport regimes during the study period. About 41% of air mass came from the Arctic Ocean, 31% originated from western Europe and 28% came from central Russia. Most of the air mass was confined to the north of 65°N , except the air mass from central Russia, which could originate from 60°N . This air mass could pass over settlement areas. The contribution of emissions from

Table 2.3 Atmospheric deposition fluxes of equivalent black carbon (EBC) in Ny-Ålesund, Svalbard, and Fairbanks, Alaska

Station	Location	Time period	Sources	Estimated atmospheric black carbon Flux ($\text{ng m}^{-2} \text{h}^{-1}$)				References
				Dry deposition flux	Wet deposition flux	Total deposition flux	Wet deposition (%)	
Ny-Ålesund Svalbard	11.60-12.06°E, 78.92-78.99°N, 13-134 m a.s.l	July, 2011	Local emissions	1.8-18	0.10-9.6	1.8-27	10-70%	This work
			Total (Local emissions + long-ranges transport)	4.3-32	2.1-12	6.4-44	22-44%	
Fairbanks Alaska	135-165°W, 65-75°N, 0.1-7.4 km a.s.l	April, 2008	Total	4.2-220	--	--	91%	[Spackman <i>et al.</i> , 2010]

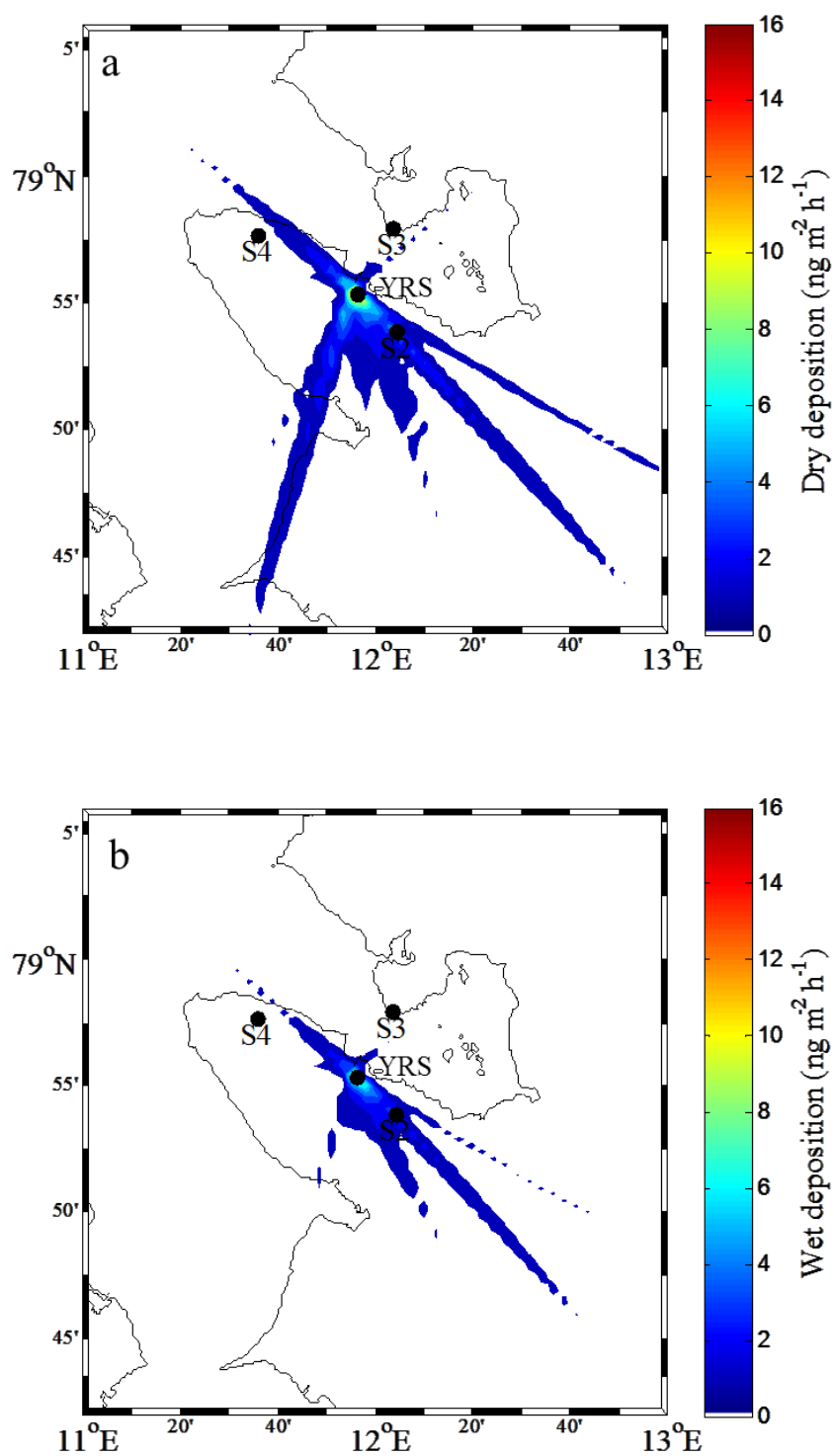


Figure 2.5 (a) Contour plot of dry deposition averaged over the entire experiment period and (b) wet deposition from local emissions.

these areas to Arctic BC not only depends on sources but also the processes that occur en route, such as precipitation. Therefore the potential precipitation along each route and the temporal variance of each pattern were combined to interpret the contribution from each sector.

Potential precipitation contribution. Removal during transport is also an important factor affecting the efficiency of pollution transportation. The analysis of the potential precipitation contribution function (PPCF) was used to link atmospheric transport regimes with precipitation, given the possibility that rainfall occurred during the passage of the plume. The PPCF values for the grid cells $PPCF_{ij}$ were the conditional probabilities that an air parcel passing through the ij -th grid cell was accompanied with precipitation and was defined as:

$$PPCF_{ij} = \frac{m_{ij}/N}{n_{ij}/N} = \frac{P[B_{ij}]}{P[A_{ij}]}, \quad (2.9)$$

where n_{ij} was the total number of end points that fall in the ij -th cell, and m_{ij} was the number of end points in the same cell that were associated with precipitation. $P(B_{ij})$ was probability of precipitation in the ij -th cell, and $P(A_{ij})$ was the probability of trajectories that pass over the ij -th cell. To reduce the effect of small values of n_{ij} , an arbitrary weight function $W(n_{ij})$ was applied to downweight the $PPCF_{ij}$ values. Here, the weight function $W(n_{ij})$, given by *Hopke et al.* [1995], was defined as:

$$W(n_{ij}) = \begin{cases} 1.0 & \text{if } n_{ij} \geq 4 \\ 0.75 & \text{if } n_{ij} = 3 \\ 0.50 & \text{if } n_{ij} = 2 \\ 0.25 & \text{if } n_{ij} = 1 \end{cases} \quad (2.10)$$

Combining the heights of transport pathway and PPCF distribution shown in Figure 2.6, indicated that air masses from western Europe experience less precipitation than air masses passing over central Russia. Western Europe was therefore a probable source for the BC ending up in Svalbard, since pollutants from central Russia were more likely to be washed out en route to the Arctic archipelago. Because of the precipitation, only pollutions originating in central Russia that existed at a higher atmospheric level were likely to be transported to the Arctic through free troposphere-level transport. However, there was no correlation with air mass back-trajectories and EBC concentrations, suggesting that the contribution of long-range transport might be not significant, while local emissions might be responsible for the elevated EBC observed at the Ny-Ålesund community.

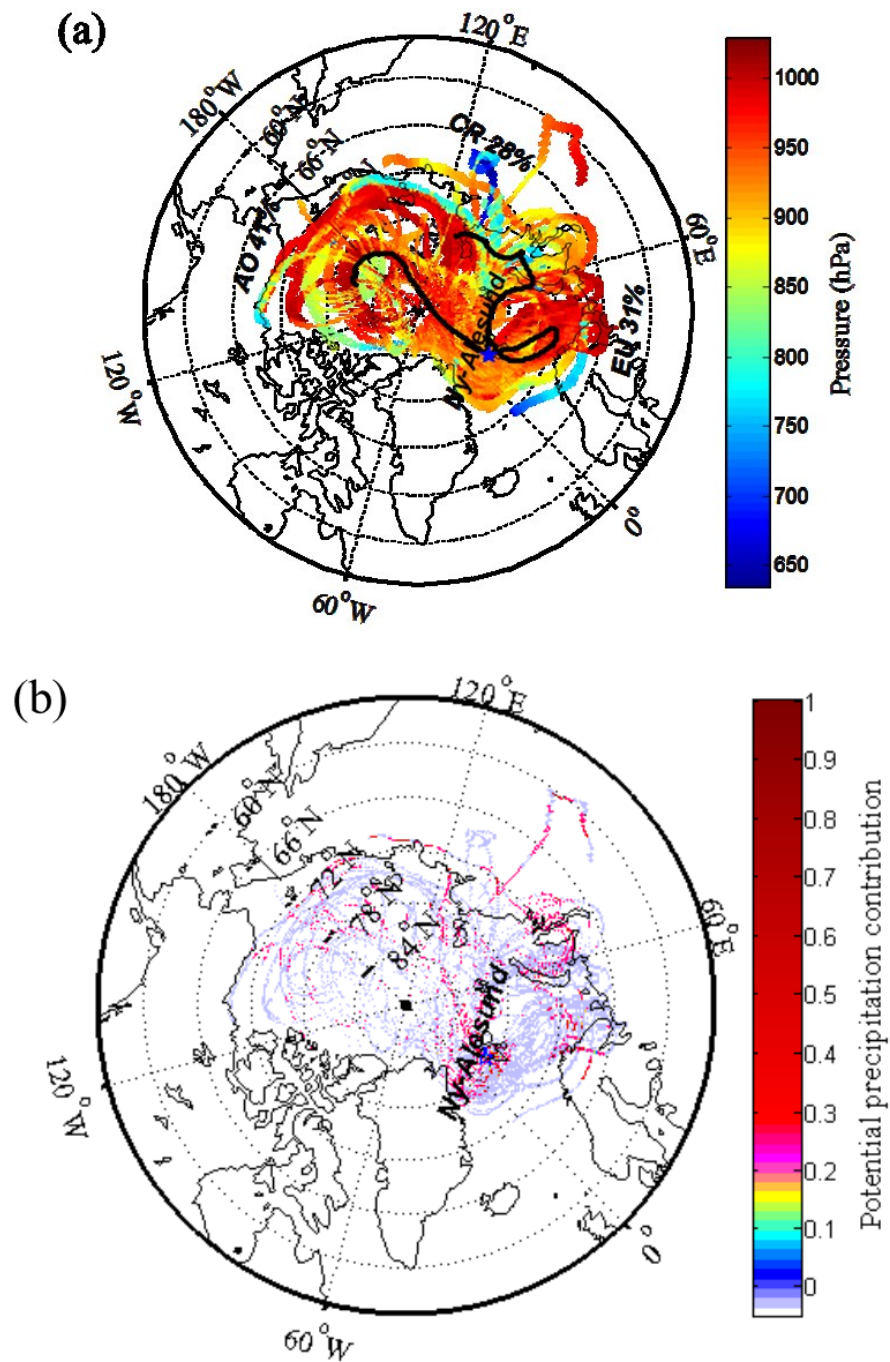


Figure 2.6 (a) Ten-day back trajectories were colored by air pressure and major transport pathways calculated by cluster analysis, labeled by identification of each cluster and frequency of occurrence. Both were generated by the HYSPLIT_4 model. AO represents the Arctic Ocean sector, EU stands for western Europe and CR stands for central Russia. (b) Map of potential precipitation contribution function probability.

2.4 Conclusions

Higher concentrations of EBC were observed within Ny-Ålesund compared with measurements outside the settlement and these were attributed to local emissions. It is estimated that about 60-70% of EBC in Ny-Ålesund was associated with local emissions, whereas emissions from outside the Arctic had less impact on local BC concentrations as a result of precipitation scavenging [Stohl *et al.*, 2006]. Additionally, meteorological parameters appear to be of minor importance and could only explain 19% the observed EBC variability.

The average emission rate at Ny-Ålesund was 8.1 g h^{-1} , equivalent to the BC emissions from about five light duty vehicles, or half the BC emissions from a bus, in constant operation. Our modeling results indicate that BC dry deposition from local emissions at Ny-Ålesund was $0.0\text{--}1.8 \text{ ng m}^{-2} \text{ h}^{-1}$, and wet deposition was 0.0 to $9.6 \text{ ng m}^{-2} \text{ h}^{-1}$ within 10 km. Dispersion and deposition patterns at Ny-Ålesund suggested that local emissions decreased to 20% within 10 km and plumes tended to affect the area to the south of the settlement.

Overall, the limited data from this study suggested that local emissions made a major contribution to EBC concentrations at Ny-Ålesund within 10 km. Even though Zeppelin Station is located 474 m a.s.l., it is still influenced by ship emissions during summer [Eckhardt *et al.*, 2013]. Researchers aiming to study pristine environments in the Arctic should consider the effects of these local emissions on air quality.

Acknowledgements

This work was funded by the National Natural Science Foundation of China (grant no. 41105094) and the Scientific Research Foundation of Third Institute of Oceanography, State Oceanic Administration of China (grant no. 2011004). The Chinese Arctic and Antarctic Administration of State Oceanic Administration supported field accommodations at YRS. The authors thanks W. Li for technical assistance and L. Chen for encouragement. The authors are also grateful for a full-time graduate assistantship provided by Rutgers University that supported the continuation and completion of this research. We gratefully acknowledge the US National Oceanic and Atmospheric Administration's Air Resources Laboratory for providing the HYSPLIT transport and dispersion model, and ECMWF and NCAR/NCEP for providing the meteorological data freely. We thank Elisabeth Bjerke Råstad at Kings Bay AS for supplying the harbor log. We thank the two reviewers for their valuable comments on this manuscript.

Chapter 3: Effects of ship emissions on summertime aerosols at Ny-Ålesund in the Arctic¹

Abstract

Selected trace elements, ionic species and organic/elemental carbon in aerosols were measured in summer at Ny-Ålesund in the Arctic, and an interpreted approach combining elemental ratios, back-trajectories and enrichment factors was used to assess the sources of aerosols observed at this location. Aerosol samples influenced by ship emissions were featured by elevated concentrations of non-crustal (nc) vanadium (V), nc-nickel (nc-Ni), non-sea salt (nss) sulfate (SO_4^{2-}) and ratios of nc-Ni/nc-V (1.7) and nss- SO_4^{2-} /nc-V (200). When two cruise ships with more than 1500 passengers visited Ny-Ålesund in July 2012, the total suspended particulate (TSP) mass reached 2290 ng m^{-3} , almost three times the median TSP concentration (609 ng m^{-3}) measured during the study period. The nc-V concentration reached 0.976 ng m^{-3} , about 38-fold higher compared to the median value of the sampling period, and this value was even higher than the annual mean value observed at the Zeppelin station and the values measured during Haze events at North American Arctic and Norwegian Arctic. The concentrations of nc-Ni and nss- SO_4^{2-} were 0.572 ng m^{-3} and 203 ng m^{-3} , which were 8-fold and 2-fold higher than the median values of the sampling period. While in the few-ship periods, defined as the period with none or only one cruise ship with less than 1000 passengers being present, aerosols at this location could be affected by a mixed impact of local emissions and long range transport, reflected by the nc-Mn/nc-V ratios and element enrichment factors often

¹ **Zhan, J.**, Gao, Y., Li, W., Chen, L., Lin, H., and Lin, Q., 2014. Effects of ship emissions on summertime aerosols at Ny-Ålesund in the Arctic. *Atmospheric Pollution Research*, in press.

found in the air masses from the North American Arctic, Iceland and North Eurasia. Results from this study suggested that cruise ship emissions contributed significantly to atmospheric particulate matter at Ny-Ålesund in the summer, effecting air quality in this area.

Keywords: Trace elements, nc-Ni/nc-V ratio, Ship emissions, Arctic Aerosols

3.1 Introduction

The Arctic is a fragile ecology and climate system, sensitive to external perturbations. Even small fluctuations, such as changes in aerosols by transported air pollutants from mid-latitudes and emissions within the Arctic, can have a profound impact on environmental changes in the region [AMAP, 2011]. Black carbon from ship emissions has been suggested to play a significant role in the observed Arctic warming, ~20% of the warming and snow-ice cover loss was due to the black carbon albedo effect [Bond *et al.*, 2013]. The Arctic atmosphere in summer is of particular interest as there are relatively low particle number concentrations in the air. Long-range transport of aerosols is limited during the summer compared with winter, as the Arctic front is weak and moves further north [Law and Stohl, 2007] and scavenging of aerosols by clouds and precipitation is high in the summer [Bourgeois and Bey, 2011]. As a result, local aerosol sources have become more important in the summer. During the past decade, human activities including aviation, shipping, oil and gas flaring and resource exploitation have increased in the summer [Vestreng *et al.*, 2009], affecting the Arctic climate through altering snow/ice albedo [Bond *et al.*, 2013] and the formation of cloud condensation nuclei [Jouan *et al.*, 2014].

It has been found that marine shipping has a significant influence on particulate matter concentrations in the Arctic [Eckhardt *et al.*, 2013]. Ship emissions contribute about 30–40% of the total PM_{2.5} and 10% of the PM₁₀ concentrations during tourist seasons in the port cities in the Gulf of Alaska [Mölders *et al.*, 2010], and marine shipping in the Arctic may increase with the retreat of Arctic sea ice [Corbett *et al.*, 2010]. The shipping emissions in the Arctic may increase black carbon by 50% in 2030 and increase ozone by 10% in the Arctic lower troposphere [Dalsøren *et al.*, 2013]. The consequence of these impacts on air quality in the Arctic has not been well studied.

Ny-Ålesund is one of the most northern communities in the world. A number of studies conducted during the summer have investigated the sources of aerosols in the Arctic. In the 1980s, elevated anthropogenic aerosols were observed during the summer months due to long-range transport from the former Soviet Union and Europe [Barrie and Barrie, 1990; Maenhaut and Cornille, 1989; Pacyna and Ottar, 1985]. However, the long-range transport of pollutants from Eurasia significantly declined since early 1990's; therefore aerosol concentrations affected by this process has declined as well [Weinbruch *et al.*, 2012]. Local sources (e.g., transportation, electric power production, coal mining and coal burning) have been proposed as potential contributors to the regional pollution [Anderson *et al.*, 1992; Geng *et al.*, 2010; Ottar *et al.*, 1986]. Ship increased in the last 10 years in Svalbard, and Ny-Ålesund accounted for 15% of all Svalbard ship landings [Hagen *et al.*, 2012]. Given the fact that a large number of ships visited Ny-Ålesund during the summer months, ship

emissions may contribute to particulate matter in the air and affect the regional aerosol chemical composition [Eckhardt *et al.*, 2013; Weinbruch *et al.*, 2012]. More recent work has recognized marine shipping in Ny-Ålesund [Eckhardt *et al.*, 2013]. In the year 2007, ship emissions were responsible for 90% of the total nitrogen oxides (NO_x) and 93% of the black carbon in the Svalbard archipelago [Vestreng *et al.*, 2009]. Eleftheriadis *et al.* [2009] suggested that 0.2% of the measured equivalent black carbon concentrations at Zeppelin station could probably be attributed to ship emissions. Soot was observed when cruise ships visited Ny-Ålesund [Weinbruch *et al.*, 2012]. Eckhardt *et al.* [2013] suggested that equivalent black carbon and 60 nm particles increased 45% and 72%, respectively, when cruise ships with more than 50 passengers were present at Ny-Ålesund. To date, few work focus on the impact of ship emissions on the chemical composition of aerosols.

In this study, we use non-crust vanadium (nc-V), nc-nickel (Ni) and non-sea salt (nss) sulfate (SO₄²⁻) in aerosols as chemical tracers to evaluate the impact of ship emissions on aerosol concentrations at Ny-Ålesund in the summer. In addition, the features of aerosol concentrations observed during the few-ship periods, defined as the period with none or only one cruise ship with less than 1000 passengers being present, were interpreted by employing the ratios of nc-V/nc-Mn, backward trajectories and enrichment factors of trace elements in aerosols at Ny-Ålesund in the summer.

3.2 Methods

3.2.1 Sampling site

Sampling of aerosols was carried out in July 2012 at the Chinese Arctic “Yellow River Station” (YRS) (78.92° N, 11.93° E, 13 m above sea level (a.s.l)) in the settlement of Ny-Ålesund, in the Svalbard Archipelago (Figure 3.1). Ny-Ålesund is a research community with up to 150 people living there in the summer, while only around 15 permanent residents are there during winter months. Pollution sources in and around Ny-Ålesund include power stations, cars, airplanes and water traffic, including small vessels and large cruise ships.

3.2.2 Meteorological conditions

The sounding profile shows that the height of boundary layer over this area was ~1 000 meters (Figure 3.2), consistent with the results derived from the Micro Pulse Lidar [Engvall *et al.*, 2008]. As hills around the station are from 400 to 1431m a.s.l., a lower starting point for trajectories could affect the accuracy of the calculations, and thus the height at 1000 m a.s.l. was chosen as the arrival elevation for each trajectory calculation. On the other hand, as shown in Figure 3.3 during the sampling period, the lower-than-average pressure over the Arctic and stronger-than-average high pressures over Greenland existed in July 2012. This pattern increased in Greenland Blocking and enhanced southward meridional winds across the Arctic, resulting in the north-west prevailing winds over Ny-Ålesund that brought in the influences from the direction of the open Arctic Ocean (Figure 3.3b and 3.3c). This feature was also reflected by a north-west sector in the wind fields at the sampling location, although there was a stronger sector of southeast winds from glacier areas due to the

topographic effects (Figure 3.4). As air masses that arrived at the 1000 m a.s.l could quickly mix with the surface air in this area [Ström *et al.*, 2009], the 96-hour samples collected at the surface could contain a mixture of both local and regional air.

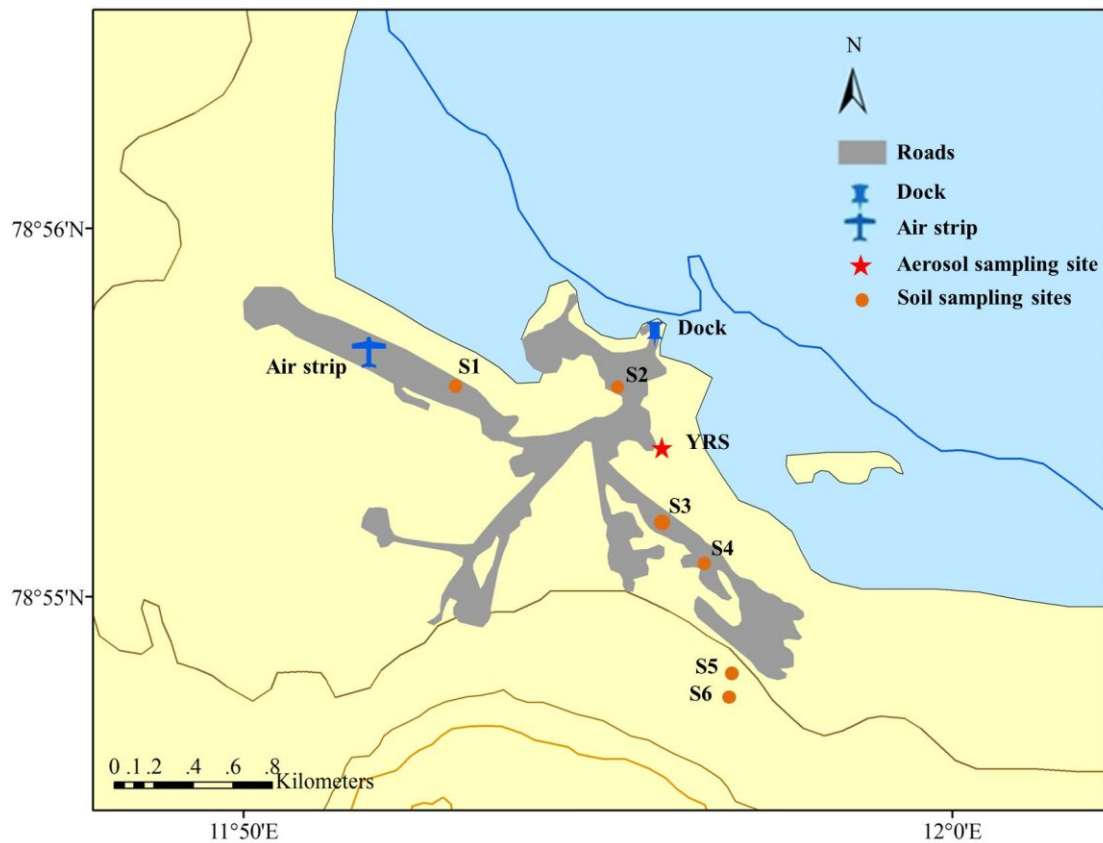


Figure 3.1 Aerosol sampling site (Yellow River Station) and soil sampling sites (S1-S5) at Ny-Ålesund.

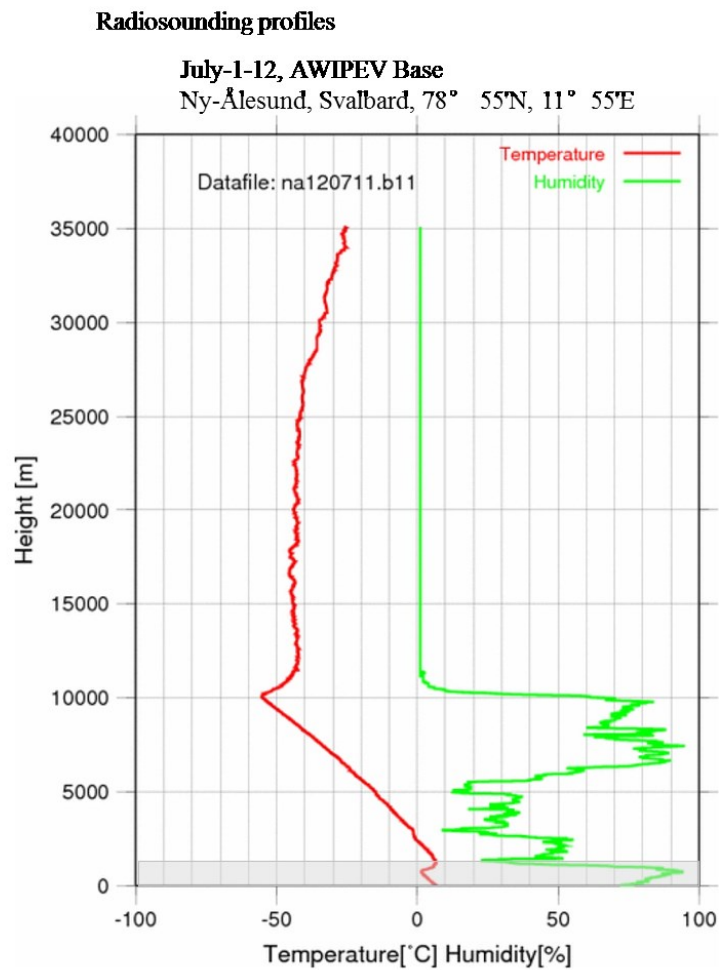


Figure 3.2 The profiles of temperature and humidity at Ny-Ålesund in July 1, 2012, based on the Radiosounding data provide by The German Alfred Wegener Institute for Polar and Marine Research (AWI) and the French Polar Institute Paul Emile Victor (IPEV).

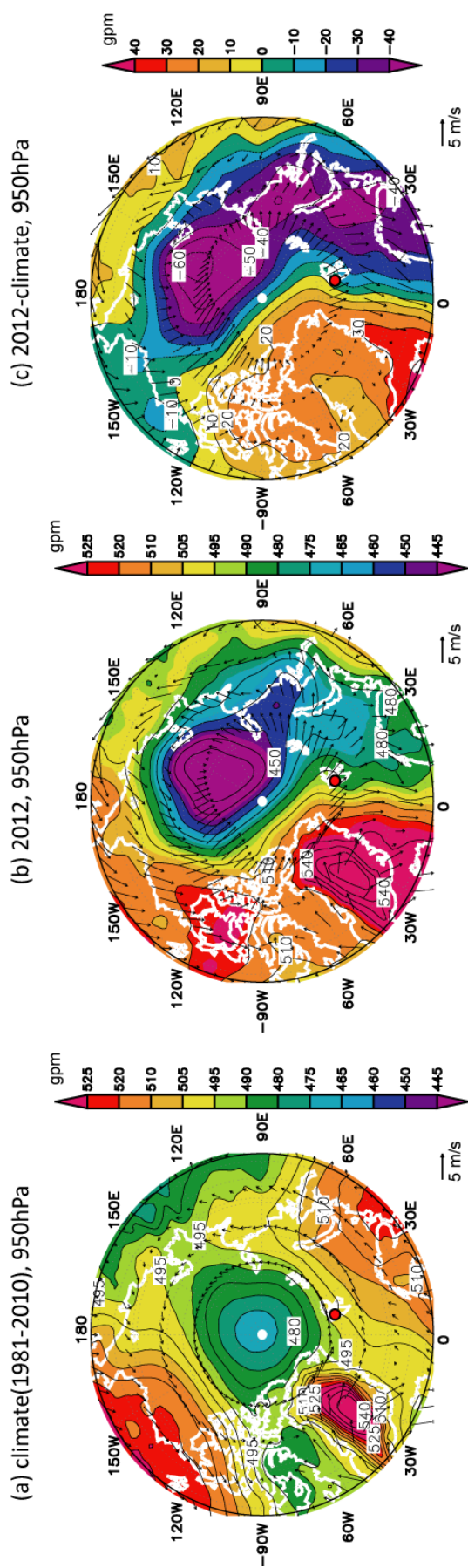


Figure 3.3 Geopotential heights (shaded colors and contour lines) and wind fields (vectors) at 950hPa based on the data from the European center for medium range weather forecasts (ECMWF) reanalysis project. (a) The averages of fields at 950 hPa in July 4-22 from 1981 to 2010, (b) the averages of fields at 950 hPa in July 4-22, 2012, and (c) the anomalies of fields in 2012 to the climate averages in 1981-2010. The unit is gpm for geopotential heights and m s^{-1} for winds. The contour line intervals are 5 gpm for both (a) and (b) and 10 gpm for (c). The red circle marks the location of this study at Ny-Ålesund.

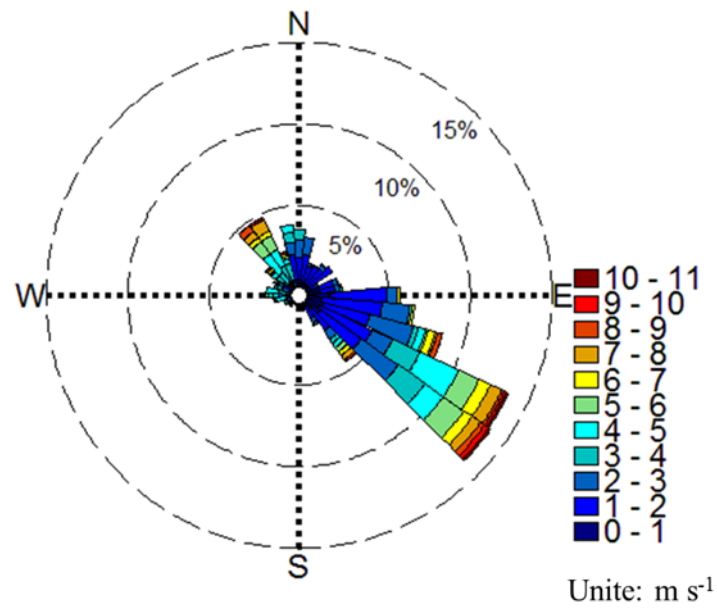


Figure 3.4 The wind rose plot for the entire experiment period (July 4-22, 2012) at Ny-Ålesund. Individual wind direction measurements were accumulated and the relative frequency is shown as a percentage. Wind speed (m s^{-1}) is expressed by different color bars.

3.2.3 Back trajectory analysis

Ten-day backward trajectories were computed by the Hybrid Single-Particle Lagrangian Integrated Trajectory Model 4 [Draxier and Hess, 1998] to trace the air history. The National Centers for Environmental Prediction (NCEP)-National Center for Atmospheric Research (NCAR) reanalysis meteorological data was fed into the model. The data showed a horizontal resolution of 2.5×2.5 degrees, 17 vertical levels up to 10hPa, and a temporal resolution of six-hour. To evaluate the relative contributions of air from different origins, cluster analysis was used to classify trajectories into different groups. The percentage of air masses from each group for each sample was calculated and listed in Table 3.1.

Table 3.1 Sampling data and time, meteorological data^b, origin of air masses arriving at Ny-Ålesund and nc-Mn/hc-V in July 2012

No. ^a	Sample Time	Temperature [°C]	Relative humidity [%]	Wind speed [m s ⁻¹]	Wind direction [°]	Pressure [hPa]	nc-Mn/ nc-V	Air mass back-trajectory ^c
1	07/04-07/07	6.5 (5.2–8.1)	76 (57–93)	2.3 (0.0–6.2)	139 (1–356)	1 008.9 (1 005.4–1 017.2)	0.2	Iceland (72%), Norwegian Sea-Barents Sea (28%)
2	07/07-07/10	5.6 (3.8–7.1)	77 (60–90)	3.4 (0.0–11)	169 (2–359)	1 018.0 (1 001.8–1 024.0)	1.01	Arctic Ocean (75%), Norwegian Sea-Barents Sea (25%)
3	07/10-07/13	5.9 (3.1–8.8)	72 (50–90)	4.7 (0.7–9.4)	214 (0–357)	1 005.9 (1 001.2–1 010.9)	1.07	Arctic Ocean (75%), Norwegian Sea-Barents Sea (25%)
4	07/13-07/16	5.9 (3.1–7.9)	76 (60–90)	3.1 (0.0–8.7)	159 (6–349)	1 009.0 (1 004.5–1 012.4)	0.31	North Russia-Laptev Sea-Arctic Ocean (75%), Norwegian Sea-Barents Sea (25%)
5	07/16-07/19	6.1 (4.4–9.1)	78 (66–86)	2.4 (0.5–7.5)	124 (1–354)	1008.8 (1 004.7–1 011.1)	0.12	Yamal Peninsula-Kara Sea-Barents Sea (100%)
6	07/19-07/22	6.0 (3.1–9.1)	75 (50–93)	3.5 (0.2–8.2)	151 (20–354)	1006.1 (1 002.9–1 010.3)	0.55	Kara Sea-Barents Sea-Yamal Peninsula (100%)

^a Chemcomb cartridges and KC-6120 collected samples parallelly.

^b Meteorological parameters were reported in the form of mean (minimum–maximum).

^c Ten days back-trajectories (HYSPLIT; Draxler and Hess, 1998; arrival height 1 000m a.s.l.).

3.2.4 Sample collection

Air Samplers were installed on the roof of the YRS building, 20 m above the ground. A Chemcomb (C) cartridge (Model 3500; Thermo Scientific, Waltham, MA, USA) was used to collect total suspended particles (TSP) operated at a flow rate of 16.7 L min^{-1} and with a sampling duration of three days, following the procedures in *Gao et al.* [2013]. Teflon filters (47mm diameter, $1.0 \mu\text{m}$ pore size; Pall Corp., Port Washington, NY, USA) were used as sampling media for the determination of trace elements, anions and cations in aerosols. A model KC-6120 comprehensive atmospheric sampler (Laoshan Electronic Instrument Factory, Qingdao, China) with a flow rate of 96 L min^{-1} was used to collect TSP for the analysis of elemental carbon (EC) and organic carbon (OC), with quartz fiber filters (MK 360; 90 mm diameter, $0.3 \mu\text{m}$ pore size; Munktell Corp., Falun, Sweden) being used as the sampling media. These quartz fiber filters were pre-fired at 550°C in a muffle furnace for 12 hours before sampling, and after then they were wrapped in aluminum foils and stored at 4°C until laboratory analysis. All filter handling was carried out in a 100-class laminar flow clean hood in the laboratory of the YRS. After sampling, each sample filter was put into a pre-cleaned petri dish, sealed in a plastic bag, and stored at 4°C until analysis. A total of 12 samples were collected (six samples on Teflon filters and six on quartz fiber filters). Soil samples were collected in small polyethylene bags around Ny-Ålesund (Figure 3.1). After collection, samples were freeze-dried and then stored in small bags in a desiccator before analysis. A total of 6 soil samples were collected.

3.2.5 Sample analysis

Water-soluble ionic species (sodium (Na^+), nitrate (NO_3^-) and SO_4^{2-}) in aerosols were analyzed by ion chromatography (IC) using a Dionex ICS-90A with RFC-30 at the Third Institute of Oceanography, State Oceanic Administration, China, following the procedures by *Zhao and Gao* [2008] and *Xu et al.* [2013]. Half of each Teflon sample filter was extracted with 25 mL Milli-Q water ($18.2 \text{ M}\Omega\text{cm}^{-1}$; Milli-Q Academic System; Millipore Corporation, Billerica, MA, USA) in an ultrasonic bath for 40 minutes and leached overnight. The extracted solution was then filtered through a PTFE syringe filter ($0.45\mu\text{m}$ pore size; Fisherbrand, Fisher Scientific, Fair Lawn, NJ, USA) and injected into the IC system via an automated sampler (AS40; Dionex) using 5.0 mL vials. A CS12A analytical column ($4\times 250 \text{ mm}^2$; Dionex), a methanesulfonic acid eluent generator cartridge (EGC II MSA; Dionex), a conductivity detector, and a 25 μL sample loop, were used to determine the concentrations of Na^+ in aerosol samples. The concentrations of NO_3^- and SO_4^{2-} in aerosol samples were determined by an AS18 analytical column, an AG18 guard column ($4\times 250 \text{ mm}^2$; Dionex), a Potassium Hydroxide (KOH) eluent generator cartridge (EGC II KOH; Dionex), a conductivity detector, and a 25 μL sample loop. National institute of Standards and Technology (NIST) traceable calibration standards were run prior to and during sample analyses. The method detection limits for Na^+ , NO_3^- and SO_4^{2-} were 20, 3 and $7\mu\text{g L}^{-1}$, respectively. The overall precision of the method was $< 5\%$. Final concentrations of these species in aerosols were corrected by their field blanks.

The other half of each Teflon sample filter was analyzed by an Inductively Coupled Plasma Mass Spectrometer (ICPMS, Model 7500ce; Agilent) at the Third Institute of

Oceanography, State Oceanic Administration in China to determine the concentrations of selected trace elements in aerosols (sodium (Na), magnesium (Mg), Aluminum(Al), potassium(K), calcium(Ca), vanadium(V), chromium (Cr), manganese (Mn), iron (Fe), cobalt (Co), nickel(Ni), copper (Cu), zinc (Zn), arsenic (As),selenium (Se),cadmium (Cd), barium(Ba), and lead (Pb)) following the procedures similar to those in *Xia and Gao* [2010]. Briefly, one half of each Teflon sample filter was digested with concentrated HNO_3 (Optima A460-500, Fisher Scientific) in a Microwave Accelerated Reaction System (MARs, CEM Corporation). There were three digestion steps: (1) heating to $170 \pm 5^\circ\text{C}$ in 5.5 minutes, (2) remaining at $170 \pm 5^\circ\text{C}$ for 30 minutes, and then (3) cooling down for 20 minutes to room temperature. Then digested solutions were diluted with Milli-Q water to 15 mL and injected to the ICPMS system. The detection limits for all trace elements analyzed in this study were less than 1ppt and the precision of the method was 2%. The digestion recoveries of the elements ranged from 91% to 104%, and overall average levels of field blanks were 2–4 times lower than the sample values. Final concentrations of the elements in samples were corrected by the field blanks.

Soil samples were dried, grounded and passed through a 100 mesh sieve. These soil samples (approximately 0.5gram each) were weighed directly into 100-mL pre-cleaned Pyrex test tubes. 7.5 mL of 10 M concentrated hydrochloric acid (HCl) and 2.5 mL of 10 M concentrated nitric acid (HNO_3) were added to each sample tube. The mixture was heated to $120\text{--}130^\circ\text{C}$ for 14–16 hours and was then added with 5mL of HClO_4 , and kept heating until dry and residue color becoming white. If the residue color was dark, another 5mL of HClO_4 was added and the sample was re-heated until

residue was white. Following digestion, the mixture was cooled and transferred into 100 mL volumetric flask. Each solution was diluted with Milli-Q water to 100 mL and was analyzed by an Inductively Coupled Plasma-Optical Emission Spectrometer (ICP-OES, Optima 7000DV; Perkin Elmer, Shelton, USA) at the Institute of Urban Environment, Chinese Academy of Sciences in China, to determine the concentrations of selected trace elements following the *DIN EN ISO 11885 protocol [1998]*. A certified reference material from China National Center for Standard Materials (GBW-07407) was digested and analyzed in the same way as samples were treated. The precision of the method was 2%. The digestion recoveries of the selected elements in the reference material ranged from 90% to 115%.

The concentrations of EC and OC in aerosols were determined using a thermal-optical transmittance carbon analyzer (Sunset Laboratory Inc., Portland, OR, USA). The details of the OC and EC analyses were as described in the *NIOSH protocol [1999]*. The uncertainties associated with the EC and OC measurements were 10%.

To obtain the total aerosol gravimetric mass, Teflon filters were weighed before and after sampling under the same controlled temperature ($20^{\circ}\text{C} \pm 2$) and humidity ($35\% \pm 2$) conditions, using a microbalance (Model XP6/52, Mettler Toledo) at the Third Institute of Oceanography, State Oceanic Administration in China. The total aerosol mass collected on each filter was calculated by the difference between the pre-sampling and after-sampling weights of the filter. Detailed information on aerosol data is provided in Table 3.2 and soil data is showed in Table 3.3.

3.2.6 Data analysis

To identify source regions and evaluate the degree of anthropogenic influence, crustal enrichment factors (EFs) were calculated as follows:

$$(EF_X)_{\text{crust}} = (C_X / C_R)_{\text{aerosol}} / (C_X / C_R)_{\text{crust}} \quad (3.1)$$

where X represents the element of interest; EF_X is the enrichment factor of X; C_X is where X represents the element of interest; EF_X is the enrichment factor of X; C_X is the concentration of X; and C_R is the concentration of a crustal reference element. The aerosol and crust subscripts refer to elements in an aerosol sample and crustal material, respectively. Al was selected as a crustal reference element. The average abundance of chemical elements in the Ny-Ålesund soil was used to calculate EFs (Table 3.3).

Elemental ratios derived from the soil data in this study and those from the table in *Taylor* [1964] were relatively comparable for most elements examined in this study (Figure 3.5). The EF values of less than five were operationally considered as indication of crustal origin, whereas the values higher than five suggested a non-crustal source.

Table 3.2 Chemical concentrations and ratios in aerosols during cruise ships present and during few-cruise ships present in Ny-Ålesund in July, 2012

Substance	Few/no-ships		Cruise ships	Ratio	Zeppelin	Ratio
	Max.	Min.		$C_{\text{ship}}/C_{\text{median}}$	Annual Average	$C_{\text{ship}}/C_{\text{zeppelin}}$
	ng m ⁻³				ng m ⁻³	
Na	7.36×10^1	8.72×10^0	2.08×10^2	3.0		
Mg	3.49×10^1	2.94×10^0	9.06×10^1	8.0		
Al	3.33×10^1	6.52×10^0	5.27×10^1	5.0		
K	9.85×10^0	1.85×10^0	2.85×10^1	5.0		
Ca	5.22×10^1	9.05×10^0	1.79×10^2	10.0		
V	8.70×10^{-2}	1.68×10^{-2}	1.04×10^0	28.0	0.07–0.20	5.2–14.8
Cr	1.89×10^{-1}	1.13×10^{-2}	7.42×10^{-2}	1.0	0.04–0.9	0.1–1.9
Mn	4.43×10^{-1}	7.95×10^{-2}	1.16×10^0	9.0	0.24–0.57	2.0–4.8
Fe	3.10×10^1	1.39×10^0	6.42×10^1	7.0		
Co	2.68×10^{-2}	1.08×10^{-3}	5.08×10^{-2}	5.0	0.055–0.14	0.4–0.9
Ni	1.77×10^{-1}	2.58×10^{-2}	5.92×10^{-1}	8.0	0.07–0.19	3.1–8.5
Cu	3.48×10^{-1}	4.45×10^{-2}	2.64×10^{-1}	1.0	0.25–0.41	0.6–1.1
Zn	9.03×10^{-1}	2.53×10^{-1}	8.88×10^{-1}	1.0	1.2–1.9	0.5–0.7
As	7.38×10^{-3}	1.14×10^{-3}	2.21×10^{-2}	4.0		
Se	7.52×10^{-2}	1.24×10^{-3}	1.11×10^{-1}	2.0		
Cd	1.21×10^{-2}	0.00×10^0	3.67×10^{-3}	1.0	0.01–0.03	0.1–0.4
Ba	1.18×10^{-1}	0.00×10^0	1.77×10^{-1}	2.0		
Pb	3.21×10^{-1}	1.10×10^{-2}	1.36×10^0	42.0	0.48–0.83	1.6–2.8
TSP	1.06×10^3	3.30×10^2	2.29×10^3	4.0		
nc-V	4.96×10^{-2}	4.31×10^{-3}	9.76×10^{-1}	39.0		
nc-Ni	1.73×10^{-1}	3.81×10^{-3}	5.72×10^{-1}	10.0		
nc-Mn	5.02×10^{-2}	2.71×10^{-3}	5.35×10^{-1}	119.0		
nss-SO ₄ ²⁻	1.08×10^2	5.07×10^1	2.03×10^2	3.0		
NO ₃ ⁻	8.42×10^1	1.41×10^1	4.59×10^1	1.0		
OC	5.42×10^1	1.66×10^1	7.73×10^1	2.0		
EC	4.64×10^0	0.00×10^0	2.76×10^0	2.0		
PAX*	4.77×10^3	4.41×10^2	6.02×10^3	3.0		
EC/OC	2.80×10^{-1}	0.00×10^0	3.57×10^{-2}	1.0		

nc-V/ nc-Ni	9.62×10^0	2.49×10^{-2}	1.70×10^0	3.0
nss-SO ₄ ²⁻ / nc-V	1.18×10^4	2.08×10^2	2.08×10^2	0.0

* PAX: the number of ship passengers; n.a.: lower than detection limit.

** Annual mean concentrations at the Zeppelin Station [*Berg et al.*, 2004].

C_{ship}/C_{median}: chemical concentrations measured during cruise ships present over median concentration of the sampling period.

*** C_{ship}/C_{zeppelin}: chemical concentrations during cruise ships present over annual mean concentration of elements at the Zeppelin Station.

Table 3.3 Element concentrations in soils at Ny-Ålesund (mg kg⁻¹)

Elements	Max.	Min	Average	LOD*
Na	1.16×10^3	3.46×10^2	7.28×10^2	8.75×10^{-1}
Mg	9.46×10^3	7.99×10^2	3.43×10^3	3.00×10^{-2}
Al	2.75×10^4	1.26×10^4	2.09×10^4	4.50×10^{-2}
K	8.60×10^3	3.64×10^3	6.01×10^3	1.00×10^{-2}
Ca	2.61×10^4	4.72×10^2	6.61×10^3	1.00×10^{-2}
V	4.67×10^1	3.43×10^0	2.35×10^1	1.00×10^{-2}
Cr	9.12×10^1	3.42×10^1	5.10×10^1	6.10×10^{-3}
Mn	4.19×10^2	7.74×10^1	2.47×10^2	1.60×10^{-3}
Fe	2.94×10^4	9.16×10^3	1.99×10^4	5.10×10^{-3}
Co	7.34×10^0	1.13×10^0	5.10×10^0	6.00×10^{-3}
Ni	1.31×10^1	2.10×10^0	7.69×10^0	1.00×10^{-2}
Cu	2.04×10^1	1.04×10^1	1.70×10^1	5.40×10^{-3}
Zn	1.36×10^2	7.13×10^1	1.15×10^2	1.80×10^{-3}
As	6.89×10^0	1.54×10^0	3.82×10^0	4.00×10^{-3}
Se	1.23×10^0	4.67×10^{-1}	8.03×10^{-1}	5.40×10^{-3}
Cd	2.08×10^{-1}	1.66×10^{-2}	1.12×10^{-1}	4.60×10^{-3}
Ba	1.46×10^2	8.00×10^1	1.10×10^2	1.30×10^{-3}
Pb	5.91×10^1	1.28×10^1	3.57×10^1	9.00×10^{-2}

* LOD: limit of detection

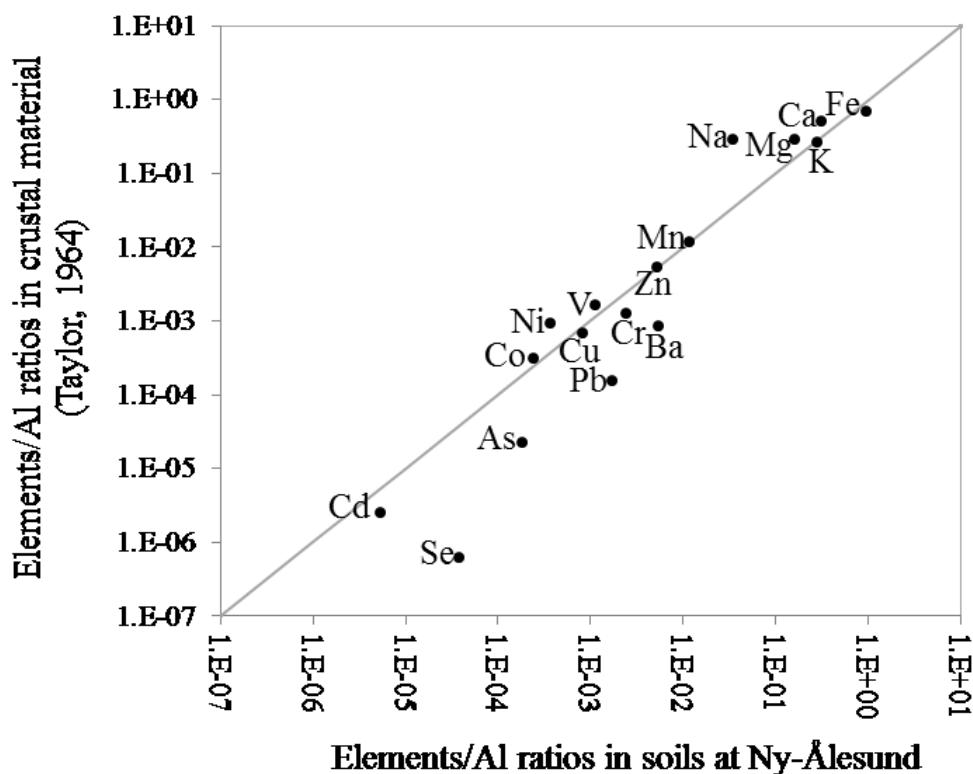


Figure 3.5 Correlation of elemental composition between soils at Ny-Ålesund and crustal materials in Taylor (1964).

The concentrations of crustal V, Ni and Mn in aerosols were calculated from the mass ratios of these elements to Al in the soil samples. The nc-V, nc-Ni, and nc-Mn were obtained by subtracting crustal V, Ni and Mn from the total V, Ni and Mn in aerosols. The concentrations of sea salt (ss)- SO_4^{2-} in aerosols were calculated from the measured Na^+ concentrations in the air and the $\text{SO}_4^{2-}/\text{Na}^+$ mass ratio for seawater of 0.252 [Millero, 2013]. The nss- SO_4^{2-} concentration was obtained by subtracting ss- SO_4^{2-} from the total SO_4^{2-} . The chemical reconstructed mass was estimated following the procedures of Malm *et al.* [2007]. Sulfate and nitrate were assumed to

be in the form of ammonium sulfate and ammonium nitrate. The organic matter (OM) was estimated from OC by assuming conversion factor (1.8) of OC to OM [*Malm et al.*, 2007]. Sea salt aerosol was estimated by multiplying sodium with a factor of 1.8, the ratio of sodium to sodium chloride in seawater [*Millero*, 2013]. Soil was estimated by sums of typical oxides of elements associated with soil (Al_2O_3 , SiO_2 , CaO , K_2O , FeO , Fe_2O_3 , TiO_2). Soil K was estimated from Fe multiplied by a factor of 0.30, a ratio of K/Fe in soil in Ny-Ålesund measured by this study. Nonsoil-K was obtained from the total K minus soil K. The formulas used in the calculation are summarized in Table 3.4.

Table 3.4 Major chemical species in aerosols derived from calculations.

Aerosol species	Calculated
Reconstructed aerosol mass	
Soil	$[\text{Soil}] = 2.20[\text{Al}] + 2.49[\text{Si}] + 1.63 [\text{Ca}] + 2.42[\text{Fe}] + 1.94 [\text{Ti}]$
Silica = Si	$[\text{Si}] = 2.93[\text{Al}]$
Soil potassium = Soil_K	$[\text{Soil_K}] = 0.30 [\text{Fe}]$
Non-soil potassium = nonsoil_K	$[\text{nonsoil_K}] = [\text{K}] - [\text{Soil_K}]$
Ammonium sulfate = $(\text{NH}_4)_2\text{SO}_4$	$[(\text{NH}_4)_2\text{SO}_4] = 1.375[\text{SO}_4^{2-}]$
Ammonium nitrate = NH_4NO_3	$[\text{NH}_4\text{NO}_3] = 1.29[\text{NO}_3^-]$
Organic matter (OM)	$[\text{OM}] = 1.8[\text{OC}]$
Sodium chloride (NaCl)	$[\text{NaCl}] = 2.5[\text{Na}]$
Reconstructed aerosol mass ^d = $\text{Mass}_{\text{recon}}$	$[\text{Mass}_{\text{recon}}] = [\text{Soil}] + [\text{NaCl}] + 1.375[\text{SO}_4^{2-}] + 1.29[\text{NO}_3^-] + [\text{OM}] + [\text{EC}] + 1.2[\text{nonsoil_K}]$
Ionic species and Elements	
non sea salt $\text{SO}_4^{2-} = \text{nss-SO}_4^{2-}$	$[\text{nss-SO}_4^{2-}] = [\text{SO}_4^{2-}]_{\text{total}} - [\text{Na}^+] \times 0.252$
non crust V = nc-V	$[\text{nc-V}] = [\text{V}] - ([\text{V}]/[\text{Al}])_{\text{crust}} \times [\text{Al}]_{\text{aerosol}}$
non crust Ni = nc-Ni	$[\text{nc-Ni}] = [\text{Ni}] - ([\text{Ni}]/[\text{Al}])_{\text{crust}} \times [\text{Al}]_{\text{aerosol}}$
non crust Mn = nc-Mn	$[\text{nc-Mn}] = [\text{Mn}] - ([\text{Mn}]/[\text{Al}])_{\text{crust}} \times [\text{Al}]_{\text{aerosol}}$

3.3 Results and discussion

3.3.1 Composition of total Aerosol mass

The mass concentrations of TSP observed at this site ranged from 330 to 2 290 ng m^{-3} , with a median concentration of 609 ng m^{-3} . These values were in the range of those previously found over the Arctic Ocean (from 0.10 to 3.8 $\mu\text{g m}^{-3}$) [*Leck and Persson, 1996b*].

The nss-SO_4^{2-} concentrations in aerosols observed at this location during this study ranged from 50.6 to 203 ng m^{-3} , with a mean of 96.5 ng m^{-3} . There could be multiple sources for nss-SO_4^{2-} observed in the Arctic marine atmosphere [*Leck and Persson, 1996a*]. The major anthropogenic contributions to nss-SO_4^{2-} included ship emissions around the Arctic Ocean [*AMAP, 2006*] and fossil fuel combustion in distant regions (such as Eurasia and North America) that affected the Arctic mainly in winter and spring through long-range transport [*Norman et al., 1999*]. In addition to volcanic emissions [*AMAP, 2006*], the dominant natural source for nss-SO_4^{2-} in the Arctic air is the oxidation of dimethylsulfide (DMS) from marine phytoplankton in sea water [*Leck and Persson, 1996a*]. In summer, regional marine biological sources contribute about one third to the sulfate aerosol in the Svalbard region, as observed at Zeppelin station by *Heintzenberg and Leck* [1994]. In this region, the melting ice edge gives rise to a spring bloom of phytoplankton (April-June), leading to the release of DMS to the atmosphere from the uppermost ocean layer, resulting in the formation of biogenic aerosol sulfate [*Park et al., 2013*].

The EC/OC ratios in aerosols in Ny-Ålesund in the summer ranged from 0.00–0.28 (median: 0.04). The observed EC/OC ratios from going marine diesel engines ranged from 0.03 to 0.07 [Agrawal *et al.*, 2010]. The variability of EC/OC ratios from heavy-duty diesel ships was large, ranging from 0.2 to 2.4, depending on engine types, model years, manufacturers, and sizes [Shah *et al.*, 2004]. The EC/OC ratios could be low in the idle phase (0.2), increase to 0.6 in the creep phase and high in the transient (2.4) and cruise (2.2) phase [Shah *et al.*, 2004].

The OC concentrations ranged from 13.8 to 64.4 ng m⁻³, with a mean of 32.8 ng m⁻³. Primary organic material could contribute significantly to the organic carbon [Decesari *et al.*, 2007]. In Svalbard, significant carbon signals were found in the X-ray spectra of aerosols, and that might be originated from humic or humic-like substances of marine origin [Weinbruch *et al.*, 2012].

Chemical reconstructed mass derived from the procedures by Malm *et al.* [2007] shows reasonable agreement with gravimetric mass (Figure 3.6), and the reconstructed aerosol composition identified 81–94% of the aerosol gravimetric mass at Ny-Ålesund. However, a more negative bias appeared toward the higher end of the mass concentration. Malm *et al.* [1994] found a similar pattern and suggested that water could be part of the unidentified mass. Bias in the multipliers used to account for the oxide forms of the crustal elements could also provide another explanation for the “missing mass in chemical reconstructed mass”. Despite uncertainties, soil, sulfate (as (NH₄)₂SO₄) and sea salt contributed to 31.5%, 24.1%, and 20.4% of the gravimetric mass, respectively. Nitrate as NH₄NO₃, organic matter, non-soil K and EC

accounted for 11.3%, 9.4%, 0.7%, and 0.3% of the gravimetric mass. The results suggested that aerosol particles at Ny-Ålesund were derived from complex sources including crustal materials, sea-spray and fuel combustion.

Highest concentration of TSP was observed in Sample #6 when two cruise ships with more than 1500 passengers visited Ny-Ålesund, which was 2290 ng m^{-3} , higher than those in Samples #1–5 ($330\text{--}1060 \text{ ng m}^{-3}$), and it was almost six times higher than that in Sample #1 which was collected when there had been a rainfall event during one of the three days sampling period (330 ng m^{-3}). The concentrations of nss-SO_4^{2-} (203 ng m^{-3}) in Sample #6 were about three times higher than the values in other samples when few ships present and the concentration of OC (64.4 ng m^{-3}) and EC (2.3 ng m^{-3}) was doubled when cruise ships visited Ny-Ålesund. This suggests that ship emissions might impact on aerosol chemical composition at this location.

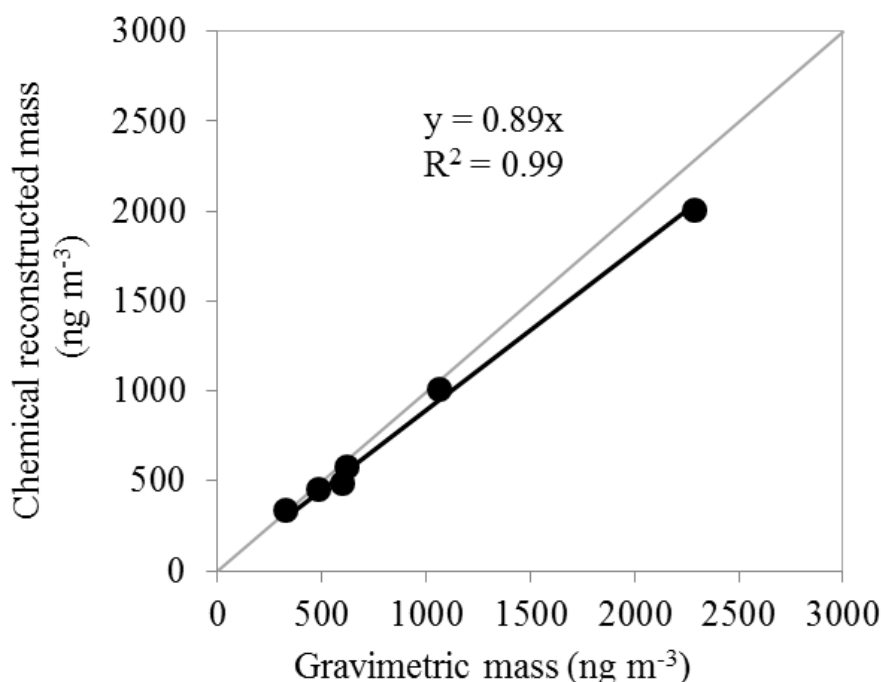


Figure 3.6 Comparison between chemical reconstructed mass and gravimetric mass.

3.3.2 Episodes from ship emissions

Identification of ship emissions. In order to estimate the influence of ship emissions on the composition of aerosols, the nc-V and nc-Ni were used as indicators of this source [Barwise, 1990; Viana *et al.*, 2009]. The nc-V concentrations ranged between 0.0043 and 0.98 ng m⁻³ and the concentrations of nc-Ni were from 0.0038 to 0.57 ng m⁻³. Elevated concentrations of nc-V (0.98 ng m⁻³) and nc-Ni (0.57 ng m⁻³) were observed in Sample #6 when two cruise ships with more than 1500 passengers visited Ny-Ålesund on July 19–22, 2012, while nc-V and nc-Ni concentrations were low at the levels of 0.0043–0.050 ng m⁻³ and 0.0038–0.17 ng m⁻³, respectively, when few cruise ships were present. The nc-V and nc-Ni concentrations in Sample #6 were 38-fold and 8-fold higher, and the nss-SO₄²⁻ concentration (203 ng m⁻³) was 2-fold higher compared to their median values found during the sampling period. The nc-V concentration in Sample #6 was 43-fold higher than the summer month average (0.022 ng m⁻³) observed at Barrow from 1976 to 1978 [Rahn, 1981] and 9-fold higher than the summer average (0.10 ng m⁻³) at Barrow from 2005 to 2008 as well [Quinn *et al.*, 2009]. Accordingly, the nc-V/nc-Ni ratio of 1.7 was observed in this study, which was higher than that in coal (0.5), gasoline (0.3) and diesel exhaust (0.5) [Pacyna and Pacyna, 2001], but it was in the range of crude oil or petroleum (1–10) [Barwise, 1990], suggesting the source of oil combustion.

In addition, the nss-SO₄²⁻/nc-V ratio in Sample #6 was low (208) compared to that in other samples (range: 1156–11767). Becagli *et al.* [2012] suggested that the nss-SO₄²⁻/nc-V ratio of 200 can be defined as the lower limit for aerosol particles originating from heavy oil combustion in summer. The signals of the concentrations

of nc-V and nc-Ni and the ratios of nc-V/nc-Ni and $\text{nss-SO}_4^{2-}/\text{nc-V}$ found in Sample #6 indicate the impact of ship emissions on the ambient particulate matter at this location.

Effects of ship emissions on the air quality. The influence of ship emissions on the ambient air quality at this location was examined by comparing certain trace elements between Sample #6 collected during cruise ship emissions and Samples# 1–5 affected by few-ship emissions. Trace elements concentrations in Sample #6 were higher than the values in Sample #1–5 and the values measured in 1980s [*Maenhaut and Cornille, 1989; Pacyna and Ottar, 1985*] (see Figure 3.7). Elements (Al, Fe, Co) in Sample #6 were 5–7 times higher than those in Sample #1–5. Anthropogenic elements, Ni, V, and Pb in Sample # 6 were found, 8–fold, 26–fold and 41–fold of the mean value of Sample #1–5.

The concentrations of trace elements typically derived from pollution sources observed at Ny-Ålesund during this study were higher than those at Zeppelin and other Arctic sites. The concentration of V in Sample #6 was 1.0 ng m^{-3} , about 4–14 times higher than the annual mean values ($0.07\text{--}0.20 \text{ ng m}^{-3}$) observed at Zeppelin Station and was higher than those measured during Haze events ($0.11\text{--}0.13 \text{ ng m}^{-3}$) at North American Arctic and Norwegian Arctic [*Sheridan and Zoller, 1989*].

The Ni concentration in Sample #6 was also 2–8 times higher than the annual mean Ni concentrations at Zeppelin Station [*Berg et al., 2004*], which was six times higher than those obtained in other samples during this study and those observed during the

summer campaigns from 1980 to 1982 at the same location [*Maenhaut and Cornille, 1989*], which was higher than the mean concentration (0.29 ng m^{-3}) observed during the winter months of 1984–1986 at Ny-Ålesund [*Maenhaut and Cornille, 1989*], and was higher than the mean concentrations of 1980–1982 at Alert (0.32 and 0.38 ng m^{-3}), Igloodik (0.14 and 0.27 ng m^{-3}) and Mould Bay (0.40 and 0.45 ng m^{-3}) in the Canadian Arctic [*Barrie and Hoff, 1985*].

Other elements that also showed similar patterns include Pb: its concentration in this sample was 1.36 ng m^{-3} , 1–2 times higher than annual mean Pb concentrations at Zeppelin station [*Berg et al., 2004*]. These comparisons indicated that ship emissions contributed significantly to the concentrations and compositions of particulate matter in the ambient air at this location in the summer.

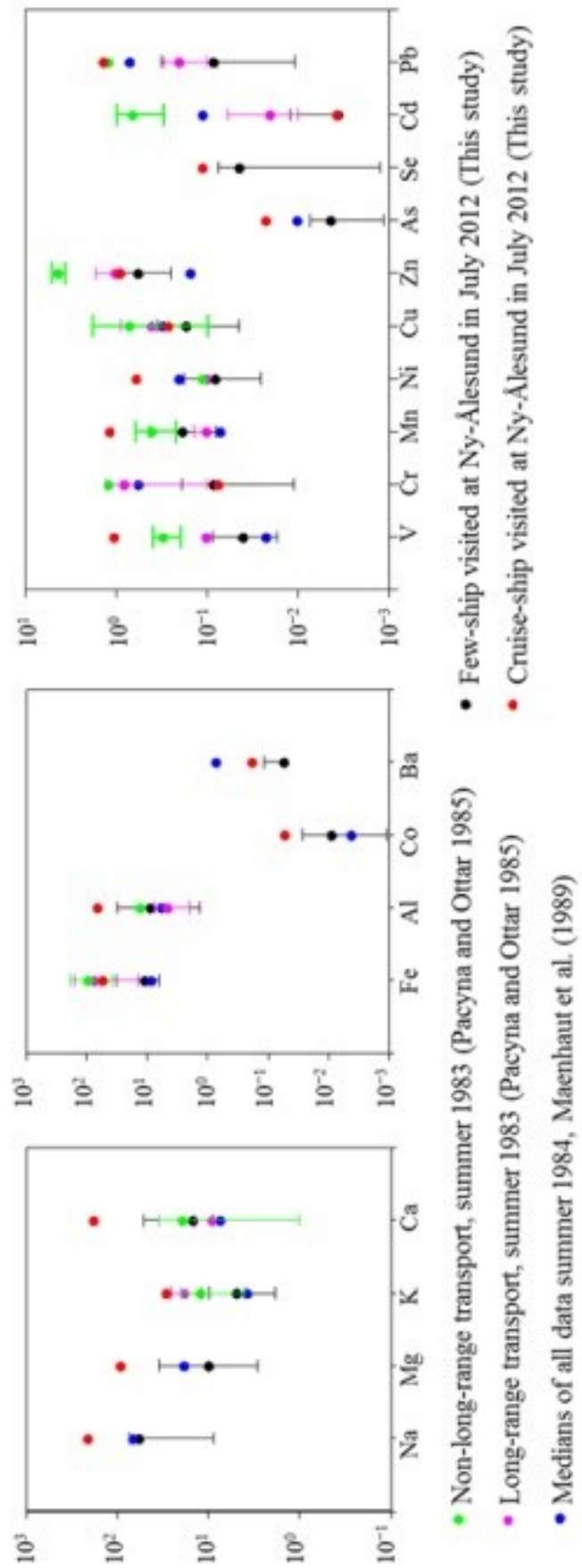


Figure 3.7 Comparison of element concentrations observed in July 2012 with the concentrations observed in the summer from others at Ny-Ålesund [Maenhaut and Cornille, 1989; Pacyna and Ottar, 1985].

3.3.3 Periods with few-ship visits

Chemical compositions. Trace elements concentrations in the aerosols collected when few-ship visited Ny-Ålesund were compared with history data collected at the Ny-Ålesund in the summer in the 1980s [Maenhaut and Cornille, 1989; Pacyna and Ottar, 1985] (see Figure 3.7). The concentration of elements (e.g., Cr, Ni, Pb, As, Se), associated with anthropogenic emissions, were lower than the values in the 1980s [Maenhaut and Cornille, 1989; Pacyna and Ottar, 1985], and V and Mn was in the lower end of the values in the 1980s [Maenhaut and Cornille, 1989; Pacyna and Ottar, 1985]. Relatively lower concentrations of Pb measured in the summer are due to a reduction in the use of leaded petrol. nc-V observed in the atmosphere results from fuel combustion [Zoller *et al.*, 1973], which concentrations ranged between 0.0004 ng m^{-3} and 0.050 ng m^{-3} at Ny-Ålesund. The nc-Mn concentrations ranged between 0.0027 ng m^{-3} and 0.05 ng m^{-3} . The comparison of the concentrations of nc-V and nc-Mn with those observed at the Alert, Bear and Spitsbergen showing that these concentrations were lower than the values reported in the literature in the summer Arctic [Quinn *et al.*, 2009; Rahn, 1981] (see Figure 3.8). The concentrations of anthropogenic elements (nc-V, nc-Ni, Cr, As, Cd and Pb) observed in this study were also lower than those in 1980s [Maenhaut and Cornille, 1989; Pacyna and Ottar, 1985]. This might be partly due to the decreased source strength since the 1990's [Berg *et al.*, 2004] and a reduction in the use of leaded gasoline. This agrees with global decrease in emissions. The declined trend of the long-range transport of pollutants is well documented, which can be seen from the decrease of BC from long-range transport since 1990's [AMAP, 2011; Eleftheriadis *et al.*, 2009] and decreased emissions from the Europe, Scandinavia and Russia since 1980's

[Weinbruch *et al.*, 2012]. However, comparable concentrations were found in metallic elements (Cu, Zn, and Mn). This generally agree with the long-term measured at Svalbard that with no significant trend in the temporal variations of Cu and Zn at Svalbard from 1994 to 2002 [Berg *et al.*, 2004]. This might be related to the temporal variation in the potential source regions [Weinbruch *et al.*, 2012].

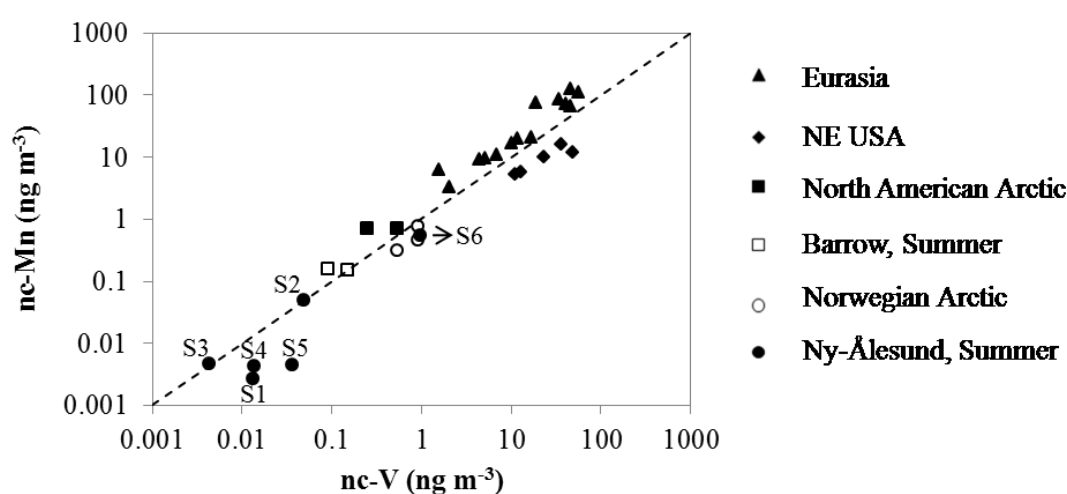


Figure 3.8 Comparison of the concentrations of nc-V versus those of nc-Mn obtained at Ny-Ålesund in the summer during this study with those from Barrow [Quinn *et al.*, 2009], Eurasia, Northeast USA, Barrow and Mould Bay in the North American Arctic and Bear Island and Spitsbergen in the Norwegian Arctic [Rahn, 1981].

nc-Mn/nc-V and Enrichment factors. The nc-Mn/nc-V ratios in aerosol samples can be used to identify aerosol sources because this ratio may reflect the signatures of pollution in source regions since sources in Eurasia were identified with a nc-Mn/nc-V ratio of 2.0, whereas sources in the northeast U.S.A. were identified with a nc-Mn/nc-V ratio of 0.41 [Quinn *et al.*, 2009; Rahn, 1981]. EFs can be used to evaluate the degree of influence of anthropogenic emissions on atmospheric aerosols

at Ny-Ålesund (Figure 3.9). Thereby, the nc-Mn/nc-V ratios, enrichment factors associated with air mass trajectories were employed to interpret the features of air masses over Ny-Ålesund while few ships visited in the summer.

The mean nc-Mn/nc-V ratio in samples from this study was 0.54, with a range of 0.12–1.1 (Table 3.1). These ratios measured in Ny-Ålesund in July 2012 had a larger range than the ratios observed at Norwegian Arctic in 1980s (range: 0.49–0.85). The nc-Mn/nc-V ratio was 1.0 in air masses from the Arctic Ocean (Sample #2 and #3). This ratio was higher than the ratios obtained in the Norwegian Arctic (0.49–0.85) and lower than the ratios observed at the Barrow Alaska (1.3–2.3) [Quinn *et al.*, 2009]. This suggested that trace elements observed in the sampling station could be affected by a mixture of air masses from the North American Arctic with those from Norwegian Arctic. Enrichment factors of elements Ni, Se, and Cd were high in these air masses.

The nc-Mn/nc-V ratio was 0.2 in the Air masses from Iceland (Sample #1), which was significantly lower than the ratios (2.1–4.3) in the air masses in Eurasia and was closed to the ratios (0.25–0.47) in the air masses in the northeast U.S.A [Rahn, 1981]. This suggested that the air masses arriving from Iceland might be linked to the air masses in the northeast USA. The nc-V/nc-Ni in Sample #1 was 0.57, which was close to coal (0.5) and diesel exhaust (0.5), higher than gasoline (0.3) [Pacyna and Pacyna, 2001] and lower than crude oil or petroleum (1–10) [Barwise, 1990], suggesting the influence from coal burning and diesel fuel combustion along the path. In addition, high EFs of Pb and Zn were observed in Sample #1 ranked second only to

Sample # 6 (influenced by ship emissions). Similar phenomenon was also found at Ny-Ålesund in the summer by *Pacyna and Ottar* [1985], who indicated that the high Zn and Pb concentrations in the air masses from Greenland and pass over Iceland were associated with lead and zinc mining along the path. This suggested the air masses arriving from Iceland could have been contaminated by mineral production along the path in addition to coal and diesel fuel combustion.

The nc-Mn/nc-V ratios ranged from 0.1 to 0.3 in the Air masses from north Russia (Sample # 4 and #5), which was lower than those from Eurasia (2.0). This might be related to the decrease in ratios during the transport as result of the difference size distribution of Mn and V [*Quinn et al.*, 2009; *Rahn*, 1981]. This ratio would decrease more in the summer than in the winter due to more precipitation and low transport efficiency in the summer. Elements Cu, Zn, Se, Cd, and Ni were found to be enriched in these air masses. Similar results were reported by *Weinbruch et al.* [2012] that high Ni, Zn, and Cu were found in air masses arriving from North Russia, possibly relating to pollutants emitted from metallurgy industry.

Thereby, when few ships visited Ny-Ålesund, the concentration of anthropogenic elements (nc-V, nc-Mn, Cr, Ni, Pb, As, Se) were lower than those values in the 1980s [*Maenhaut and Cornille*, 1989; *Pacyna and Ottar*, 1985; *Rahn*, 1981], suggesting Ny-Ålesund can be counted as a “clean” region in the summer. Anthropogenic signal reflected by nc-V/nc-Mn and enrichment factors, however, can still be seen in the air arriving from the North American Arctic, Iceland and North Eurasia in Ny-Ålesund in the summer.

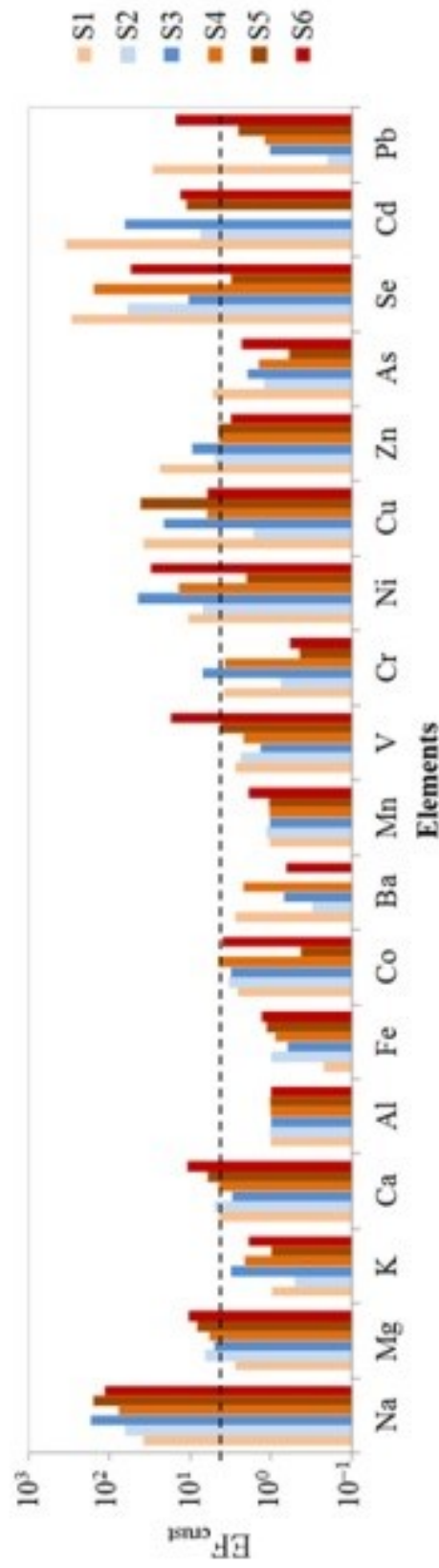


Figure 3. 9. Enrichment factors of elements in aerosols at Ny-Ålesund against crustal composition, with Al as the reference element. The dash line indicates the value of 5 that operationally separates crustal/sea water and non-crustal sources/non-sea water sources.

3.4 Conclusions

The selected trace elements, ionic species and organic/elemental carbon in aerosols and elemental composition of local soils were measured to assess the origins of aerosols and their impact on aerosol chemical composition in Ny-Ålesund in the summer. The concentrations of anthropogenic elements (nc-V, nc-Mn, Cr, Ni, Pb, As, Se) were lower than the values in the 1980s [Maenhaut and Cornille, 1989; Pacyna and Ottar, 1985; Rahn, 1981] when few-ship visited Ny-Ålesund; however, anthropogenic signal reflected by nc-V/nc-Mn and enrichment factor can be seen in the air arriving from the North American Arctic, Iceland and North Eurasia in Ny-Ålesund in the summer.

Significantly enhanced levels of nc-V and nc-Ni were observed when two cruise ships with more than 1500 passengers visited Ny-Ålesund. The nc-V, nc-Ni and Pb concentration in Sample #6 was 38-fold, 8-fold and 40-fold, respectively, higher than the median values observed during the sampling period. Elevated concentrations of TSP, nss-SO_4^{2-} , OC, EC and trace elements (Mn, Fe, Co, Ni, As, and Se) in aerosols were also observed when the presence of cruise ships, suggesting that ship emissions contributed significantly to pollutants in Ny-Ålesund in the summer.

The results indicate that ship emissions significantly contribute to aerosol concentrations in Ny-Ålesund in the summer. This study may serve for future research that seeks to examine the impact of anthropogenic emissions on the physiochemical properties of aerosol, particularly in identifying tracers that track the aerosol sources.

Acknowledgements

The work was funded by the National Natural Science Foundation of China (41105094) and the Scientific Research Foundation of Third Institute of Oceanography, SOA (2011004). The Chinese Arctic and Antarctic Administration of the State Oceanic Administration of China supported the field accommodation at the YRS. Additional support was provided by the Rutgers University for the continuation and completion of this research. We gratefully acknowledge the NOAA Air Resources Laboratory (ARL) for the provision of HYSPLIT transport and dispersion model and NCAR/NCEP for providing the meteorological data freely. We thank Elisabeth Bjerke Råstad at Kings Bay AS for supplying the harbor log, and Guojie Xu and Rafael Jusino Atresino for help with field sampling preparation. Discussions with Guojie Xu, Rafael Jusino Atresino, Tianyi Xu, and Pami Mukherjee were helpful.

Chapter 4: Characterization of major ionic species and carbonaceous components in summertime aerosols at Ny-Ålesund in the Arctic¹

Abstract

Aerosol sampling was conducted at Ny-Ålesund in the Arctic in July 2012 to assess the formation of secondary inorganic aerosols (SIAs), aerosol acidity and chloride depletion. Water soluble components (Na^+ , NH_4^+ , K^+ , Mg^{2+} , Ca^{2+} , F^- , methanesulfonate (MSA^-), Cl^- , NO_2^- , NO_3^- , SO_4^{2-} , and PO_4^{3-}) and organic/elemental carbon (OC/EC) in aerosols were measured by ion chromatography and thermal–optical transmittance carbon analysis. The mean sea salt concentration was 373 ng m^{-3} , and the mean Cl^- concentration was 210 ng m^{-3} . Na^+ and Cl^- accounted for $57 \pm 17\%$ of the measured ionic species. The mean SIAs concentration, defined as the sum of nss-SO_4^{2-} , NO_3^- and NH_4^+ , was 158 ng m^{-3} , accounting for 33% of the total mass of ionic species. The mean concentration of OC was 55 ng m^{-3} , and 88% of the variance in OC could be explained by oceanic emissions and ship emissions. The mean neutralization ratio (NR) was 0.53, indicating that SO_4^{2-} and NO_3^- was not fully neutralized by NH_4^+ . Aerosols in this area were generally acidic, with the mean $[\text{H}^+]_{\text{total}}$ of 3.17 nmol m^{-3} and $[\text{H}^+]_{\text{free}}$ of 3.06 nmol m^{-3} . The Cl^- depletion occurred in samples when $[\text{nss-SO}_4^{2-} + \text{NO}_3^- - \text{NH}_4^+]$ and sea salt concentrations were high, indicating that the Cl^- depletion could be affected by interactions of acidic species (SO_4^{2-} , NO_3^-) with sea salt.

¹ **Zhan, J**, Gao, Y., Li, W., Chen, L., and Lin, Q., 2014. Characterization of major ionic species and carbonaceous components in the aerosols at Ny-Ålesund in the summer Arctic, submitted to *Polar Research*.

Keywords: Water-soluble ionic species, carbonaceous aerosol, secondary inorganic aerosols, aerosol acidity, chloride depletion, Arctic.

4.1 Introduction

The relative abundances of different chemical species in the atmosphere affect aerosol radiative forcing [*Martin et al.*, 2004], aerosol-cloud interactions [*Leck et al.*, 2002], and heterogeneous chemistry [*Weinbruch et al.*, 2012]. Heterogeneous processes involving oxides of sulfur and nitrogen lead to secondary aerosol formation that may alter aerosol acidity [*Sievering et al.*, 1992; *Weinbruch et al.*, 2012]. The extent to which aerosols are neutralized can influence the ability of particles acting as cloud condensation nuclei [*Abbatt et al.*, 2006; *Girard et al.*, 2013; *Yang et al.*, 2011] and change the ability of particles to scatter and absorb light [*Martin et al.*, 2004]. Aerosol acidity can therefore have an effect on aerosol radiative forcing.

Aerosol acidity and the formation of secondary inorganic aerosols (SIAs) depend on the concentrations of strong acids (e.g., sulfuric and nitric acids) and the availability of ammonia in aerosols [*Quinn et al.*, 2009], which vary spatially and temporally [*Fisher et al.*, 2011]. Ground-based observations at Barrow, Alaska, have revealed that the ammonium concentrations in aerosols have declined more rapidly than that of sulfate over the last decade, and that aerosol acidity has increased as a result [*Quinn et al.*, 2009]. In contrast, at Alert, Canada, the ammonium concentrations have decreased less rapidly than the sulfate concentrations, implying that the aerosols have become more neutral [*Hole et al.*, 2009]. The results obtained from

the projects “the Arctic Research of the Composition of the Troposphere from Aircraft and Satellites (ARCTAS) and the Aerosol, Radiation, and Cloud Processes Affecting Arctic Climate (ARCPAC)” conducted in April 2008 showed that aerosols were more acidic below 2 km than those above 2 km, with the median neutralized fraction $[\text{NH}_4^+]/(2[\text{SO}_4^{2-}]+[\text{NO}_3^-])$ being 0.5 below 2 km and 0.7 above 2 km. This vertical pattern could be attributed to the influences of biomass burning and NH_3 emissions from eastern Asia [Fisher *et al.*, 2011]. When aerosols become acidic, the acid displacement of chloride (Cl^-) in sea-salt leads to the production of Cl containing gases such as HC , Cl_2 , HOCl , and ClNO_2 [Finlayson-Pitts, 2003], resulting in lower Cl^-/Na^+ ratios, and the Cl^- depletion in aerosols [Quinn *et al.*, 2009]. A lack of Cl^- has been observed in some particles, with both Na^+ , NO_3^- and SO_4^{2-} being detected because of the transformation of HNO_3 and H_2SO_4 [Behrenfeldt *et al.*, 2008].

Aerosols observed in the unpolluted air at Ny-Ålesund were dominated by NaCl particles [Geng *et al.*, 2010]. These particles could be modified by pollution-derived compounds from local emission sources including diesel generators, cars and ships. Modified sea salt aerosols have occasionally been observed at Ny-Ålesund [Anderson *et al.*, 1992; Geng *et al.*, 2010]. However, the formation of secondary inorganic aerosols, aerosol acidity and chloride depletion impacted by local pollution and natural processes in the summer have not been assessed for this site. The purpose of this study is to investigate ionic composition of aerosols and potential sources of ionic species and carbonaceous aerosol and to assess the

formation of SIAs, aerosol acidity and chloride depletion that may occur in summer at this location.

4.2 Methods

4.2.1 Sample and data collection

Sampling of aerosols was carried out at the Chinese Arctic “Yellow River Station (YRS)” (78.92° N, 11.93° E, 13 m above sea level (a.s.l)) in the village of Ny-Ålesund in Svalbard (see Figure 4.1) in July 2012. Two aerosol samplers were used simultaneously to collect aerosol particles on the roof of the YRS building, approximately 7 m above the ground. A Chemcomb (C) cartridge (Model 3500; Thermo Scientific, Waltham, MA, USA) was used to collect total suspended particles (TSP) for the analysis of water soluble species. Particles were collected on Teflon filters (47 mm diameter, 1.0 μm pore size; Pall Corp., USA) at a flow rate of 16.7 L min^{-1} with sampling duration of 3 day. Another sampler was a model KC-6120 comprehensive atmospheric sampler (Laoshan Electronic Instrument Factory, Qingdao, China) for collection of TSP for elemental carbon (EC) and organic carbon (OC) analyses. Particles were collected on quartz fiber filters (MK 360; 90 mm diameter, 0.3 μm pore size; Munktell Corp., Falun, Sweden) at a flow rate of 96 L min^{-1} with 3 days duration. Prior to sampling, the quartz fiber filters were baked at 550 °C in a muffle furnace for ca.12 hours and after then wrapped in aluminum foil until their use. In the laboratory at the YRS, the filters were handled in a 100-class laminar flow clean hood. After sampling, each sample filter was put into a cleaned petri dish, sealed in a plastic bag, and stored at 4 °C until analysis. A total of 12 samples were collected (six samples on Teflon filters and six on quartz fiber filters).

Meteorological parameters (air temperature, wind speed, wind direction, and relative humidity (RH)) were measured by weather detectors and probes (Vaisala Company; Helsinki, Finland) throughout the study, with a temporal resolution of 1 hour. The times and dates of the arrivals and departures of ships, and the numbers of passengers (hereafter PAX) visiting Ny-Ålesund, were obtained from the Kings Bay AS Company. Detailed sampling information and results of analyses are shown in Table 4.1.

4.2.2 Chemical analysis

Aerosol particles collected on Teflon filters were analyzed for major water-soluble ionic species by ion chromatography (IC), using a Dionex ICS-90A with an RFC-30 reagent-free controller (Dionex, Sunnyvale, CA, USA) at the Third Institute of Oceanography, State Oceanic Administration, China. Half of each Teflon filter sample was extracted with 25 mL of ultra-pure water ($18.2 \text{ M}\Omega \text{ cm}^{-1}$; Milli-Q Academic system; Millipore Corp., Billerica, MA, USA) in an ultrasonic bath for 40 min and after then leached overnight. The extract was then filtered through a PTFE syringe filter ($0.45 \mu\text{m}$ pore size; Fisherbrand, Fisher Scientific, Fair Lawn, NJ, USA) and injected into the IC system using an automated sampler (AS40; Dionex), using 5.0 mL vials. Cation analysis was made using a CS12A analytical column (4 mm I.D., 250 mm long; Dionex), a methanesulfonic acid eluent generator cartridge (EGC II MSA; Dionex), a conductivity detector, and a 25 μL sample loop. Anions were analyzed using an AS18 analytical column (4 mm I.D., 250 mm long; Dionex), an AG18 guard column (Dionex), a KOH eluent generator cartridge (EGC II KOH; Dionex), a conductivity detector, and a 25 μL sample loop. Standards from National Institute of

Standards and Technology (NIST) were run before and during sample analyses. The method detection limits for Na^+ , NH_4^+ , K^+ , Mg^{2+} , Ca^{2+} , F^- , MSA, Cl^- , NO_2^- , NO_3^- , SO_4^{2-} , and PO_4^{3-} were 20, 9, 20, 20, 50, 0.9, 0.4, 1, 0.5, 3, 7, and $8 \mu\text{g L}^{-1}$, respectively. The overall precision of the method was $< 5\%$. The final concentrations of the species analyzed in the aerosols were corrected for the amounts found in the field blanks. The EC and OC were determined using a thermal–optical transmittance carbon analyzer (Sunset Laboratory Inc., Portland, OR, USA), following the National Institute of Occupational and Health protocol [NIOSH, 1999]. The uncertainties associated with the EC and OC measurements were ca. 10%.

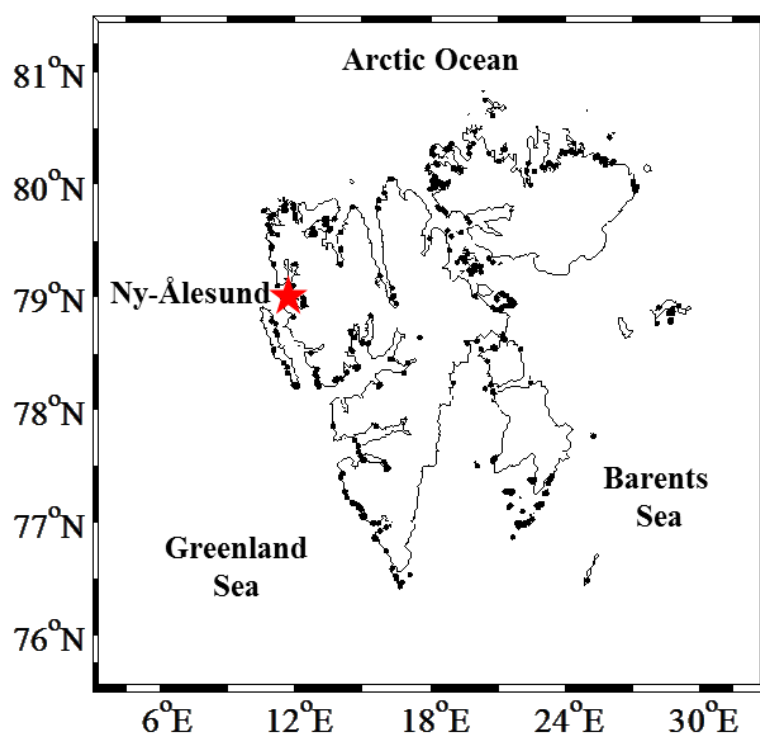


Figure 4.1 Sampling location at Ny-Ålesund, Svalbard

4.2.3 Data analysis

Sea salt calculation. The sea salt (SS) concentration was calculated using equation 4.1.

$$[\text{SS}] = [\text{Cl}^-] + 1.47 \times [\text{Na}^+], \quad (4.1)$$

where 1.47 is the seawater ratio $(\text{Na}^+ + \text{K}^+ + \text{Mg}^{2+} + \text{Ca}^{2+} + \text{SO}_4^{2-} + \text{HCO}_3^-)/\text{Na}^+$ [Millero, 2013]. This calculation assumes that all the Na^+ in aerosols came from sea spray. Most of the Na^+ in Arctic aerosols has been found to be associated with sea salt was either unmodified or modified [Geng *et al.*, 2010]. The concentrations of sea salt sulfate (ss-SO_4^{2-}) were calculated from the measured Na^+ concentration and the $\text{SO}_4^{2-}/\text{Na}^+$ mass ratio of 0.252 derived from seawater [Millero, 2013].

Non-sea salt calculation. The concentrations of non-sea salt sulfate (nss-SO_4^{2-}) were calculated as the difference between the total SO_4^{2-} and the ss-SO_4^{2-} , as shown in equation 2.

$$[\text{nss-SO}_4^{2-}] = [\text{SO}_4^{2-}] - 0.252 \times [\text{Na}^+] \quad (4.2)$$

Secondary inorganic aerosols. In this study, the sum of nss-SO_4^{2-} , NO_3^- , and NH_4^+ is defined as SIAs, as these species are the main components of SIAs. This approach has been used by other investigators [Squizzato *et al.*, 2013].

The neutralization ratio (NR). In this study, NR was calculated by equation 4.3.

NR was used to determine the extent to which the acidic SO_4^{2-} and NO_3^- were neutralized by NH_4^+ (expressed as equivalents) [Tsai and Cheng, 1999]. The aerosol was defined to be acidic if it had an NR of less than 0.9, propagating a 10%

uncertainty in the NR calculation from the analytical error and measurement uncertainties [Quinn *et al.*, 2000].

$$NR = [NH_4^+]/([SO_4^{2-}] + [NO_3^-]) \quad (4.3)$$

Aerosol acidity. Aerosol acidity is an important factor influencing aerosol properties [Pathak *et al.*, 2009]. In the past, the total acidity ($[H^+]_{total}$), strong acidity ($[H^+]_{strong}$), free acidity ($[H^+]_{free}$), and pH were among the parameters that were used to evaluate aerosol acidity [Behera *et al.*, 2013; Zhang *et al.*, 2007; Zhou *et al.*, 2012]. In this study, $[H^+]_{total}$, which is referred to as the ion-balanced acidity, is the sum of anions minus the sum of cations [Pathak *et al.*, 2009]. However, $[H^+]_{total}$ does not represent the in situ acidity of aerosols well because of the excessive amounts of water present in aqueous extracts [Keene and Savoie, 1998]. $[H^+]_{free}$ was defined as the number of moles of free hydrogen ions in the aqueous phase of the aerosol per unit air volume ($nmol\ m^{-3}$), or as the pH of the aqueous aerosol phase; [Zhang *et al.*, 2007]. $[H^+]_{free}$ was obtained from the Extended Aerosol Inorganic Model Aerosol Thermodynamics Model - Inorganic Model IV (hereafter E-AIM 4) [Frieze and Ebel, 2010]. In addition, water content ($[H_2O]$) was computed from E-AIM 4 model as well.

Chloride depletion. In this study, Cl^- depletion (%) was calculated using equation 4 based on the work [Zhao and Gao, 2008].

$$Cl^- \text{ depletion (\%)} = 100 \times (1.174[Na^+] - [Cl^-]) / (1.174[Na^+]), \quad (4.4)$$

where $[Na^+]$ and $[Cl^-]$ are the concentrations ($nmol\ m^{-3}$) measured in the aerosol.

1.174 is the $[Na^+]/[Cl^-]$ ratio for sea water [Millero, 2013].

Table 4.1 Sampling dates, meteorological data, chemical concentrations (ng m^{-3}), neutralization ratios, $[\text{H}^+]_{\text{total}}$, $[\text{H}^+]_{\text{strong}}$, $[\text{H}^+]_{\text{free}}$ (nmol m^{-3}), and pH

	Sample 1 7/4–7/7	Sample 2 7/7–7/10	Sample 3 7/10– 7/13	Sample 4 7/13– 7/16	Sample 5 7/16– 7/19	Sample 6 7/19– 7/22
T[°C]	6.5	5.6	5.9	5.9	6.1	6
RH[%]	76	77	72	76	78	75
WS[m s ⁻¹]	2.3	3.4	4.7	3.1	2.4	3.5
WD[°]	139	169	214	159	124	151
P[hPa]	1008.9	1018	1005.9	1009	1008.8	1006.1
PAX	1898	4770	1335	2386	441	6018
ng m^{-3}						
F ⁻	3.86×10^{-1}	7.10×10^{-1}	7.78×10^{-1}	n.a.	n.a.	n.a.
MSA ⁻	2.65×10^1	1.46×10^1	4.61×10^0	8.61×10^0	8.80×10^0	1.71×10^1
Cl ⁻	5.86×10^1	3.08×10^2	1.75×10^2	1.69×10^2	2.55×10^2	2.95×10^2
NO ₂ ⁻	7.71×10^{-1}	1.24×10^0	6.58×10^{-1}	2.17×10^0	1.98×10^0	1.69×10^0
NO ₃ ⁻	8.42×10^1	8.30×10^1	3.54×10^1	1.41×10^1	4.52×10^1	4.59×10^1
SO ₄ ²⁻	6.79×10^1	1.13×10^2	7.27×10^1	1.20×10^2	1.24×10^2	2.49×10^2
nss-SO ₄ ²⁻	6.50×10^1	5.73×10^1	5.07×10^1	1.08×10^2	9.49×10^1	2.03×10^2
PO ₄ ³⁻	n.a.	n.a.	n.a.	n.a.	n.a.	2.41×10^0
Na ⁺	1.11×10^1	2.19×10^2	8.76×10^1	4.85×10^1	1.15×10^2	1.84×10^2
NH ₄ ⁺	1.53×10^1	1.18×10^{-1}	n.a.	1.39×10^1	2.45×10^1	4.58×10^0
K ⁺	n.a.	n.a.	n.a.	n.a.	5.39×10^0	0.00×10^0
Mg ²⁺	n.a.	n.a.	n.a.	n.a.	n.a.	3.58×10^1
Ca ²⁺	n.a.	n.a.	n.a.	n.a.	n.a.	6.07×10^1
TSP	3.30×10^2	1.06×10^3	5.98×10^2	4.82×10^2	6.20×10^2	2.29×10^3
OC	2.06×10^1	5.42×10^1	1.66×10^1	3.46×10^1	3.29×10^1	7.73×10^1
EC	1.31×10^0	1.95×10^0	4.64×10^0	n.a.	2.51×10^{-1}	2.76×10^0
Sea Salt	7.50×10^1	6.30×10^2	3.03×10^2	2.40×10^2	4.24×10^2	5.65×10^2
SIAAs	1.65×10^2	1.40×10^2	8.61×10^1	1.36×10^2	1.65×10^2	2.54×10^2
nmol m^{-3}						
$[\text{H}^+]_{\text{free}}$	2.61×10^0	2.07×10^0	2.64×10^0	3.75×10^0	3.26×10^0	4.03×10^0
$[\text{H}^+]_{\text{total}}$	3.41×10^0	3.04×10^0	3.31×10^0	4.75×10^0	4.13×10^0	3.3×10^{-1}
$[\text{H}_2\text{O}]$	3.68×10^1	1.11×10^2	5.84×10^1	6.74×10^1	9.59×10^1	8.68×10^1
NR	4.10×10^{-1}	2.61×10^{-3}	0.00×10^0	5.20×10^{-1}	6.72×10^{-1}	7.61×10^{-2}

n.a.: lower than detection limit; PAX: Number of ship passengers

4.3 Results and discussion

4.3.1 Major ions in aerosols

The major inorganic ions in aerosols were Cl^- , SO_4^{2-} , NO_3^- , MSA^- , Na^+ , and NH_4^+ , together contributing to ca. 98% of the total ionic species by mass measured in this study. Other anions (F^-) and cations (Ca^{2+} , Mg^{2+} , and K^+) contributed to the remaining ca. 2% fraction. The mean SIAs concentration was 158 ng m^{-3} , accounting for 33% of the total mass of water-soluble ionic species. The highest SIAs contribution to the total mass of water-soluble ionic species was 62%, which was associated with a rainfall on July 4–9, 2012. NO_3^- , nss-SO_4^{2-} , and NH_4^+ contributed 51%, 40%, and 1%, respectively. The oxidation of gaseous precursors, including nitrogen oxides (NO_x), SO_2 , and NH_3 , which could react with O_3 and hydroxyl radicals ($\text{HO}\cdot$), could lead to the production of SO_4^{2-} , NO_3^- , and NH_4^+ [Squizzato *et al.*, 2013].

Sea salt Aerosol. The Na^+ concentrations in aerosol samples ranged from 11.1 to 219 ng m^{-3} , with a mean of 111 ng m^{-3} , which was within the range of the Na^+ concentrations ($10\text{--}1000 \text{ ng m}^{-3}$) previously measured at the Zeppelin Mountain station in the Ny-Ålesund [Ström *et al.*, 2003]. The Cl^- concentrations in aerosols samples ranged from 58.6 to 295 ng m^{-3} , with a mean of 210 ng m^{-3} . $[\text{Cl}^-]$ and $[\text{Na}^+]$ dominated the water soluble inorganic species, accounting for $57\pm 17\%$ of the total ionic species in aerosols observed at this location. The concentrations of sea salt aerosol ranged from 75.0 to 630 ng m^{-3} , with a mean of 373 ng m^{-3} , accounting for ca. 46% of the TSP. Sea salt aerosol was the dominant aerosol type observed in

Ny-Ålesund settlement [Anderson *et al.*, 1992; Geng *et al.*, 2010] and the Zeppelin station [Weinbruch *et al.*, 2012].

Nss-SO₄²⁻ and MSA⁻. The nss-SO₄²⁻ concentration measured in this study ranged from 50.6 to 203 ng m⁻³, with a mean of 96.5 ng m⁻³, consistent with concentrations measured at other Arctic sites (see Table 4.2). The MSA concentrations in Ny-Ålesund ranged from 4.61 to 26.5 ng m⁻³, similar to the concentrations found at other Arctic sites in summer (Table 4.2). The highest MSA concentration (26.5 ng m⁻³) was found during the period 4–7 July, when the air mass passed over the productive waters of the Atlantic Ocean (Figure 4.2), where the monthly average chlorophyll concentration was as high as 0.3 mg m⁻³ [Feldman and McClain, 2009]. Chang *et al.* [2011] found high marine biogenic production when air masses originated in the Barents and Kara Seas. The lowest MSA concentration (1.13 ng m⁻³) was found when the marine biogenic sulfur concentration was low, when the air mass had passed over the Arctic Ocean.

The oxidation of dimethylsulfide (DMS, CH₃SCH₃) from microbial activity in the ocean contributes to the nss-SO₄²⁻ formation [Leck and Persson, 1996a]. MSA, which is only derived from the photo-oxidation of DMS [Leaitch *et al.*, 2013], was used to evaluate the contribution of marine biogenic SO₄²⁻ to the total nss-SO₄²⁻ concentration. The MSA⁻/nss-SO₄²⁻ ratio was 0.08–0.40, and this range is similar to that found at other Arctic sites in summer (see Table 4. 2). However, the range of MSA⁻/nss-SO₄²⁻ ratios from this study was lower than those found in summer at Alert, Canada [Li and Barrie, 1993; Norman *et al.*, 1999]. Results from previous

studies showed that variability in the $\text{MSA}^-/\text{nss-SO}_4^{2-}$ ratio was affected by the temperature [Bates *et al.*, 1992]. However, the relationship between the $\text{MSA}^-/\text{nss-SO}_4^{2-}$ ratio and the temperature obtained in this study was not significant, with the Pearson correlation coefficient r being 0.47 ($p = 0.35$). The temperature ranged from 5.6 to 6.5 °C during the sampling periods that may not be sufficient to affect the production of MSA^- . Similar results (i.e., no significant relationships between the $\text{MSA}^-/\text{nss-SO}_4^{2-}$ ratio and temperature) were found in the Southern Ocean and in coastal Antarctica [Chen *et al.*, 2012; Xu *et al.*, 2013]. These results suggest that changes in the $\text{MSA}^-/\text{nss-SO}_4^{2-}$ ratio at Ny-Ålesund in summer were not controlled by temperature. A positive correlation was found between the $\text{MSA}^-/\text{nss-SO}_4^{2-}$ ratio and the MSA^- concentration (excluding the sample that was influenced by ship emissions), with an R^2 of 0.94 (Figure 4.3), indicating that biogenic emissions from the ocean influenced the ratio. However, the slope of MSA^- vs. $\text{MSA}^-/\text{nss-SO}_4^{2-}$ decreased by 13% and R^2 decreased to 0.68 when the sample influenced by ship emissions was included in regression analysis, suggesting the contribution of ship emissions to the nss-SO_4^{2-} concentrations.

NH_4^+ . The mean NH_4^+ concentration was 9.72 ng m^{-3} , with the range from lower than detection limit to 24.5 ng m^{-3} , comparable to the mean of 11 ng m^{-3} found at Alert, Canada in summers between 1980 and 1995 [Sirois and Barrie, 1999], and 15.8 ng m^{-3} at the Summit station (Central Greenland, 72° N , 37° W , 3 240 m a.s.l.) in summer 1991. The NH_4^+ concentrations were lower than those seen during the haze season at Ny-Ålesund (about 153 ng m^{-3}) that was impacted by mid-latitude transport [Heintzenberg *et al.*, 2011]. Few sources of NH_4^+ existed in the Arctic

[AMAP, 2006]. A negative correlation was found between NH_4^+ and sea salt concentration, with a Pearson correlation coefficient r of -0.42 ($p = 0.41$), suggesting that emissions from the ocean might not make a significant contribution to the NH_4^+ concentration.

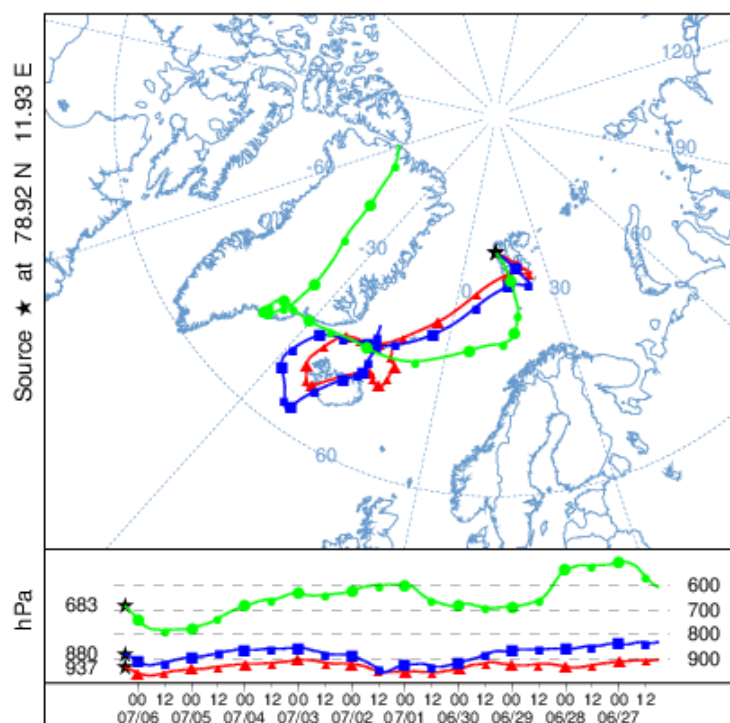


Figure 4.2 Ten days air mass backward trajectories associated with the high concentrations of MSA. The trajectories were calculated at the 500m, 1000m, and 5000m heights every 6 hours by the Hybrid Single-Particle Lagrangian Integrated Trajectory Model 4 (HYSPLIT_4) [Draxier and Hess, 1998]. The National Centers for Environmental Prediction (NCEP)-National Center for Atmospheric Research (NCAR) reanalysis meteorological data was fed into the model.

Table 4.2 Non-sea salt sulfate (nss-SO_4^{2-}) and methanesulfonate (MSA^-) concentrations and the $\text{nss-SO}_4^{2-}/\text{MSA}^-$ ratio in the Arctic in summer

Location or study	nss-SO_4^{2-} ($\mu\text{g m}^{-3}$)	MSA^- ($\mu\text{g m}^{-3}$)	$\text{MSA}^-/\text{nss-SO}_4^{2-}$	Reference
IAOE-91	0.0027–0.66	0.0002–0.13	0.22	<i>Leck and Persson</i> [1996b]
AOE-96	0.0036–1.185	0.002–0.104		<i>Kerminen and Leck</i> [2001]
ASCOS	<0.008–0.42	<0.01–0.08	0.25 ± 0.02	<i>Chang et al.</i> [2011]
CHINARE	0.049–5.55	0.0068–0.19	$0.0051\text{--}0.39$	<i>Chen et al.</i> [2012]
Alert, Canada		0.03–0.05	0.6 ± 0.3	<i>Li and Barrie</i> [1993]
	0.03–0.22		0.39 ± 0.21	<i>Norman et al.</i> [1999]
Barrow, USA	0.09–0.23	0.02	$0.09\text{--}0.22$	<i>Quinn et al.</i> [2002]
Ny-Ålesund, Svalbard	0.39	0.0118		<i>Heintzenberg and Leck</i> [1994]
	0.065–0.20	0.008–0.026	$0.08\text{--}0.40$	This study

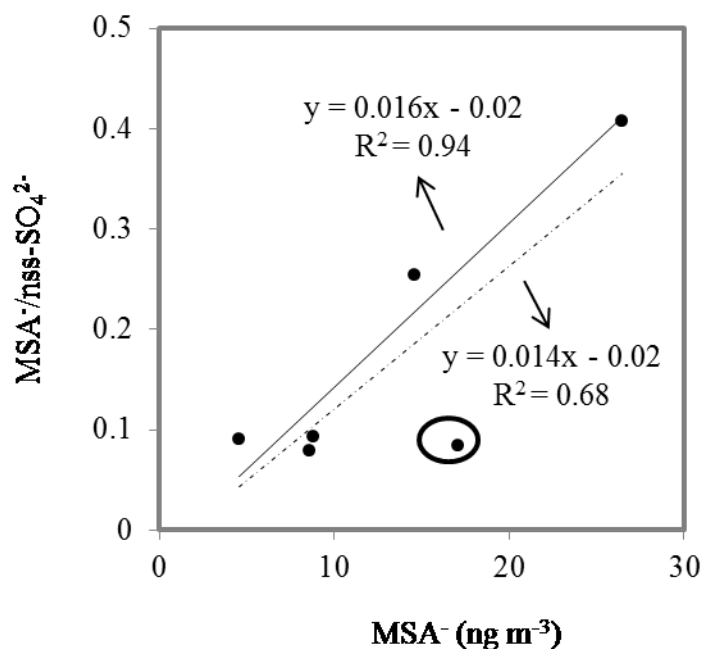


Figure 4.3 Relationships between the methanesulfonate/non-sea salt sulfate ($\text{MSA}^-/\text{nss-SO}_4^{2-}$) ratios and the MSA^- concentrations. The dashed line was the result from linear regression model using all of the data. The solid line was the result from linear regression model excluding one sample affected by ship emission which was highlighted with back circle.

NO_3^- . The NO_3^- concentrations ranged from 14.1 to 84.2 ng m^{-3} , with a mean of 51.3 ng m^{-3} . Comparable concentrations (30–100 ng m^{-3}) were found at Alert, Canada in summer between 1980 and 1991 [Sirois and Barrie, 1999]. However, the NO_3^- concentrations in this study were higher than the NO_3^- concentrations found in summer over the Arctic Ocean, for which the first and third quartiles were 5.1 ng m^{-3} and 7.2 ng m^{-3} , respectively [Chang *et al.*, 2011]. This might be related to local pollution emissions in the summer at this location. A positive correlation was found between NO_3^- and Na^+ , with a Pearson correlation coefficient r of 0.22 ($p = 0.67$). This might be related to NO_3^- formation through the reaction $\text{HNO}_{3(\text{g})} + \text{NaCl}_{(\text{s})} \rightarrow \text{HCl}_{(\text{g})} + \text{NaNO}_{3(\text{s})}$. Similar results were found at Sevetijärvi, northern Finland, where the highest NO_3^- concentrations were found during periods of high Na^+ concentrations, and NO_3^- was not found to be associated with anthropogenic emissions [Ricard *et al.*, 2002]. The reaction of DMS with nitrate radicals ($\text{NO}_3\cdot$) in the marine boundary layer has been proposed to be an important route for the formation of NO_3^- [Allan *et al.*, 2000; Savarino *et al.*, 2013]. The Pearson correlation coefficient of NO_3^- and MSA^- , was 0.74 ($p = 0.095$). Similar results have been reported by Allan *et al.* [2000], who found a strong correlation between NO_3^- and DMS concentrations. About 80–90% of the NO_3^- present was found to be removed by its reaction with DMS in the marine boundary layer at Mace Head, western Ireland [Allan *et al.*, 2000]. Savarino *et al.* [2013] also suggested that DMS is a sink for NO_3^- in the marine boundary layer, and that this occurs predominantly at night. Interestingly, the NO_3^- concentration was negatively correlated with the nss-SO_4^{2-} concentrations, with $r = -0.33$ ($p = 0.53$). Other sources including ship emissions,

vehicles, power station, and aircraft may also contribute to the abundance of NO_3^- in aerosols in the Ny-Ålesund in summer [Eckhardt *et al.*, 2013].

4.3.2 Formation of secondary inorganic aerosols

In this study, the formation of SIAs was determined from the relative abundances of NO_3^- , nss-SO_4^{2-} , and NH_4^+ . NH_4^+ made up about 20% of the SIAs, compared to the contributions of NO_3^- and nss-SO_4^{2-} , of 38% and 42%, respectively (calculated as the molar concentration ratio ($\text{nmol m}^{-3}/\text{nmol m}^{-3}$)). The NR was used to assess the extent to which the acidic sulfate and nitrate compounds were neutralized by NH_4^+ . The TSP was of a generally acidic nature, with an NR of 0.53 ± 0.13 (mean \pm standard deviation) because of the low NH_4^+ concentration at Ny-Ålesund. This indicates a deficit of NH_4^+ in Ny-Ålesund. The nss-SO_4^{2-} aerosol at Ny-Ålesund was therefore not fully neutralized by NH_4^+ , and could remain in more acidic forms, such as NH_4HSO_4 or H_2SO_4 rather than as $(\text{NH}_4)_2\text{SO}_4$, as observed by Barrie and Barrie [1990] and report from AMAP [2006]. The presence of acidic species increased the hygroscopicity of the particles, causing them to remain as liquid-coated on the aerosol surface [Hoffman *et al.*, 2004; Laskin *et al.*, 2002].

The $[\text{NH}_4^+]/[\text{nss-SO}_4^{2-}]$ ratio was used to study ammonium nitrate formation [Squizzato *et al.*, 2013]. Previous studies have shown that $[\text{NH}_4^+]/[\text{nss-SO}_4^{2-}] > 1.5$ indicates that NH_3 can stabilize the NO_3^- , whereas $[\text{NH}_4^+]/[\text{nss-SO}_4^{2-}] < 1.5$ indicates that NO_3^- formation may depend on reactions between gas phase HNO_3 and sea salt particles [Squizzato *et al.*, 2013]. The average $[\text{NH}_4^+]/[\text{nss-SO}_4^{2-}]$ ratio was 0.57 with a range from 0 to 1.37 obtained from this study. The $[\text{NH}_4^+]/[\text{nss-SO}_4^{2-}]$ ratio less than 1.5 suggested a deficit of NH_4^+ in aerosols at

Ny-Ålesund, and thus the ionic composition of aerosols and associated reactions may not be in favor of the formation of NH_4NO_3 at this location.

4.3.3 Aerosol acidity

The $[\text{H}^+]_{\text{total}}$ ranged from 0.332 to 4.75 nmol m^{-3} in aerosols obtained during this study. The average $[\text{H}^+]_{\text{total}}$ was 3.17 nmol m^{-3} . The lowest $[\text{H}^+]_{\text{total}}$ of 0.332 was found in sample S6, which also had the nss-Mg concentration of 0.50 nmol m^{-3} and the nss-Ca concentration of 1.34 nmol m^{-3} , suggesting that acidic particles were neutralized by the Mg- and Ca-containing substances, decreasing the $[\text{H}^+]_{\text{total}}$. These cations (Mg^{2+} , Ca^{2+}) could be from a natural source (e.g., dust) [AMAP, 2006] and anthropogenic emissions (e.g., ship emissions) [Zhan *et al.*, 2014]. The remainder of the samples had undetectable Ca^{2+} and Mg^{2+} concentrations, and the $[\text{H}^+]_{\text{total}}$ ranged from 3.04 to 4.75 nmol m^{-3} . A positive correlation was found between $[\text{H}^+]_{\text{total}}$ and $[\text{nss-SO}_4^{2-}]$ ($r = 0.96$, $p = 0.008$), suggesting the $[\text{H}^+]_{\text{total}}$ in these samples could be affected by nss-SO_4^{2-} .

Free hydrogen ions in the aqueous phase of the aerosol $[\text{H}^+]_{\text{free}}$ is an important factor affecting the heterogeneous chemical processes (e.g., oxidation of SO_2 , NO_x , and organic aerosols) on particles [Pathak *et al.*, 2009]. The $[\text{H}^+]_{\text{free}}$, which was estimated using the E-AIM 4 thermodynamic model, was $3.06 \pm 0.75 \text{ nmol m}^{-3}$, which was in the range of results from previous studies at Singapore ($5.23 \pm 4.52 \text{ nmol m}^{-3}$) [Behera *et al.*, 2013] and in the Po Valley in Italy ($1.2 \pm 1.1 \text{ nmol m}^{-3}$) [Squizzato *et al.*, 2013] and lower than the sampling site in Beijing, China ($228 \pm 344 \text{ nmol m}^{-3}$) and Shanghai ($96 \pm 136 \text{ nmol m}^{-3}$), where only a small portion of $[\text{SO}_4^{2-}]$

and $[\text{NO}_3^-]$ were neutralized by ammonia [*Pathak et al.*, 2009] (see Table 4.3). The $[\text{H}^+]_{\text{free}}$ is a complex function of water content in particles, ambient temperature and the levels of SIAs. The correlations between aerosol acidity, particle species, and meteorological parameters were summarized in Table 4.4. A positive correlation was found between $[\text{nss-SO}_4^{2-}]$ and $[\text{H}]_{\text{free}}$ ($r = 0.86$, $p = 0.02$). In contrast, $[\text{NO}_3^-]$ was negatively correlated with $[\text{H}]_{\text{free}}$ ($r = -0.69$, $p = 0.13$). The displacement of Cl^- from sea salt through reactions with HNO_3 may lead to a decrease in $[\text{H}^+]$ and the formation of NO_3^- in aerosols.

The water content has been proposed to be an important parameter that could increase the hygroscopic growth of the SIAs and increase the aqueous phase acidity [*Behera et al.*, 2013]. There were no correlations between the water content and $[\text{H}^+]_{\text{free}}$, or SIAs in this study. The influence of water content on aerosol acidity is complex. Aerosols tend to contain more water under acidic conditions than under neutral conditions, and high water content is able to sorb acidic species and increase the aerosol acidity further [*Badger et al.*, 2006; *Wise et al.*, 2007]. However, high water content is in favor of absorbing acidic species and increase the aerosol acidity [*Behera et al.*, 2013].

Table 4.3 Aerosol acidities found at Ny-Ålesund and at other sites

Site	Study periods	$[\text{H}^+]_{\text{Free}}$ nmol m^{-3}	References
Ny-Ålesund, Svalbard	2012 Jul.	3.06 ± 0.75	This study
Singapore (urban site, day time)	2011 Sep.–Nov.	5.23 ± 4.52	<i>Behera et al.</i> [2013]
Singapore (urban site, nighttime time)		4.97 ± 3.69	
Mt. Tai, China (1532 m)	2007 Mar.–Apr	25.25 ± 32.23	<i>Zhou et al.</i> [2012]
	2007 Jun.–Jul.	35.27 ± 30.88	
Beijing, China (280 m rural site)	2005 Jun.–Aug.	228 ± 344	<i>Pathak et al.</i> [2009]
Shanghai, China (urban site)	2005 May–Jun.	96 ± 136	
Lanzhou, China (suburban site)	2006 Jun.–Jul.	7 ± 6	
Guangzhou, China (suburban site)	2004 May	25 ± 29	
Po Valley, Italy (Semi-rural coastal background)	2009–2010	1.2 ± 1.1	<i>Squizzato et al.</i> [2013]
Po Valley, Italy (urban background)	2009–2010	1.2 ± 1.0	
Po Valley, Italy (industrial emissions)	2009–2010	2.0 ± 1.7	

Table 4.4 Correlation matrix for the parameters measured

	F ⁻	MSA	Cl ⁻	NO ₃ ⁻	SO ₄ ²⁻	PO ₄ ³⁻	Na ⁺	NH ₄ ⁺	OC	SS	SIA _s	[H ⁺] _{free}	[H ₂ O]	NR	T	RHPAX			
F ⁻	1																		
MSA ⁻	-0.06	1																	
Cl ⁻	-0.09	-0.34	1																
NO ₃ ⁻	0.45	0.74	-0.04	1															
SO ₄ ²⁻	-0.58	0.07	0.64	-0.21	1														
-	-0.73	0.13	0.41	-0.33	.96**	1													
PO ₄ ³⁻	-0.42	0.23	0.44	-0.10	.93**	.92**	1												
Na ⁺	0.14	-0.14	.95**	0.22	0.57	0.31	0.45	1											
NH ₄ ⁺	-0.68	0.1	-0.30	-0.14	-0.11	0.05	-0.26	-0.50	1										
OC	-0.35	0.19	0.76	0.07	.91*	0.78	.82*	0.78	-0.30	1									
SS	0.04	-0.23	.98**	0.11	0.61	0.36	0.45	.99**	-0.42	0.78	1								
SIA _s	-0.65	0.52	0.35	0.14	.86*	.876*	.85*	0.34	0.16	0.79	0.35	1							
[H ⁺] _{free}	- .88*	-0.13	0.14	-0.69	0.72	.862*	0.64	-0.08	0.33	0.42	0.02	0.6	1						
[H ⁺] _{total}	0.04	-0.35	-0.44	-0.23	-0.76	-0.68	- .91*	-0.57	0.49	-0.76	-0.52	-0.73	-0.26	1					
[H ₂ O]	-0.09	-0.31	.95**	0.06	0.46	0.22	0.2	.89*	-0.13	0.64	.93**	0.24	-0.01	-0.20	1				
NR	-0.68	0.01	-0.34	-0.26	-0.17	0	-0.34	-0.56	*	-0.35	-0.47	0.05	0.35	0.62	-0.16	1			
T	-0.31	0.6	-0.73	0.21	-0.19	0.04	0	-0.72	0.6	-0.39	-0.73	0.25	0.15	0.04	-0.72	0.51	1		
RH	-0.47	0.29	0.25	0.31	0.1	0.06	-0.16	0.17	0.63	0.23	0.21	0.33	0.02	0.26	0.48	0.61	0.07	1	
PAX	-0.03	0.33	0.56	0.23	0.72	0.59	0.73	0.69	-0.60	.90*	0.64	0.62	0.18	-0.78	0.42	-0.62	-0.41	0	1

The numbers in bold were statistically significant; * = Correlation is significant at the 0.05 level (2-tailed); ** = Correlation is significant at the 0.01 level (2-tailed).

4.3.4 Chloride depletion

The Cl^- depletion only occurred in samples 2 and 6, at about 11% and 22%, respectively when both sea salt concentrations and excess acidic species concentrations (defined as $[\text{nss-SO}_4^{2-} + \text{NO}_3^- - \text{NH}_4^+]$) were high, based on the assumption that SO_4^{2-} and NO_3^- were neutralized by NH_4^+ and that the remaining of SO_4^{2-} and NO_3^- reacted with sea salt. The Cl^- depletion occurred in sample 6 collected when cruise ships visited Ny-Ålesund. In this sample, nss-SO_4^{2-} was doubled and NO_3^- was comparable to the samples collected when few cruise ships visited [Zhan *et al.*, 2014]. This suggested that the Cl^- depletion was affected by nss-SO_4^{2-} from ship emissions. A higher degree of Cl^- depletion (22%) in sample 2 was associated with the highest $\text{NO}_3^-/\text{nss-SO}_4^{2-}$ ratio 1.44, but the $[\text{NH}_4^+]/[\text{nss-SO}_4^{2-}]$ ratio in this sample was 0.01, lower than 1.5. This suggested that gas-phase reaction involves HNO_3 and sea salt particles could be important for Cl^- depletion in this area during summer. Similar results were found by Sirois and Barrie [1999], who suggested that alkaline sea salt surfaces are preferred by gaseous acids, such as HNO_3 , over the more acidic anthropogenic SO_4^{2-} particles. The Cl^- depletion didn't occur in other samples. A positive correlation was found between $[\text{Cl}^-]$ and $[\text{H}_2\text{O}]$ ($r = 0.95$, $p = 0.004$), indicating that $[\text{Cl}^-]$ can remain in the aqueous phase in a high humidity environment at the low temperatures over the Arctic. No significant correlation was found between Cl^- depletion and $[\text{H}]_{\text{free}}$ ($r = 0.14$, $p = 0.79$). The Cl^- depletion from sea salt aerosol resulting from reactions with acidic species is often a function of particle sizes [Quinn *et al.*, 2002]. However, the results from this study were not sufficient to address this issue that will be explored through future studies.

4.3.5 Organic carbon and elemental carbon

The OC concentrations measured in this study ranged from 13.8 to 64.4 ng m⁻³, with a mean of 55 ng m⁻³. This range is comparable to those found over the Arctic Ocean [Chang *et al.*, 2011] and at Barrow, Alaska [Shaw *et al.*, 2010]. The mean OC/EC ratio in our study was 45, which was relatively high compared with the ratios typically found for domestic combustion, bio-fuel combustion, and open biomass burning [AMAP, 2011]. High OC concentrations could be caused by organic matter from seawater. A significant relationship was found between the sea salt and OC concentrations in aerosols ($R^2 = 0.62$, $p = 0.074$) (see Figure 4.4a), suggesting that marine sources could be important contributors to OC in the air. This could be linked to biogenic emissions of gases from the ocean in summer, which could be photo-oxidized to form particulate organic matter. Similar results were found in previous research. For example, organic matter was found to be a major component in marine aerosol [Facchini *et al.*, 2008; O'Dowd *et al.*, 2008]. Weinbruch *et al.* [2012] found significant carbon signals in the X-ray spectra of aerosols, possibly originating from humic or humic-like substances in the marine environment. In addition, a strong correlation was found between the OC concentration and the number of ship passengers (PAX) ($R^2=0.80$, $p=0.015$) (see Figure 4.4b), indicating that emissions from ships were among major contributors to the OC concentrations in aerosols in Ny-Ålesund. The OC concentrations were more than ten times higher than the EC concentrations in emissions from low-speed marine diesel engines [Agrawal *et al.*, 2008], and high OC concentrations have been found to be emitted by ship emissions [AMAP, 2011]. Open biomass burning has been also found to give higher particulate organic matter/black carbon ratios than the combustion of biofuels. Wood smoke from

forest fires is one of the most important sources of aerosols in the Arctic in summer [Stohl *et al.*, 2006]. The nss-K^+ is a useful tracer for aerosols derived from biomass burning [Quinn *et al.*, 2002]. However, in this study, nss-K^+ was undetectable, indicating that biomass burning did not contribute to the TSP. Regression analysis showed that the sea salt concentration and the ship emissions together explained 88% ($p = 0.043$) of the variance in the OC concentration. Therefore, marine sources and emissions from ships play important roles in controlling the OC abundance in aerosols at Ny-Ålesund. Similar results were found by [Shaw *et al.*, 2010], who suggested that the organic mass found in aerosols at Barrow, Alaska, was associated with both combustion and ocean-derived sources. Other factors may also contribute to the OC abundance, such as secondary organic aerosol formed through the oxidization of volatile organic compounds by $\text{HO}\cdot$ radicals [Kanakidou *et al.*, 2005].

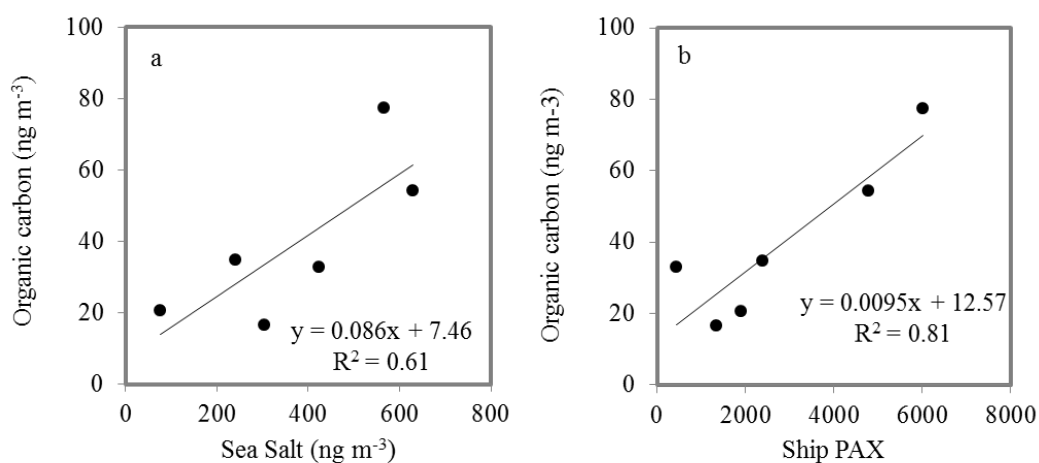


Figure 4.4 (a) The relationships between the organic carbon and sea salt concentrations. (b) The relationship between the organic carbon concentrations and the number of ship passengers.

4.4 Conclusions

The results from this study showed that sea salt was a dominant aerosol component, accounting 46% of the aerosol mass concentration. SIAs accounted for 33% of the water soluble ionic species in aerosols, making up with 42% nss-SO_4^{2-} , 38% of NO_3^- , and 20% of NH_4^+ , respectively. The mean of OC was 55 ng m^{-3} , contributed by both marine and ship emissions.

The mean neutralization ratio was 0.53, indicating that there was a deficit of NH_4^+ and that SO_4^{2-} might remain in more acidic forms, such as NH_4HSO_4 or H_2SO_4 , rather than forming $(\text{NH}_4)_2\text{SO}_4$. The E-AIM 4 simulation results showed that the aerosols were generally acidic, with $[\text{H}^+]_{\text{free}} = 3.06 \pm 0.75 \text{ nmol m}^{-3}$.

The Cl^- depletion of 11% and 22% was evident in two samples. High $[\text{nss-SO}_4^{2-} + \text{NO}_3^- - \text{NH}_4^+]$ concentrations were found when the Cl^- depletion in those samples occurred, and this coincided with high sea salt concentrations. This indicates that the mixing of sea salt and excess acidic species $[\text{nss-SO}_4^{2-} + \text{NO}_3^- - \text{NH}_4^+]$ resulted in the Cl^- depletion. There was no clear correlation between $[\text{H}^+]_{\text{free}}$ and Cl^- depletion.

The aerosol measurements presented here allowed evaluating the formation of secondary inorganic aerosols, aerosol acidity, and Cl^- depletion. More investigations on the size distributions of aerosol particles over a longer period are needed to further assess these processes in order to better understand their impacts on atmospheric chemistry and regional climate.

Acknowledgments

This work was funded by the National Natural Science Foundation of China (41105094). The Chinese Arctic and Antarctic Administration of the State Oceanic Administration of China supported the field accommodation at YRS. Support was also provided by Rutgers University for the continuation and completion of this research. We gratefully acknowledge the NOAA Air Resources Laboratory (ARL) for the provision of HYSPLIT transport and dispersion model and NCAR/NCEP for providing the meteorological data freely. We thank Elisabeth Bjerke Råstad at Kings Bay AS for supplying the harbor log.

Chapter 5: Conclusions and future work

5.1. Overall conclusions

EBC calculated from aethalometer measurements of light attenuation, selected trace elements, ionic species and organic/elemental carbon in aerosols and elemental composition of local soils were measured to determine chemical composition, their potential sources and sinks, and the chemical properties of aerosols at Ny-Ålesund in summer. The major conclusions from this study are as follows.

The median EBC concentration of 17 ng m^{-3} was observed in the settlement of Ny-Ålesund, which was higher than median values (5.4 ng m^{-3}) observed outside the settlement. This suggests that EBC concentrations measured in the settlement were influenced by local emissions. The average emission rate at Ny-Ålesund was 8.1 g h^{-1} , equivalent to the EBC emissions from about five light duty vehicles, or half the BC emissions from a bus, in constant operation. Total deposition from local emissions estimated to be $6.4\text{--}4.4 \text{ ng m}^{-2} \text{ h}^{-1}$. This may affect snow black carbon concentrations in nearby glaciated areas. This suggests that local human activities might impact the concentration of EBC at Ny-Ålesund in the summer.

The highest concentration of TSP was observed in the sample collected when two cruise ships with more than 1500 passengers visited Ny-Ålesund, which was 2290 ng m^{-3} , three times higher than the median value of the sampling period. The concentrations of nss-SO_4^{2-} (203 ng m^{-3}) were about three times higher. The concentration of OC (64.4 ng m^{-3}) and EC (2.3 ng m^{-3}) was doubled. The nc-V

concentration reached 0.976 ng m^{-3} , about 38-fold higher, and the concentrations of nc-Ni were 0.572 ng m^{-3} , which was 8-fold higher when compared to the mean value of the sampling period. This indicated that ship emissions contributed significantly to the concentrations and compositions of particulate matter in the ambient air at this location in the summer. When few ships were present, aerosols at this location and the concentrations of anthropogenic elements (nc-V, nc-Mn, Cr, Ni, Pb, As, Se) were low; however, anthropogenic signal reflected by nc-V/nc-Mn and enrichment factor can be seen in the air arriving from the North American Arctic, Iceland and North Eurasia in Ny-Ålesund in the summer.

Sea salt was a dominant aerosol component, accounting for 46% of the aerosol mass concentration. SIAs accounted for 33% of the water soluble ionic species in aerosols, making up 42% of nss-SO_4^{2-} , 38% of NO_3^- , and 20% of NH_4^+ , respectively. The mean of OC was 55 ng m^{-3} , and 88% of the variance in OC could be explained by oceanic emissions and ship emissions. The mean neutralization ratio was 0.53, indicating that there was a deficit of NH_4^+ and that SO_4^{2-} might remain in more acidic forms, such as NH_4HSO_4 or H_2SO_4 , rather than forming $(\text{NH}_4)_2\text{SO}_4$. Aerosols were generally acidic, with $[\text{H}^+]_{\text{free}} = 3.06 \pm 0.75 \text{ nmol m}^{-3}$. The Cl^- depletion of 11% and 22% was evident in the samples with high $[\text{nss-SO}_4^{2-} + \text{NO}_3^- - \text{NH}_4^+]$ concentrations and high sea salt concentrations, indicating the interaction of sea salt and excess acidic species $[\text{nss-SO}_4^{2-} + \text{NO}_3^- - \text{NH}_4^+]$.

5.2. Recommendations for future research

Arduous effort has been dedicated to studying aerosol emissions, concentrations, transport and aerosol climate forcing in the last decade. However, the implemented measurements and analyses could elucidate the characterization of aerosols in the Arctic, including:

- a. Long-term measurements of aerosol chemical composition, size distributions, mixing states (internal or external mixture), and aerosol scattering/absorption coefficients should be obtained to improve source identification and to evaluate aerosol climate forcing.
- b. Additional vertical observations should be carried out to obtain vertical profiles of aerosols in the Arctic.
- c. Implement routine measurements of rain and snow to investigate aerosol deposition processes and sources of deposited aerosols.

Reference

- Abbatt, J. P. D., S. Benz, D. J. Cziczo, Z. Kanji, U. Lohmann, and O. Möhler (2006), Solid ammonium sulfate aerosols as ice nuclei: a pathway for cirrus cloud formation, *Science*, 313(5794), 1770-1773, doi:10.1126/science.1129726.
- Agrawal, H., Q. G. J. Malloy, W. A. Welch, J. W. Miller, and D. R. Cocker, III (2008), In-use gaseous and particulate matter emissions from a modern ocean going container vessel, *Atmospheric Environment*, 42(21), 5504-5510, doi:10.1016/j.atmosenv.2008.02.053.
- Agrawal, H., W. A. Welch, S. Henningsen, J. W. Miller, and D. R. Cocker (2010), Emissions from main propulsion engine on container ship at sea, *Journal of Geophysical Research: Atmospheres*, 115, D23205, doi:10.1029/2009jd013346.
- Allan, B. J., G. McFiggans, J. M. C. Plane, H. Coe, and G. G. McFadyen (2000), The nitrate radical in the remote marine boundary layer, *Journal of Geophysical Research: Atmospheres*, 105(D19), 24191-24204, doi:10.1029/2000JD900314.
- AMAP (2006), *AMAP Assessment 2006: Acidifying Pollutants, Arctic Haze, and Acidification in the Arctic*. Arctic Monitoring and Assessment Programme (AMAP), Oslo, Norway. xii+112 pp.
- AMAP (2011), *The Impact of Black Carbon on Arctic Climate (2011)*. By: P.K. Quinn, A. Stohl, A. Arneth, T. Berntsen, J. F. Burkhart, J. Christensen, M. Flanner, K. Kupiainen, H. Lihavainen, M. Shepherd, V. Shevchenko, H. Skov, and V. Vestreng. Arctic Monitoring and Assessment Programme (AMAP), Oslo. 72 pp
- Anderson, J. R., P. R. Buseck, D. A. Saucy, and J. M. Pacyna (1992), Characterization of individual fine-fraction particles from the Arctic aerosol at Spitsbergen, May–June 1987, *Atmospheric Environment. Part A. General Topics*, 26(9), 1747-1762, doi:10.1016/0960-1686(92)90072-S.
- Badger, C. L., I. George, P. T. Griffiths, C. F. Braban, R. A. Cox, and J. P. D. Abbatt (2006), Phase transitions and hygroscopic growth of aerosol particles containing humic acid and mixtures of humic acid and ammonium sulphate, *Atmospheric Chemistry and Physics*, 6(3), 755-768, doi:10.5194/acp-6-755-2006.
- Barrie, L. A. (1996), *Occurrence and trends of pollution in the Arctic troposphere, in Chemical Exchange Between the Atmosphere and Polar Snow*, 93-130 pp., NATO ASI Ser., New York.
- Barrie, L. A., and M. J. Barrie (1990), Chemical components of lower tropospheric aerosols in the high Arctic: Six years of observations, *Journal of Atmospheric Chemistry*, 11(3), 211-226, doi:10.1007/BF00118349.
- Barrie, L. A., and R. M. Hoff (1985), Five years of air chemistry observations in the Canadian Arctic, *Atmospheric Environment*, 19(12), 1995-2010, doi:10.1016/0004-6981(85)90108-8.

- Barwise, A. J. G. (1990), Role of nickel and vanadium in petroleum classification, *Energ Fuel*, 4(6), 647-652, doi:10.1021/ef00024a005.
- Bates, T. S., J. A. Calhoun, and P. K. Quinn (1992), Variations in the methanesulfonate to sulfate molar ratio in submicrometer marine aerosol particles over the south Pacific Ocean, *Journal of Geophysical Research: Atmospheres*, 97(D9), 9859-9865, doi:10.1029/92JD00411.
- Bauer, S. E., and S. Menon (2012), Aerosol direct, indirect, semidirect, and surface albedo effects from sector contributions based on the IPCC AR5 emissions for preindustrial and present-day conditions, *Journal of Geophysical Research: Atmospheres*, 117, D01206, doi:10.1029/2011JD016816.
- Becagli, S., et al. (2012), Evidence for heavy fuel oil combustion aerosols from chemical analyses at the island of Lampedusa: a possible large role of ships emissions in the Mediterranean, *Atmospheric Chemistry and Physics*, 12(7), 3479-3492, doi:10.5194/acp-12-3479-2012.
- Behera, S. N., R. Betha, P. Liu, and R. Balasubramanian (2013), A study of diurnal variations of PM_{2.5} acidity and related chemical species using a new thermodynamic equilibrium model, *Science of the Total Environment*, 452-453(0), 286-295, doi:10.1016/j.scitotenv.2013.02.062.
- Behrenfeldt, U., R. Krejci, J. Strom, and A. Stohl (2008), Chemical properties of Arctic aerosol particles collected at the Zeppelin station during the aerosol transition period in May and June of 2004, *Tellus Series B: Chemical and Physical Meteorology*, 60(3), 405-415, doi:10.1111/j.1600-0889.2008.00349.x.
- Berg, T., R. Kallenborn, and S. Manø (2004), Temporal trends in atmospheric heavy metal and organochlorine concentrations at Zeppelin, Svalbard, *Arctic, Antarctic, and Alpine Research*, 36(3), 284-291, doi:10.1657/1523-0430(2004)036[0284:TTIAHM]2.0.CO;2.
- Bond, T. C., et al. (2013), Bounding the role of black carbon in the climate system: A scientific assessment, *Journal of Geophysical Research: Atmospheres*, 118(11), 5380-5552, doi:10.1002/jgrd.50171.
- Bourgeois, Q., and I. Bey (2011), Pollution transport efficiency toward the Arctic: Sensitivity to aerosol scavenging and source regions, *Journal of Geophysical Research: Atmospheres*, 116, D08213, doi:10.1029/2010JD015096.
- Chang, R. Y. W., et al. (2011), Aerosol composition and sources in the central Arctic Ocean during ASCOS, *Atmospheric Chemistry and Physics*, 11(20), 10619-10636, doi:10.5194/acp-11-10619-2011.
- Chen, L., J. Wang, Y. Gao, G. Xu, X. Yang, Q. Lin, and Y. Zhang (2012), Latitudinal distributions of atmospheric MSA and MSA/nss-SO₄²⁻ ratios in summer over the high latitude regions of the Southern and Northern Hemispheres, *Journal of Geophysical Research: Atmospheres*, 117, D10306, doi:10.1029/2011jd016559.

- Corbett, J. J., D. A. Lack, J. J. Winebrake, S. Harder, J. A. Silberman, and M. Gold (2010), Arctic shipping emissions inventories and future scenarios, *Atmospheric Chemistry and Physics*, 10(19), 9689-9704, doi:10.5194/acp-10-9689-2010.
- Dalsøren, S. B., Ø. Endresen, I. S. A. Isaksen, G. Gravir, and E. Sørgård (2007), Environmental impacts of the expected increase in sea transportation, with a particular focus on oil and gas scenarios for Norway and northwest Russia, *Journal of Geophysical Research: Atmospheres*, 112, D02310, doi:10.1029/2005JD006927.
- Dalsøren, S. B., B. H. Samset, G. Myhre, J. J. Corbett, R. Minjares, D. Lack, and J. S. Fuglestad (2013), Environmental impacts of shipping in 2030 with a particular focus on the Arctic region, *Atmospheric Chemistry and Physics*, 13(4), 1941-1955, doi:10.5194/acp-13-1941-2013.
- DeAngelo, B. E. (2011), *An assessment of emissions and mitigation options for black carbon for the Arctic Council. Technical report of the Arctic Council Task Force on Short-Lived Climate Forcers*. Tromsø: Arctic Council.
- Decesari, S., M. Mircea, F. Cavalli, S. Fuzzi, F. Moretti, E. Tagliavini, and M. C. Facchini (2007), Source attribution of water-soluble organic aerosol by nuclear magnetic resonance spectroscopy, *Environmental Science & Technology*, 41(7), 2479-2484, doi:10.1021/Es061711l.
- Devasthale, A., U. Willén, K. G. Karlsson, and C. G. Jones (2010), Quantifying the clear-sky temperature inversion frequency and strength over the Arctic Ocean during summer and winter seasons from AIRS profiles, *Atmospheric Chemistry and Physics*, 10(12), 5565-5572, doi:10.5194/acp-10-5565-2010.
- Di Liberto, L., et al. (2012), Estimate of the Arctic Convective Boundary Layer Height from Lidar Observations: A Case Study, *Advances in Meteorology*, 2012, 851927, doi:10.1155/2012/851927.
- Doherty, S. J., S. G. Warren, T. C. Grenfell, A. D. Clarke, and R. E. Brandt (2010), Light-absorbing impurities in Arctic snow, *Atmospheric Chemistry and Physics*, 10(23), 11647-11680, doi:10.5194/acp-10-11647-2010.
- Draxier, R. R., and G. D. Hess (1998), An overview of the HYSPLIT_4 modelling system for trajectories, dispersion and deposition, *Australian Meteorological Magazine*, 47(4), 295-308.
- Eckhardt, S., O. Hermansen, H. Grythe, M. Fiebig, K. Stebel, M. Cassiani, A. Baecklund, and A. Stohl (2013), The influence of cruise ship emissions on air pollution in Svalbard - a harbinger of a more polluted Arctic?, *Atmospheric Chemistry and Physics*, 13(16), 8401-8409, doi:10.5194/acp-13-8401-2013.
- Eleftheriadis, K., S. Vratolis, and S. Nyeki (2009), Aerosol black carbon in the European Arctic: Measurements at Zeppelin station, Ny-Ålesund, Svalbard from 1998–2007, *Geophysical Research Letters*, 36, L02809, doi:10.1029/2008gl035741.

- Engvall, A. C., R. Krejci, J. Ström, R. Treffeisen, R. Scheele, O. Hermansen, and J. Paatero (2008), Changes in aerosol properties during spring-summer period in the Arctic troposphere, *Atmospheric Chemistry and Physics*, 8(3), 445-462, doi:10.5194/acp-8-445-2008.
- Facchini, M. C., et al. (2008), Primary submicron marine aerosol dominated by insoluble organic colloids and aggregates, *Geophysical Research Letters*, 35, L17814, doi:10.1029/2008gl034210.
- Feldman, G. C., and C. R. McClain (2009), Ocean Color Web, MODIS-Aqua Reprocessing 2009.1, NASA Goddard Space Flight Center. Eds. Kuring, N., Bailey, S. W. May 2010. <http://oceancolor.gsfc.nasa.gov/>. MODIS Monthly Chlorophyll concentration, http://oceancolor.gsfc.nasa.gov/cgi/l3/A20121532012182.L3m_MO_CHL_chlor_a_9km.png?sub=img.
- Finlayson-Pitts, B. J. (2003), The Tropospheric Chemistry of Sea Salt: A Molecular-Level View of the Chemistry of NaCl and NaBr, *Chemical Review*, 103(12), 4801-4822, doi:10.1021/cr020653t.
- Fisher, J. A., et al. (2011), Sources, distribution, and acidity of sulfate-ammonium aerosol in the Arctic in winter-spring, *Atmospheric environment*, 45(39), 7301-7318, doi:10.1016/j.atmosenv.2011.08.030.
- Flanner, M. G., C. S. Zender, P. G. Hess, N. M. Mahowald, T. H. Painter, V. Ramanathan, and P. J. Rasch (2009), Springtime warming and reduced snow cover from carbonaceous particles, *Atmospheric Chemistry and Physics*, 9(7), 2481-2497, doi:10.5194/acp-9-2481-2009.
- Friese, E., and A. Ebel (2010), Temperature Dependent Thermodynamic Model of the System $\text{H}^+ - \text{NH}_4^+ - \text{Na}^+ - \text{SO}_4^{2-} - \text{NO}_3^- - \text{Cl}^- - \text{H}_2\text{O}$, *The Journal of Physical Chemistry A*, 114(43), 11595-11631, doi:10.1021/jp101041j.
- Gao, Y., G. Xu, J. Zhan, J. Zhang, W. Li, Q. Lin, L. Chen, and H. Lin (2013), Spatial and particle size distributions of atmospheric dissolvable iron in aerosols and its input to the Southern Ocean and coastal East Antarctica, *Journal of Geophysical Research: Atmospheres*, 118(22), 2013JD020367, doi:10.1002/2013JD020367.
- Garrett, T. J., S. Brattstrom, S. Sharma, D. E. J. Worthy, and P. Novelli (2011), The role of scavenging in the seasonal transport of black carbon and sulfate to the Arctic, *Geophysical Research Letters*, 38, L16805, doi:10.1029/2011gl048221.
- Geng, H., J. Ryu, H.-J. Jung, H. Chung, K.-H. Ahn, and C.-U. Ro (2010), Single-Particle Characterization of Summertime Arctic Aerosols Collected at Ny-Ålesund, Svalbard, *Environmental Science & Technology*, 44(7), 2348-2353, doi:10.1021/es903268j.
- Girard, E., G. Dueymes, P. Du, and A. K. Bertram (2013), Assessment of the effects of acid-coated ice nuclei on the Arctic cloud microstructure, atmospheric

- dehydration, radiation and temperature during winter, *International Journal of Climatology*, 33(3), 599-614, doi:10.1002/joc.3454.
- Granier, C., U. Niemeier, J. H. Jungclaus, L. Emmons, P. Hess, J. F. Lamarque, S. Walters, and G. P. Brasseur (2006), Ozone pollution from future ship traffic in the Arctic northern passages, *Geophysical Research Letters*, 33, L13807, doi:10.1029/2006GL026180.
- Hadley, O. L., and T. W. Kirchstetter (2012), Black-carbon reduction of snow albedo, *Nature Climate Change*, 2(4), 437-440, doi:10.1038/nclimate1433.
- Hagen, D., O. I. Vistad, N. E. Eide, A. C. Flyen, and K. Fangel (2012), Perspective: Managing visitor sites in Svalbard: from a precautionary approach towards knowledge-based management, *Polar Research*, 31, 18432, doi:10.3402/polar.v31i0.18432.
- Hansen, A. D. A., J. R. Turner, and A. G.A. (2007), An algorithm to compensate Aethalometer™ data for the effects of optical shadowing and scattering, in *Paper presented at the 5th Asian Aerosol Conference, 26-29 August, Kaohsiung, Taiwan.*, edited.
- Hegg, D. A., A. D. Clarke, S. J. Doherty, and J. StrÖM (2011), Measurements of black carbon aerosol washout ratio on Svalbard, *Tellus Series B: Chemical and Physical Meteorology*, 63(5), 891-900, doi:10.1111/j.1600-0889.2011.00577.x.
- Heintzenberg, J., H.-C. Hansson, and H. Lannefors (2011), The chemical composition of arctic haze at Ny-Ålesund, Spitsbergen, *Tellus Series A: Dynamic Meteorology and Oceanography*, 33(2), 162-171, doi:10.1111/j.2153-3490.1981.tb01741.x.
- Heintzenberg, J., and C. Leck (1994), Seasonal variation of the atmospheric aerosol near the top of the marine boundary layer over Spitsbergen related to the Arctic sulphur cycle*, *Tellus Series B: Chemical and Physical Meteorology*, 46(1), 52-67, doi:10.1034/j.1600-0889.1994.00005.x.
- Held, A., D. A. Orsini, P. Vaattovaara, M. Tjernstrom, and C. Leck (2011), Near-surface profiles of aerosol number concentration and temperature over the Arctic Ocean, *Atmospheric Measurement Techniques*, 4(8), 1603-1616, doi:10.5194/amt-4-1603-2011.
- Hermansen, O., J. Wasseng, A. Bäcklund, B. Noon, T. Hennig, D. Schulze, and V. L. Barth (2011), *Air quality Ny-Ålesund. Monitoring of local air quality 2008-2010. Measurement results*. Kjeller, Norway: Norwegian Institute for Air Research.
- Hirdman, D., J. F. Burkhart, H. Sodemann, S. Eckhardt, A. Jefferson, P. K. Quinn, S. Sharma, J. Strom, and A. Stohl (2010a), Long-term trends of black carbon and sulphate aerosol in the Arctic: changes in atmospheric transport and source region emissions, *Atmospheric Chemistry and Physics*, 10(19), 9351-9368, doi:DOI 10.5194/acp-10-9351-2010.

- Hirdman, D., H. Sodemann, S. Eckhardt, J. F. Burkhart, A. Jefferson, T. Mefford, P. K. Quinn, S. Sharma, J. Ström, and A. Stohl (2010b), Source identification of short-lived air pollutants in the Arctic using statistical analysis of measurement data and particle dispersion model output, *Atmospheric Chemistry and Physics*, *10*(2), 669-693, doi:10.5194/acp-10-669-2010, 2010.
- Hoffman, R. C., A. Laskin, and B. J. Finlayson-Pitts (2004), Sodium nitrate particles: physical and chemical properties during hydration and dehydration, and implications for aged sea salt aerosols, *Journal of Aerosol Science*, *35*(7), 869-887, doi:DOI 10.1016/j.jaerosci.2004.02.003.
- Hole, L. R., J. H. Christensen, T. Ruoho-Airola, K. Torseth, V. Ginzburg, and P. Glowacki (2009), Past and future trends in concentrations of sulphur and nitrogen compounds in the Arctic, *Atmospheric Environment*, *43*(4), 928-939, doi:10.1016/j.atmosenv.2008.10.043.
- Hopke, P. K., L. A. Barrie, S. M. Li, M. D. Cheng, C. Li, and Y. Xie (1995), Possible sources and preferred pathways for biogenic and non-sea-salt sulfur for the high Arctic, *Journal of Geophysical Research: Atmospheres*, *100*(D8), 16595-16603, doi:10.1029/95JD01712.
- Huang, L., S. L. Gong, S. Sharma, D. Lavoue, and C. Q. Jia (2010), A trajectory analysis of atmospheric transport of black carbon aerosols to Canadian high Arctic in winter and spring (1990-2005), *Atmospheric Chemistry and Physics*, *10*(11), 5065-5073, doi:10.5194/acp-10-5065-2010.
- IPCC (2007), Climate change 2007: The physical science basis. Contribution of Working Group I to the fourth assessment report of the Intergovernmental Panel on Climate Change, 996pp., 2007.
- IPCC (2013), IPCC, 2013: Climate Change 2013: The Physical Science Basis. Contribution of Working Group I to the Fifth Assessment Report of the Intergovernmental Panel on Climate Change, edited by: Stocker, T. F., Qin, D., Plattner, G.-K., Tignor, M., Allen, S. K., Boschung, J., Nauels, A., Xia, Y., Bex, V., and Midgley, P. M., Cambridge University Press, Cambridge, United Kingdom and New York, NY, USA, 1535 pp., 2013.
- Jacob, D. J., et al. (2010), The Arctic Research of the Composition of the Troposphere from Aircraft and Satellites (ARCTAS) mission: design, execution, and first results, *Atmospheric Chemistry and Physics*, *10*(11), 5191-5212, doi:10.5194/acp-10-5191-2010.
- Johnson, M. R., R. W. Devillers, and K. A. Thomson (2011), Quantitative Field Measurement of Soot Emission from a Large Gas Flare Using Sky-LOSA, *Environmental Science & Technology*, *45*(1), 345-350, doi:10.1021/es102230y.
- Jouan, C., J. Pelon, E. Girard, G. Ancellet, J. P. Blanchet, and J. Delanoë (2014), On the relationship between Arctic ice clouds and polluted air masses over the North

- Slope of Alaska in April 2008, *Atmospheric Chemistry and Physics*, 14(3), 1205-1224, doi:10.5194/acp-14-1205-2014.
- Kanakidou, M., et al. (2005), Organic aerosol and global climate modelling: a review, *Atmospheric Chemistry and Physics*, 5(4), 1053-1123, doi:10.5194/acp-5-1053-2005.
- Keene, W. C., and D. L. Savoie (1998), The pH of deliquesced sea-salt aerosol in polluted marine air, *Geophysical Research Letters*, 25(12), 2181-2184, doi:10.1029/98gl01591.
- Keogh, D. U., J. Kelly, K. Mengersen, R. Jayaratne, L. Ferreira, and L. Morawska (2010), Derivation of motor vehicle tailpipe particle emission factors suitable for modelling urban fleet emissions and air quality assessments, *Environ Sci Pollut R*, 17(3), 724-739, doi:10.1007/s11356-009-0210-9.
- Kerminen, V.-M., and C. Leck (2001), Sulfur chemistry over the central Arctic Ocean during the summer: Gas-to-particle transformation, *Journal of Geophysical Research: Atmospheres*, 106(D23), 32 087-032 099, doi:10.1029/2000jd900604.
- Klonecki, A., P. Hess, L. Emmons, L. Smith, J. Orlando, and D. Blake (2003), Seasonal changes in the transport of pollutants into the Arctic troposphere-model study, *Journal of Geophysical Research: Atmospheres*, 108(D4), 8367, doi:10.1029/2002JD002199.
- Koch, D., et al. (2011), Coupled Aerosol-Chemistry-Climate Twentieth-Century Transient Model Investigation: Trends in Short-Lived Species and Climate Responses, *Journal of Climate*, 24(11), 2693-2714, doi:10.1175/2011JCLI3582.1.
- Lack, D., B. Lerner, C. Granier, T. Baynard, E. Lovejoy, P. Massoli, A. R. Ravishankara, and E. Williams (2008), Light absorbing carbon emissions from commercial shipping, *Geophysical Research Letters*, 35, L13815, doi:10.1029/2008GL033906.
- Laskin, A., M. J. Iedema, and J. P. Cowin (2002), Quantitative time-resolved monitoring of nitrate formation in sea salt particles using a CCSEM/EDX single particle analysis, *Environmental Science & Technology*, 36(23), 4948-4955, doi:10.1021/es020551k.
- Law, K. S., and A. Stohl (2007), Arctic air pollution: Origins and impacts, *Science*, 315(5 818), 1537-1540, doi:10.1126/science.1137695.
- Leaitch, W. R., et al. (2013), Dimethyl sulfide control of the clean summertime Arctic aerosol and cloud, *Elementa: Science of the Anthropocene*, 1(1), 000017, doi:10.12952/journal.elementa.000017.
- Leck, C., J. Heintzenberg, and M. Engardt (2002), A meridional profile of the chemical composition of submicrometre particles over the East Atlantic Ocean:

- regional and hemispheric variabilities, *Tellus Series B: Chemical and Physical Meteorology*, 54(4), 377-394, doi:10.1034/j.1600-0889.2002.01318.x.
- Leck, C., and C. Persson (1996a), The central Arctic Ocean as a source of dimethyl sulfide - Seasonal variability in relation to biological activity, *Tellus Series B: Chemical and Physical Meteorology*, 48(2), 156-177, doi:DOI 10.1034/j.1600-0889.1996.t01-1-00003.x.
- Leck, C., and C. Persson (1996b), Seasonal and short-term variability in dimethyl sulfide, sulfur dioxide and biogenic sulfur and sea salt aerosol particles in the arctic marine boundary layer during summer and autumn, *Tellus Series B: Chemical and Physical Meteorology*, 48(2), 272-299, doi:10.1034/j.1600-0889.48.issue2.1.x.
- Lee, D. S., et al. (2010), Transport impacts on atmosphere and climate: Aviation, *Atmospheric Environment*, 44(37), 4678-4734, doi:10.1016/j.atmosenv.2009.06.005.
- Li, S.-M., and L. A. Barrie (1993), Biogenic sulfur aerosol in the Arctic troposphere: 1. Contributions to total sulfate, *Journal of Geophysical Research: Atmospheres*, 98(D11), 20613-20622, doi:10.1029/93JD02234.
- Liu, J., S. Fan, L. W. Horowitz, and H. Levy, II (2011), Evaluation of factors controlling long-range transport of black carbon to the Arctic, *Journal of Geophysical Research: Atmospheres*, 116, D04307, doi:10.1029/2010jd015145.
- Mölders, N., S. E. Porter, C. F. Cahill, and G. A. Grell (2010), Influence of ship emissions on air quality and input of contaminants in southern Alaska National Parks and Wilderness Areas during the 2006 tourist season, *Atmospheric Environment*, 44(11), 1400-1413, doi:10.1016/j.atmosenv.2010.02.003.
- Maenhaut, W., and P. Cornille (1989), Trace element composition and origin of the atmospheric aerosol in the Norwegian arctic, *Atmospheric Environment*, 23(11), 2551-2569, doi:10.1016/0004-6981(89)90266-7.
- Malm, W. C., M. L. Pitchford, C. McDade, and L. L. Ashbaugh (2007), Coarse particle speciation at selected locations in the rural continental United States, *Atmospheric Environment*, 41(10), 2225-2239, doi:10.1016/j.atmosenv.2006.10.077.
- Malm, W. C., J. F. Sisler, D. Huffman, R. A. Eldred, and T. A. Cahill (1994), Spatial and seasonal trends in particle concentration and optical extinction in the United States, *Journal of Geophysical Research: Atmospheres*, 99(D1), 1347-1370, doi:10.1029/93jd02916.
- Martin, S. T., H. M. Hung, R. J. Park, D. J. Jacob, R. J. D. Spurr, K. V. Chance, and M. Chin (2004), Effects of the physical state of tropospheric ammonium-sulfate-nitrate particles on global aerosol direct radiative forcing, *Atmospheric Chemistry and Physics*, 4, 183-214, doi:10.5194/acp-4-183-2004.

- Millero, F. J. (2013), *Chemical oceanography*, Fourth edition, 591 pp., CRC Press, Boca Raton, FL.
- Nilsson, E. D., and U. Rannik (2001), Turbulent aerosol fluxes over the Arctic Ocean 1. Dry deposition over sea and pack ice, *Journal of Geophysical Research: Atmospheres*, 106(D23), 32125-32137, doi:Doi 10.1029/2000jd900605.
- NIOSH (1999), Elemental carbon (Diesel Particulate): Method 5040, <http://www.cdc.gov/noish/docs/2013-154/pdfs/5040.pdf>.
- Norman, A. L., L. A. Barrie, D. Toom-Sauntry, A. Sirois, H. R. Krouse, S. M. Li, and S. Sharma (1999), Sources of aerosol sulphate at Alert: Apportionment using stable isotopes, *Journal of Geophysical Research: Atmospheres*, 104(D9), 11619-11631, doi:10.1029/1999jd900078.
- Nyeki, S., H. Bauer, H. Puxbaum, C. Dye, K. Teinila, R. Hillamo, J. Ström, and K. Eleftheriadis (2005), *Comparison of black carbon concentrations derived by filter-based light transmission and thermo-optical techniques for Arctic aerosol*, Paper presented at European Aerosol Conference 2005, 28 August – 2 September, Ghent, Belgium.
- O'Dowd, C. D., B. Langmann, S. Varghese, C. Scannell, D. Ceburnis, and M. C. Facchini (2008), A combined organic-inorganic sea-spray source function, *Geophysical Research Letters*, 35, L01801, doi:10.1029/2007gl030331.
- Ottar, B., J. M. Pacyna, and T. C. Berg (1986), Aircraft measurements of air pollution in the Norwegian Arctic, *Atmospheric Environment*, 20(1), 87-100, doi:10.1016/0004-6981(86)90209-x.
- Pacyna, J. M., and B. Ottar (1985), Transport and chemical composition of the summer aerosol in the Norwegian Arctic, *Atmospheric Environment*, 19(12), 2109-2120, doi:10.1016/0004-6981(85)90118-0.
- Pacyna, J. M., and E. G. Pacyna (2001), An assessment of global and regional emissions of trace metals to the atmosphere from anthropogenic sources worldwide, *Environmental Reviews*, 9(4), 269-298, doi:10.1139/er-9-4-269.
- Park, K.-T., K. Lee, Y.-J. Yoon, H.-W. Lee, H.-C. Kim, B.-Y. Lee, O. Hermansen, T.-W. Kim, and K. Holmén (2013), Linking atmospheric dimethyl sulfide and the Arctic Ocean spring bloom, *Geophysical Research Letters*, 40(1), 155-160, doi:10.1029/2012GL054560.
- Pathak, R. K., W. S. Wu, and T. Wang (2009), Summertime PM_{2.5} ionic species in four major cities of China: nitrate formation in an ammonia-deficient atmosphere, *Atmospheric Chemistry and Physics*, 9(5), 1711-1722, doi:10.5194/acp-9-1711-2009.
- DIN EN ISO 11885 (1998), *Determination of 33 elements by inductively coupled plasma atomic emission spectroscopy*. European Committee for Standardization, Brussels.

- Quinn, P. K., et al. (2000), Surface submicron aerosol chemical composition: What fraction is not sulfate?, *Journal of Geophysical Research: Atmospheres*, 105(D5), 6785-6805, doi:10.1029/1999jd901034.
- Quinn, P. K., T. S. Bates, K. Schulz, and G. E. Shaw (2009), Decadal trends in aerosol chemical composition at Barrow, Alaska: 1976-2008, *Atmospheric Chemistry and Physics*, 9(22), 8883-8888, doi:10.5194/acp-9-8883-2009.
- Quinn, P. K., T. L. Miller, T. S. Bates, J. A. Ogren, E. Andrews, and G. E. Shaw (2002), A 3-year record of simultaneously measured aerosol chemical and optical properties at Barrow, Alaska, *Journal of Geophysical Research: Atmospheres*, 107(D11), 4130, doi:10.1029/2001jd001248.
- Rahn, K. A. (1981), The Mn/V ratio as a tracer of large-scale sources of pollution aerosol for the Arctic, *Atmospheric Environment*, 15(8), 1457-1464, doi:10.1016/0004-6981(81)90352-8.
- Ricard, V., J. L. Jaffrezo, V. M. Kerminen, R. E. Hillamo, K. Teinila, and W. Maenhaut (2002), Size distributions and modal parameters of aerosol constituents in northern Finland during the European Arctic Aerosol Study, *Journal of Geophysical Research: Atmospheres*, 107(D14), 4208, doi:10.1029/2001jd001130.
- Savarino, J., S. Morin, J. Erbland, F. Grannec, M. D. Patey, W. Vicars, B. Alexander, and E. P. Achterberg (2013), Isotopic composition of atmospheric nitrate in a tropical marine boundary layer, *Proceedings of the National Academy of Sciences*, 110(44), 17668-17673, doi:10.1073/pnas.1216639110.
- Scott, B. C. (1978), Parameterization of sulfate removal by precipitation, *Journal of Applied Meteorology* 17, 1375-1389, doi:10.1175/1520-0450(1978)017<1375:POSRBP>2.0.CO;2.
- Shah, S. D., D. R. Cocker, J. W. Miller, and J. M. Norbeck (2004), Emission rates of particulate matter and elemental and organic carbon from in-use diesel engines, *Environmental Science & Technology*, 38(9), 2544-2550, doi:10.1021/es0350583.
- Sharma, S., E. Andrews, L. A. Barrie, J. A. Ogren, and D. Lavoué (2006), Variations and sources of the equivalent black carbon in the high Arctic revealed by long-term observations at Alert and Barrow: 1989-2003, *Journal of Geophysical Research: Atmospheres*, 111(D14208), doi:10.1029/2005JD006581.
- Sharma, S., D. Lavoué, H. Cachier, L. A. Barrie, and S. L. Gong (2004), Long-term trends of the black carbon concentrations in the Canadian Arctic, *Journal of Geophysical Research: Atmospheres*, 109(D15), doi:10.1029/2003JD004331.
- Shaw, P. M., L. M. Russell, A. Jefferson, and P. K. Quinn (2010), Arctic organic aerosol measurements show particles from mixed combustion in spring haze and from frost flowers in winter, *Geophysical Research Letters*, 37, L10803, doi:10.1029/2010gl042831.

- Sheridan, P. J., and W. H. Zoller (1989), Elemental composition of particulate material sampled from the Arctic haze aerosol, *Journal of Atmospheric Chemistry*, 9(1-3), 363-381, doi:10.1007/Bf00052843.
- Shindell, D., and G. Faluvegi (2009), Climate response to regional radiative forcing during the twentieth century, *Nature Geoscience*, 2, 294-300, doi:10.38/ngeo473.
- Sievering, H., J. Boatman, E. Gorman, Y. Kim, L. Anderson, G. Ennis, M. Luria, and S. Pandis (1992), Removal of Sulfur from the Marine Boundary-Layer by Ozone Oxidation in Sea-Salt Aerosols, *Nature*, 360(6404), 571-573, doi:10.1038/360571a0.
- Sirois, A., and L. A. Barrie (1999), Arctic lower tropospheric aerosol trends and composition at Alert, Canada: 1980-1995, *Journal of Geophysical Research: Atmospheres*, 104(D9), 11599-11618, doi:10.1029/1999jd900077.
- Spackman, J. R., R. S. Gao, W. D. Neff, J. P. Schwarz, L. A. Watts, D. W. Fahey, J. S. Holloway, T. B. Ryerson, J. Peischl, and C. A. Brock (2010), Aircraft observations of enhancement and depletion of black carbon mass in the springtime Arctic, *Atmospheric Chemistry and Physics*, 10(19), 9667-9680, doi:10.5194/acp-10-9667-2010.
- Squizzato, S., M. Masiol, A. Brunelli, S. Pistollato, E. Tarabotti, G. Rampazzo, and B. Pavoni (2013), Factors determining the formation of secondary inorganic aerosol: a case study in the Po Valley (Italy), *Atmospheric Chemistry and Physics*, 13(4), 1927-1939, doi:10.5194/acp-13-1927-2013.
- Stohl, A., et al. (2006), Pan-Arctic enhancements of light absorbing aerosol concentrations due to North American boreal forest fires during summer 2004, *Journal of Geophysical Research: Atmospheres*, 111, D22214, doi:10.1029/2006jd007216.
- Ström, J., A.-C. Engvall, F. Delbart, R. Krejci, and R. Treffeisen (2009), On small particles in the Arctic summer boundary layer: observations at two different heights near Ny-Ålesund, Svalbard, *Tellus Series B: Chemical and Physical Meteorology*, 61(2), 473-482, doi:10.1111/j.1600-0889.2008.00412.x.
- Ström, J., J. Umegård, K. Tørseth, P. Tunved, H. C. Hansson, K. Holmén, V. Wismann, A. Herber, and G. König-Langlo (2003), One year of particle size distribution and aerosol chemical composition measurements at the Zeppelin Station, Svalbard, March 2000-March 2001, *Physics and Chemistry of the Earth*, 28(28-32), 1181-1190, doi:10.1016/j.pce.2003.08.058.
- Taylor, S. (1964), Abundance of chemical elements in the continental crust: A new table, *Geochim Cosmochim Acta*, 28(8), 1273-1285.
- Tjernström, M. (2005), The Summer Arctic Boundary Layer during the Arctic Ocean Experiment 2001 (AOE-2001), *Boundary-layer meteorology*, 117(1), 5-36, doi:10.1007/s10546-004-5641-8.

- Tjernström, M., and R. G. Graversen (2009), The vertical structure of the lower Arctic troposphere analysed from observations and the ERA-40 reanalysis, *Quarterly Journal of the Royal Meteorological Society*, 135(639), 431-443, doi:10.1002/qj.380.
- Tsai, Y. I., and M. T. Cheng (1999), Visibility and aerosol chemical compositions near the coastal area in Central Taiwan, *Science of the Total Environment*, 231(1), 37-51, doi:10.1016/S0048-9697(99)00093-5.
- Vestreng, V., R. Kallenborn, and E. Økstad (2009), *Norwegian Arctic climate: climate influencing emissions, scenarios and mitigation options at Svalbard*. Oslo: Climate and Pollution Agency.
- Viana, M., F. Amato, A. Alastuey, X. Querol, T. Moreno, S. García Dos Santos, M. Dolores Herce, and R. Fernández-Patier (2009), Chemical tracers of particulate emissions from commercial shipping, *Environmental Science & Technology*, 43(19), 7472-7477, doi:10.1021/es901558t.
- Vignati, E., M. Karl, M. Krol, J. Wilson, P. Stier, and F. Cavalli (2010), Sources of uncertainties in modelling black carbon at the global scale, *Atmospheric Chemistry and Physics*, 10(6), 2595-2611, doi:10.5194/acp-10-2595-2010.
- Wang, Q., et al. (2011), Sources of carbonaceous aerosols and deposited black carbon in the Arctic in winter-spring: implications for radiative forcing, *Atmospheric Chemistry and Physics*, 11(23), 12453-12473, doi:10.5194/acp-11-12453-2011.
- Weinbruch, S., D. Wiesenmann, M. Ebert, K. Schütze, R. Kallenborn, and J. Ström (2012), Chemical composition and sources of aerosol particles at Zeppelin Mountain (Ny Ålesund, Svalbard): An electron microscopy study, *Atmospheric Environment*, 49, 142-150, doi:10.1016/j.atmosenv.2011.12.008.
- Wise, M. E., T. A. Semeniuk, R. Bruintjes, S. T. Martin, L. M. Russell, and P. R. Buseck (2007), Hygroscopic behavior of NaCl-bearing natural aerosol particles using environmental transmission electron microscopy, *Journal of Geophysical Research: Atmospheres*, 112, D10224, doi:10.1029/2006jd007678.
- Worthy, D. E. J., N. B. A. Trivett, J. F. Hopper, J. W. Bottenheim, and I. Levin (1994), Analysis of long-range transport events at Alert, Northwest Territories, during the Polar Sunrise Experiment, *Journal of Geophysical Research: Atmospheres*, 99(D12), 25329, doi:10.1029/94jd01209.
- Wu, Z. H., and N. E. Huang (2004), A study of the characteristics of white noise using the empirical mode decomposition method, *Proceedings of the Royal Society A: Mathematical, Physical & Engineering Sciences*, 460(2046), 1597-1611, doi:10.1098/rspa.2003.1221.
- Wu, Z. H., and N. E. Huang (2009), Ensemble empirical mode decomposition: a noise assisted data analysis method, *Advances in Adaptive Data Analysis*, 1, 1-41, doi:10.1142/S1793536909000047.

- Xia, L., and Y. Gao (2010), Chemical composition and size distributions of coastal aerosols observed on the US East Coast, *Marine Chemistry*, 119(1-4), 77-90, doi:10.1016/j.marchem.2010.01.002.
- Xu, G., Y. Gao, Q. Lin, W. Li, and L. Chen (2013), Characteristics of water-soluble inorganic and organic ions in aerosols over the Southern Ocean and coastal East Antarctica during austral summer, *Journal of Geophysical Research: Atmospheres*, 118(23), 2013JD019496, doi:10.1002/2013JD019496.
- Yang, Z., A. K. Bertram, and K. C. Chou (2011), Why do sulfuric acid coatings influence the ice nucleation properties of mineral dust particles in the atmosphere?, *The Journal of Physical Chemistry Letters*, 2(11), 1232-1236, doi:10.1021/jz2003342.
- Zhan, J., Y. Gao, W. Li, L. Chen, H. Lin, and Q. Lin (2014), Effects of ship emissions on summertime aerosols at Ny-Ålesund in the Arctic, *Atmospheric Pollution Research*, In press.
- Zhang, Q., J. L. Jimenez, D. R. Worsnop, and M. Canagaratna (2007), A case study of urban particle acidity and its influence on secondary organic aerosol, *Environmental Science & Technology*, 41(9), 3213-3219, doi:10.1021/Es061812j.
- Zhao, Y., and Y. Gao (2008), Mass size distributions of water-soluble inorganic and organic ions in size-segregated aerosols over metropolitan Newark in the US east coast, *Atmospheric Environment*, 42(18), 4063-4078, doi:10.1016/j.atmosenv.2008.01.032.
- Zhou, Y., L. K. Xue, T. Wang, X. M. Gao, Z. Wang, X. F. Wang, J. M. Zhang, Q. Z. Zhang, and W. X. Wang (2012), Characterization of aerosol acidity at a high mountain site in central eastern China, *Atmospheric Environment*, 51, 11-20, doi:10.1016/j.atmosenv.2012.01.061.
- Zoller, W. H., G. E. Gordon, E. S. Gladney, and A. E. Jones (1973), The sources and distribution of vanadium in the atmosphere, in *Trace Elements in the Environment*, edited, pp. 31-47, Trace Elements in the Environment.

Curriculum vitae

- 2003** Graduated from Longyan No.2 High School, Fujian, China
- 2003 – 2007** B.Sc. in Oceanography, Ocean University of China, Qingdao, China.
- 2007 – 2010** M.Sc. in Marine Chemistry, Third Institute of Oceanography, State Oceanic Administration (SOA), Xiamen, China.
- 2010 – 2011** Research Assistance, Third Institute of Oceanography, State Oceanic Administration (SOA), Xiamen, China.
- 2011** Peer-reviewed article: Chen, L., Xu, S., Gao, Z., Chen, H., Zhang, Y., **Zhan, J.**, Li, W., 2011. Estimation of monthly air-sea CO₂ flux in the southern Atlantic and Indian Ocean using in-situ and remotely sensed data. *Remote Sensing of Environment* 115, 1935-1941.
- 2011 – 2014** Teaching Assistance, Rutgers University, New Jersey, USA.
- 2011 – 2014** Ph.D. student, in Environmental Sciences, Rutgers University, New Jersey, USA.
- 2013** Peer-reviewed article: Gao, Y., G. Xu, J. **Zhan, J.** Zhang, W. Li, Q. Lin, L. Chen, and H. Lin., 2013, Spatial and Particle-Size Distributions of Atmospheric Dissolved Iron in Aerosols and Its Input to the Southern Ocean and Coastal East Antarctica, *Journal of Geophysical Research – Atmospheres*, VOL. 118, 1–15, doi:10.1002/2013JD020367, 2013.
- 2014** Peer-reviewed article: **Zhan, J.**, Gao, Y., 2014. Impact of summertime anthropogenic emissions on atmospheric black carbon at Ny-Ålesund in the Arctic. *Polar Research* 33, 21821.
- 2014** Peer-reviewed article: **Zhan, J.** Gao, Y., Li, W., Chen, L., Lin, H., and Lin, Q., 2014. Effects of ship emissions on summertime aerosols at Ny-Ålesund in the Arctic. *Atmospheric Pollution Research*, in press.
- 2014** Peer-reviewed article: **Zhan, J.** Gao, Y., Li, W., Chen, L., and Lin, Q., 2014. The Influence of Acidity on Chloride Depletion and Secondary Aerosol Formation. In review.